Simulation of the Cystic Fibrosis patient airway habitats using microfluidic devices

Skolimowski, Maciej; Emnéus, Jenny; Geschke, Oliver; Dufva, Martin; Sternberg, Claus; Molin, Søren

Publication date:
2013

DTU Nanotech
Department of Micro- and Nanotechnology

Simulation of the Cystic Fibrosis patient airway habitats using microfluidic devices

PhD Thesis

Maciej Skolimowski

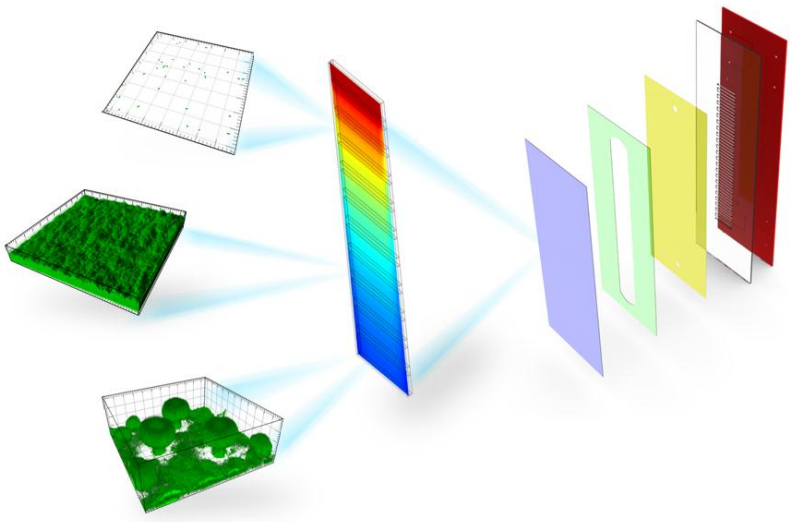

Supervisor: Jenny Emnéus (2010-2011) and Oliver Geschke (2008-2010)

Co-supervisors: Martin Dufva, Claus Sternberg, Søren Molin

Department of Micro- and Nanotechnology

Technical University of Denmark

June 2011

Abstract

Many severe infections in humans affect the airways. Different types of pneumonia are major causes of morbidity and mortality in patients with various weakening conditions, and often ineffective anti-microbial therapies fail to remove the infecting microbes. One of the most severe genetic diseases affecting human airways is cystic fibrosis.

Cystic fibrosis (CF) patients suffer from a genetic defect that influences the salt transport over the cell membranes. Due to this effect, the mucus layer becomes very viscous as the defect in salt transport inhibit diffusion of and establishment of the important airway surface liquid (ASL). A direct consequence of the impaired ASL is the impairment of the mucocilliary clearance mechanisms. This results in frequent infections in the airways of CF patients, with the risk of pneumonia. Since bacteria infect the lungs of these patients in large numbers, the immune system tries to eradicate the infections, but with reduced success. This is due to the fact that the bacteria reside embedded in mucus and are more or less recalcitrant to the attack. Instead, the lung tissue is gradually damaged by the ongoing immunological exposure, eventually leading to massive pulmonary deficiency and death.

The classical ways of studying CF related bacterial infections, primarily *Pseudomonas aeruginosa*, are either to use animal models or to grow the bacteria in flow cell systems. The use of animal models raises ethical concerns and is costly. Besides, CF related animal models are still not ideal, mainly because the immune response differs between man and e.g. mouse, and because the lung pathology after infection is very different in animals compared to humans.

In flow cell based systems the bacteria are allowed to form a biofilm on the surface, as in the airways, and their growth is then monitored using confocal microscopy. However, this is not either a suitable CF model as the human airways are subdivided into aerobic and anaerobic compartments.

To investigate the different compartments of the human airways system it is crucial importance to construct a microfluidic model system in which the oxygen level can be regulated and the migration of cells between individual compartments can be controlled and monitored. Furthermore, the special conditions in the CF bronchi need to be mimicked as the thick mucus plug present there seems to be another essential factor in the failure of treating infections in CF patients. Therefore, in this work we propose novel microfluidic devices that on one hand can mimic different airway environments by controlling the oxygen levels and on the other hand can mimic the microenvironment of the cystic fibrosis bronchi.

Résumé

Mange alvorlige infektioner i mennesket påvirker luftvejene. Forskellige typer af lungebetændelse er primære årsager til sygelighed og dødelighed i patienter med forskellige svækkende omstændigheder hvor ineffektive anti-mikrobiel terapi slår fejl i bekæmpelsen af de inficerende mikrober. En af de mest alvorlige genetiske sygdomme der påvirker de menneskelig luftveje, er cystisk fibrose.

Cystisk fibrose (CF) patienter lider af en genetisk defekt der påvirker salt transporten over cellemembranerne. På grund af denne defekt, bliver slimlaget meget viskøst da den defekte salt transport hæmmer diffusion og etableringen af den vigtige overflade associerede overflade væske (Airway surface liquid, ASL). En direkte konsekvens af den hæmmede ASL er en hæmning af cilia slim transporten.

Dette resulterer i hyppige infektioner i luftvejene hos CF patienter med risiko for lungebetændelse. Eftersom bakterier i hobetal inficerer lungerne hos disse patienter, forsøger immunsystemet at fjerne disse infektioner, dog med begrænset held. Dette skyldes at bakterierne lever indpakket i slimlaget og er mere eller mindre modstandsdygtige overfor immunologiske angreb. I stedet bliver lungevævet gradvist ødelagt grundet den kontinuerlige immunologiske påvirkning der med tiden fører til den massive lunge defekt og død.

Den klassiske måde at studere CF relaterede bakterielle infektioner på, primært med Pseudomonas aeruginosa, er enten i dyremodeller eller ved dyrkning af bakterierne i flow celle systemer. Brug af dyremodeller er omkostningskrævende og fører til etiske betænkeligheder. Ud over dette er CF relaterede dyremodeller stadig ikke idelle, primært fordi de immunologiske reaktioner afviger kraftigt mellem menneske og eksempelvis mus og ydermere fordi at lunge patologien efter infektioner er meget forskellige i dyr sammenlignet med mennesker.

I flow celle systemer lader bakterierne sig fæstne og danne biofilm på overfladerne, som i luftvejene, og deres vækst kan blive monitoreret ved brug af konfokal mikroskopi. Dette er dog ikke et passende CF model system da de humane luftveje er underinddelt i aerobe og anaerobe grene.

For at udnersøger de forskellige grene af det humane luftvejs system er det er yderst vigtigt at konstruere et mikrofluidt model system hvor oxygen niveauerne kan blive reguleret og migrationen af bakterierne mellem den individuelle grene kan blive kontrolleret og monitoreret.

Ydermere, de specielle omstændigheder i CF bronkierne nødvendiggør efterligning da de viskøse slim ansamlinger syntes at være en anden essentiel faktor i de mislykkede forsøg i at behandle infektioner i CF patienter. Af denne årsag foreslår vi en nytænkning indenfor mikrofluide systemer,

der på den ene side kan efterligne forskellige luftvejs miljøer ved at kontrollere oxygen niveauer og på den anden side kan efterligne de mikromiljøer der eksisterer i bronkier hos cystisk fibrose patienter.

Acknowledgements

I would like to thank Assoc. Prof. Oliver Geschke, Prof. Jenny Emnéus, Assoc. Prof. Martin Dufva, Assoc. Prof. Claus Sternberg and Prof. Søren Molin for proposing this very exciting project to me and accepting me for the PhD studies at DTU Nanotech and DTU Biosys. Furthermore, I would like to express my deepest gratitude to them for providing me with excellent working and studying conditions, scientifically developing environment and all the care and supervision during my PhD studies. I would also like to thank Assoc. Prof. Rafael Taboryski and Assoc. Prof. Kristian Mølhave for their support and feedbacks to the project.

The realisation of the project would not be possible without the collaboration with Martin Weiss Nielsen. I would like to express the deepest gratitude for his help, inputs, patience and, most importantly, friendship during the time we spend for our projects.

For the great time as well as for the help and support I would like to thank to all the past and present members of the two research group I belonged: POEM and BIOANALYTICS. I would like to express my special gratitude to Jan Kafka, Jörg Vogel and Kamila Pszon-Bartosz who welcomed me at DTU Nanotech and showed me the first steps in the field of microfabrication.

During my PhD project I received a great help from fellow students. I had a great occasion to work with: Terje Rosquist Tofteberg, Joanna Łopacińska, Maria Matschuk, Simas Mickevičius, Niels Brehm Nielsen, Søren Matthias Goldschmidt, Yang Liu, Rafał Wierzbicki and Fabien Abeille. I would like to express my inmost appreciation to them and all former and present employees and students at DTU Nanotech and DTU Biosys.

Furthermore, I would like to thank to Prof. Dmitri B. Papkovsky and his research group from Department of Biochemistry, University College Cork, Ireland for providing me a great opportunity for a research stay at their University and all the help and support with oxygen concentration measurements.

I would also like to acknowledge for the funding of Ph.D. stipend by The Technical University of Denmark as well as the EU funded FP7 project EXCELL for financing my external stay in Ireland.

Table of contents

1 List of publications

This thesis is based on the following papers, which will be referred to in the text by their Roman numerals. The papers are appended at the end of the thesis.

I. **Skolimowski, M.**, Tofteberg, T., Andreassen, E., and Geschke, O., *A novel passive micromixer suitable for mass production in polymers.* The 25th Annual meeting of The Polymer Processing Society, conference proceedings, 2009.

II. Tofteberg, T**., Skolimowski, M.**, Andreassen, E., and Geschke, O., *A novel passive micromixer: lamination in a planar channel system.* Microfluidics and Nanofluidics, 2010. 8(2): p. 209-215, DOI: 10.1007/s10404-009-0456-z.

III. **Skolimowski, M.**, Nielsen, M.W., Emnéus, J., Molin, S., Dufva, M., Taboryski, R., Sternberg, C., and Geschke, O., *Microfluidic biochip as a model of the airways of cystic fibrosis patients.* Proceedings of the Thirteenth International Conference on Miniaturized Systems for Chemistry and Life Sciences, p. 1091-1093, 2009.

IV. **Skolimowski, M.**, Nielsen, M.W., Emnéus, J., Molin, S., Taboryski, R., Sternberg, C., Dufva, M., and Geschke, O., *Microfluidic dissolved oxygen gradient generator biochip as a useful tool in bacterial biofilm studies.* Lab on a Chip, 2010. 10(16): p. 2162-2169, DOI: 10.1039/c003558k.

V. **Skolimowski, M.**, Nielsen, M.W., Abeille, F., Skafte-Pedersen, P., Sabourin, D., Fercher, A., Papkovsky, D., Molin, S., Taboryski, R., Sternberg, C., Dufva, M., Geschke, O. and Emnéus, J, *Modular microfluidic system as a model of cystic fibrosis airways.* Submitted manuscript to Lab on a Chip, 2011.

VI. **Skolimowski, M.**, Abeille, F., Nielsen, M.W., Lopacinska, J., D., Molin, S., Taboryski, R., Sternberg, C., Dufva, M., Geschke, O. and Emnéus, J., *Microfluidic model of cystic fibrosis*

bronchi. Accepted for Proceedings of the Fifteenth International Conference on Miniaturized Systems for Chemistry and Life Sciences, 2011.

VII. Abeille, F.**, Skolimowski, M.**, Nielsen, M.W., Lopacinska, J., D., Molin, S., Taboryski, R., Sternberg, C., Dufva, M., Geschke, O. and Emnéus, J., Microfluidic system for *in vitro* study of bacterial infections in cystic fibrosis bronchi. Manuscript in preparation, 2011.

Other related publications not included in this thesis:

1. Lopacinska, J.M., Gradinaru, C., Wierzbicki, R., Schmidt M.S., Madsen M. T., **Skolimowski, M.**, Dufva, M., Flyvbjerg, H., Mølhave, K., *Cell motility, morphology, viability and proliferation changes as a response to the nanotopography cues*. 2011, manuscript for submission to Biomaterials

2. Kwapiszewski, R., **Skolimowski, M.**, Ziolkowska, K., Jedrych, E., Chudy, M., Dybko, A., and Brzozka, Z., *A microfluidic device with fluorimetric detection for intracellular components analysis.* Biomedical Microdevices, 2011. 13(3): p. 431-40, DOI: 10.1007/s10544-011-9511-0.

3. Ziolkowska, K., Jedrych, E., Kwapiszewski, R., Lopacinska, J., **Skolimowski, M.**, and Chudy, M., *PDMS/glass microfluidic cell culture system for cytotoxicity tests and cells passage.* Sensors and Actuators B-Chemical, 2010. 145(1): p. 533-542, DOI: 10.1016/j.snb.2009.11.010.

4. Ciosek, P., Zawadzki, K., Lopacinska, J., **Skolimowski, M.**, Bembnowicz, P., Golonka, L.J., Brzozka, Z., and Wroblewski, W., *Monitoring of cell cultures with LTCC microelectrode array.* Analytical and Bioanalytical Chemistry, 2009. 393(8): p. 2029-38, DOI: 10.1007/s00216-009-2651-x.

5. Chudy, M., Grabowska, I., Ciosek, P., Filipowicz-Szymanska, A., Stadnik, D., Wyzkiewicz, I., Jedrych, E., Juchniewicz, M., **Skolimowski, M.**, Ziolkowska, K., and Kwapiszewski, R., *Miniaturized tools and devices for bioanalytical applications: an overview.* Analytical and Bioanalytical Chemistry, 2009. 395(3): p. 647-668, DOI: 10.1007/s00216-009-2979-2.

6. **Skolimowski, M.**, Churski, K., Cabaj, M., and Brzózka, Z., *Kontrola przepływu cieczy w mikrourządzeniach typu Lab-on-a-Chip*, (*Control of fluid flow in Lab-on-a-Chip microdevices*), in *Mikrobioanalityka*, Z. Brzózka, Editor 2009, Oficyna Wydawnicza Politechniki Warszawskiej: Warsaw. p. 208, ISBN: 978-83-7207-809-4.

7. Łopacińska, J., **Skolimowski, M**., Dąbrowski, M., Jacewicz, M., Kuciński, M., Stefanek, K., and Brzózka, Z., Miniaturowe układy typu Lab-on-a-chip w chemii, biologii i medycynie, (Miniaturized Lab-on-a-chip devices for chemistry, biology and medicine), in Na pograniczu chemii i biologii 2008, Wydawnictwo Naukowe UAM: Poznań. p. 316, ISBN: 978-83-232184-5-6.

2 Contribution to the papers and manuscripts

Paper I. *A novel passive micromixer suitable for mass production in polymers*

I took part in the designing of the micromixer together with the second author, Terje Tofteberg. I designed and performed the fabrication of the device and performed the measurements of the mixer efficiency. I wrote the part of the paper concerning fabrication and confocal laser scanning microscopy. The paper was further corrected by Oliver Geschke and Erik Andreassen.

Paper II. *A novel passive micromixer: lamination in a planar channel system*

I took part in the design of the micromixer together with the first author, Terje Tofteberg. I designed and performed fabrication of the device and performed the measurements of the mixer efficiency. I wrote the part of the paper concerning fabrication and confocal laser scanning microscopy. The paper was further corrected by Oliver Geschke and Erik Andreassen.

Paper III. *Microfluidic biochip as a model of the airways of cystic fibrosis patients*

I designed and fabricated the devices and performed the numerical simulation of the generation of oxygen gradient in the device. Together with the second author, Martin Weiss Nielsen, I took part in the bacterial biofilm culturing. I wrote most of the paper, which was further corrected by the rest of the co-authors.

Paper IV. *Microfluidic dissolved oxygen gradient generator biochip as a useful tool in bacterial biofilm studies*

I designed and fabricated the device and performed the numerical simulation of the generation of oxygen gradient in the device. Together with the second author, Martin Weiss Nielsen, I took part in the bacterial biofilm culturing and the result analysis. I and Martin Weiss Nielsen wrote the paper, which was further corrected by the rest of the co-authors.

Paper V. *Modular microfluidic system as a model of cystic fibrosis airways*

I designed the devices and the fabrication steps. I performed the fabrication together with the third author, Fabien Abeille. Together with two co-authors: Martin Weiss Nielsen and Fabien Abeille, I took part in the bacterial biofilm culture. Together with Andreas Fercher and Dmitry Papkovsky I performed the oxygen concentration measurements. Together with Martin Weiss Nielsen I took part in the result analysis. I wrote most of the paper, which was further corrected by the rest of the co-authors.

Paper VI. *Microfluidic model of cystic fibrosis bronchi*

I, together with Martin Weiss Nielsen, developed the idea of cystic fibrosis bronchi model. Together with Fabien Abeille, I designed the device and fabricated it. Together with Martin Weiss Nielsen, Fabien Abeille and Joanna Łopacińska I took part in the mammalian cell culturing, bacterial biofilm culturing and the result analysis. Fabien Abeille and I wrote the paper, which was further corrected by the rest of the co-authors.

Paper VII. *Microfluidic system for in vitro study of bacterial infections in cystic fibrosis bronchi*

I, together with Martin Weiss Nielsen, developed the idea of cystic fibrosis bronchi model. Together with Fabien Abeille, I designed the device and fabricated it. Together with Martin Weiss Nielsen, Fabien Abeille and Joanna Łopacińska, I took part in the mammalian cell culturing, bacterial biofilm culturing and the result analysis. Fabien Abeille and I wrote most of the paper, which was further corrected by the rest of the co-authors.

3 Introduction

3.1 Motivation

Cystic fibrosis (CF) is one of the most spread genetic diseases among European and European-descendant populations. The disease attacks multiple organs among which, the dysfunction of the airways clearance is most severe. So far there is no treatment that can alleviate the effects of this disease. CF gradually lowers the quality of life and eventually leads to premature death of a patient as a result of the recurrent airways infections and decline in respiratory function of the lungs. Due to the development of early diagnostics, the prognosis for the patients and their life expectancy has improved over recent years. However, a successful therapy that efficiently can treat the infections and stop their recurrence has not yet been realised. There is therefore a need for new therapeutic strategies based on improved understanding of the infection cycles and the specific interactions between the bacteria and the environment in the host organism.

The current *in vivo* models of CF related infections are animal models, among which, the mouse - either inbred laboratory mice or transgenic cystic fibrosis mice - are the most widely used. These models are far from ideal, mainly because of the differences in immune response and the efficiency of airways clearing mechanism between mice and human. Besides, the growing ethical concern of using animals for medical research makes it especially important to replace or at least reduce the use of animals and move toward the use of better *in vitro* model systems.

The present *in vitro* models are mainly based on flow-cell based systems. These models lack to describe the complexity of the different compartments of the human airways as well as the interaction between these compartments. Irrespective of the quick advancement in the *in vivo* and *in vitro* models of the CF airways, there is a need for microfluidic models that better resemble the scale and conditions met by invading pathogens. Therefore, an advanced microfluidic cell culture system that mimics the environmental conditions in three relevant compartments of the airways, i.e., nasal sinus cavities, the conductive zones of trachea, bronchi and bronchioles, and the alveolar aerobic zone is required, and was developed during this thesis.

The ability to provide a high-throughput way of studying differences in metabolism, adaptation and genetic variability of bacteria living in the airways compartments with different oxygen tension

should allow in the future to develop safer, better and more efficient strategies for treatment of CF related infections.

3.2 Aim of the work

The primary goal of this project was to develop and apply a novel *in vitro* microfluidic airways model that potentially could replace existing, but insufficient animal models. Using the above proposed microfluidic artificial airways model, one can look into the bacterial details in the three interconnected compartments, their transmitting interaction and the states of the bacterial inhabitants before, during, and after antibiotic treatment. The development of an artificial microfluidic model, with particular emphasis on resembling the oxygen microenvironments in the different compartments should lead to better understanding of the airways and the interactions within the complex lung-airway-nasal sinus system.

Furthermore, a model of the CF bronchi epithelia covered with a thick mucus layer was needed to better understand the hindered diffusion of the antimicrobial agent to the focal point of infections.

3.3 Structure of the thesis

The content of this thesis is based on the results obtained during the three-year period of the author's Ph.D. studies. The thesis has been divided into three main parts: the biological background of CF (**chapters 4-5**), the microfabrication aspects of developing a microfluidic CF airways model (**chapter 6-7**), and the collection of the core results gathered in the published papers and prepared manuscripts (**chapter 8**).

Chapter 4 is an introduction to the genetic, physiological and microbiological aspects related to CF that needs to be considered and that has led up to the design of the microfluidic CF airways model in this thesis. Special attention is put on the known reasons for the common failures in the treatment of CF related infections alongside with the hypothesis for the causes of the persistent and recurrent bacterial colonisation of the airways. The theories that try to explain the impairment of mucociliary clearance as well as the resistance of the *P. aeruginosa* infections to the treatment of different antibiotics are presented. The impact of changes in the oxygen tension in the different compartments of the CF airways is emphasized in this chapter.

Chapter 5 contains a brief review of the few microfluidics models of different human organs reported in recent literature.

Chapter 6 discusses different ways to control the dissolved oxygen concentration in microfluidic devices. The techniques used for measurement of dissolved oxygen at the microscale, with special focus on the optical methods are presented in this chapter.

Chapter 7 describes different aspects of microfabrication of microfluidic systems, and finally shows the different solutions pursued in this thesis.

Chapter 8 contains the collection of original papers and manuscripts.

Paper I (conference proceeding) presents a novel passive micromixer concept that creates direct lamination in a 2D channel. This concept is further described in **paper II** (full published paper). This passive micromixer was further used in the microfluidic airways model described in **paper V** (manuscript).

Paper III (conference proceeding) reports the work performed towards development of a dissolved oxygen gradient generator as part of a microfluidic system that can simulate the aerobic and anaerobic conditions in the human airways. This system is further described in **paper IV** (full published paper).

Paper V (manuscript) contains the description of a modular microfluidic system as a model of the CF airways.

Paper VI (accepted conference proceeding) presents the work towards mimicking the CF bronchi, which is followed by **Paper VII** (manuscript) where this system is described in more detail.

The collection of the papers is followed by **chapter 9**, that contains some brief conclusions and future perspectives of the systems developed in this work. The thesis is concluded by a list of references.

4 Biological background

4.1 Human airways

The human airways consist of at least three independent compartments, the conductive airways (the trachea, bronchi and bronchioles), the oxygen exchange compartment also called respiratory zone (respiratory bronchioles, alveolar ducts and alveolar sacs), and a third less recognized compartment, the paranasal sinuses (maxillary sinuses, frontal sinuses and ethmoid sinuses) (Figure 1). In the first and the last compartment, the environment is essentially anaerobic or micro-aerobic, while the alveoli are highly aerated[1]. Traditionally, the airways are divided into the upper respiratory tract (nasal cavity, paranasal sinuses, pharynx) and lower respiratory tract (trachea, bronchi, bronchioles and pulmonary alveoli)[2].

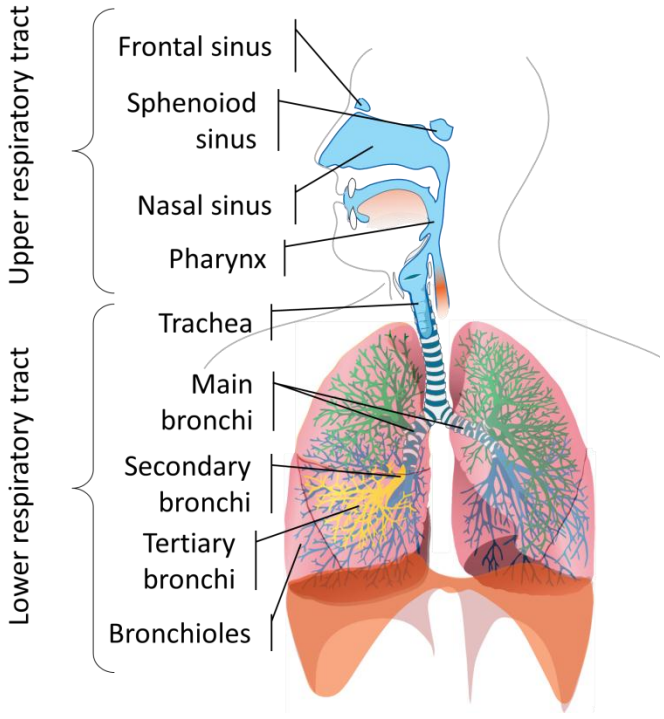

Figure 1. The human airways.

The upper respiratory tract is the home for bacterial flora[3, 4], while the lower respiratory tract in healthy persons, usually remains sterile.

4.2 Cystic fibrosis

4.2.1 Mutation in the CFTR gene

Cystic fibrosis (CF) is a severe genetic multiorgan disease, common in European and European-descendant populations[5]. A mutation in the Cystic Fibrosis Transmembrane Conductance Regulator (CFTR) gene cause dysfunction of the mucosa[1][6]. Due to this dysfunction, the secreted mucus is less hydrated and therefore much more viscous than in a healthy person. This make the natural mechanisms of clearing and renewing of the mucous layer impaired. The epithelia of the exocrine pancreas, intestine, hepatobiliary system, male genital tract, exocrine sweat glands and, most importantly, the airways are affected by this defect[7].

The product of CFTR gene, the CFTR protein, has many roles as an ionic channel and regulator[8]. The protein plays a main role as the chloride channel and the chloride ions regulator, but it is also involved in regulation and inhibition of sodium transport (epithelial sodium channels), regulation of ATP channels and regulation of vesicle transport in the cells. The CFTR protein also plays a role in acidification of intracellular organelles[9-14].

There are more than 1 800 different mutations of CFTR gene[15], but in about 70% of the CF cases the mutation is a deletion of three-pairs of nucleotides at position 508 (ΔF508) [16]. These three-pairs are coding for phenylalanine[17, 18] and the lack of this amino acid residue results in improper folding of the CFTR protein and its quick ubiquitination and degradation[14]. Different CFTR gene mutations have been gathered and classified according to its effects by Welsh and Smith[19].

4.2.2 Diagnosis of cystic fibrosis

The final effect of most of the mutations is impaired transport of the chloride ions by the CFTR protein. Therefore diagnosis of CF is usually made clinically by measuring of the chloride ions concentration in sweat.

Sweat produced by glands in the dermis contains chloride ions in concentration of approx. 105 mM and is equal to the concentration of chloride in serum. Sweat is transported from the gland to the surface through dermal ducts, where the chloride should be absorbed by the epithelial cells in

[1] The membrane lining bodily cavities containing cells that secrete mucus

a CFTR-dependent manner (Figure 2). In healthy individuals the chloride concentration in secreted sweat is below 40 mM [20].

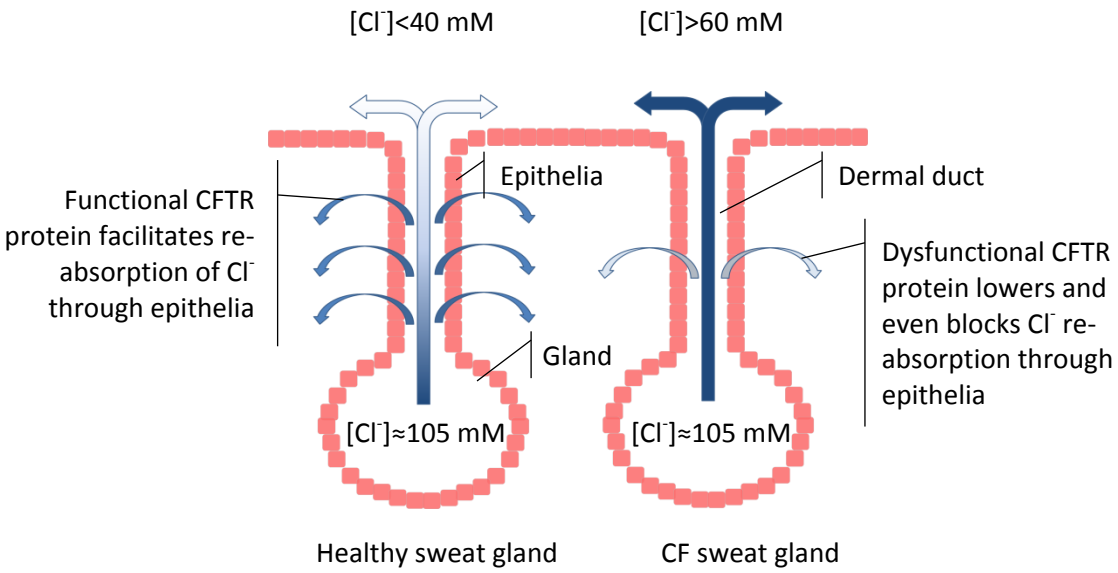

Figure 2. Scheme of the healthy and cystic fibrosis sweat gland[20].

A chloride concentration in the sweat above 60 mM, determined at least twice or more by quantitative pilocarpine ionophoresis, indicate CF[21]. The need for more than one measurement at different occasions arises from the risk of false-positive test results. The temporary increase in the chloride concentration in sweat can sometimes occur in the healthy person, especially for older adults[20, 22].

False-negative sweat test results can occur for patients with CF. There are some CFTR mutations (patients homozygous for ΔF508 with additional R553Q mutation in one of the alleles) that masks improper chloride channel function[23]. False-negative sweat test results can also occur in malnourished patients with pulmonary oedema[24]. Therefore, positive sweat test result should be followed by genetic screening. Even the genetic screening, due to the numerous possible mutations in CFTR gene, is not always 100% conclusive[20].

4.3 The dysfunction of the salt transport in CF epithelia

The dysfunction of the CFTR protein in conductance and regulation of the chloride transport, exemplified for sweat glands (Figure 2), hinder secretion of the fluids by pulmonary epithelial cells. This leads to changes in the mucus physical and chemical properties and impairment of the

mucociliary clearance mechanism in the airways[25]. There are several theories that try to explain this impairment, but two of them seem to be most probable, referred to in literature as 'high salt' and 'low salt' theories[26]. The 'high salt´ theory assumes that the mucus in CF patients has elevated sodium chloride concentration. This phenomenon is explained in the same way as in the case of the high chloride concentration in sweat, i.e. a high mucus osmolality deactivates the antimicrobial peptides secreted by the epithelia, called defensins. This allows bacteria to successfully colonise the airways[27, 28].

The 'low salts theory' also refers to CFTR proteins, which is involved in control of the sodium and chloride ions transport mechanism in airway epithelial cells. In healthy epithelia, CFTR allows the cell to reabsorb sodium and secrete chloride ions. A high salt concentration in the mucus, osmotically drives the water out from the epithelia and rehydrates the mucus (Figure 3). In CF patients, the CFTR protein, acting as a chloride channel, is dysfunctional, and thus hinders the salt transport. This leads to high salt concentration in the epithelia and low concentration in the mucus, which stops water from rehydrating it[26]. Most of the recent publications assume the 'low salt' theory and dehydration of the mucus.

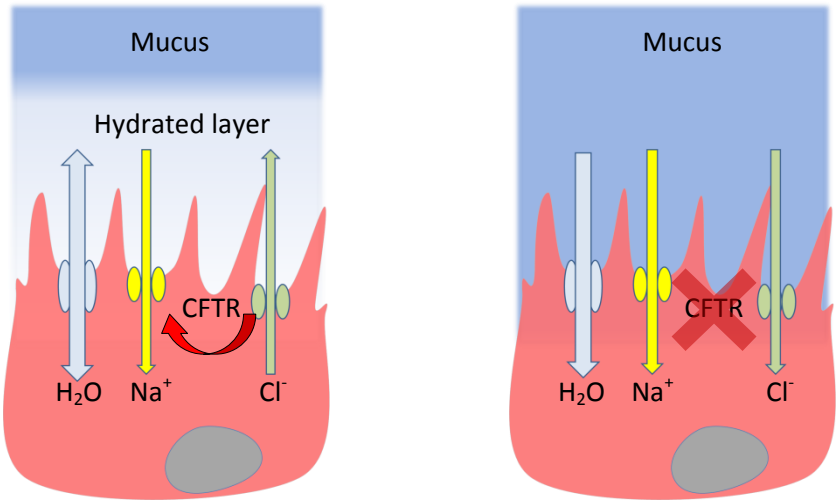

Figure 3. Hydration control and salt transport mechanism in airway epithelial cell in healthy individuals and CF patients (adopted from [26]).

4.4 Mucociliary clearance mechanism in healthy individuals and CF patients

The epithelia of the airways is covered by a layer of airway surface liquid (ASL). This liquid, in healthy individual airways, can be further divided into two layers according to the viscosity. The lower layer, with low viscosity, embeds the cilia growing out the ciliated epithelial cells. It contains mainly water and salts and is about 7 µm thick[29]. This layer is referred to in literature as perciliary liquid (PCL). The top layer is more viscous and contains, besides water (approx. 98%), salts (approx. 1%) and mucin (approx. 1%)[30]. Mucin is a glycosylated protein secreted in the upper respiratory tract and lungs by goblet cells and by Clara cells in the terminal bronchioles[31].

These two layers protect the lower respiratory tract from infections. In the healthy person, the lower respiratory tract is basically sterile while the upper tract is not, which therefore can be a source of infecting germs to the lower tract. The sterility of the lower respiratory tract is maintained by the fact that the invading germs adhere to the top viscous mucus layer. This layer is then transported up the respiratory tract and is removed either by coughing it out or swallowing. The transport of the viscous layer is possible only if the lubricating PCL between the top layer and epithelium has low viscosity, implying proper hydration. This transport is facilitated by small cilia where each cilium performs a slow movement actuating the flow of the mucus. The linear velocity of the mucus is in order of tens of micrometres per second[30]. Therefore, in a healthy person´s airways the mucus layer is constantly cleared and renewed by the mucociliary system (Figure 4)[32, 33].

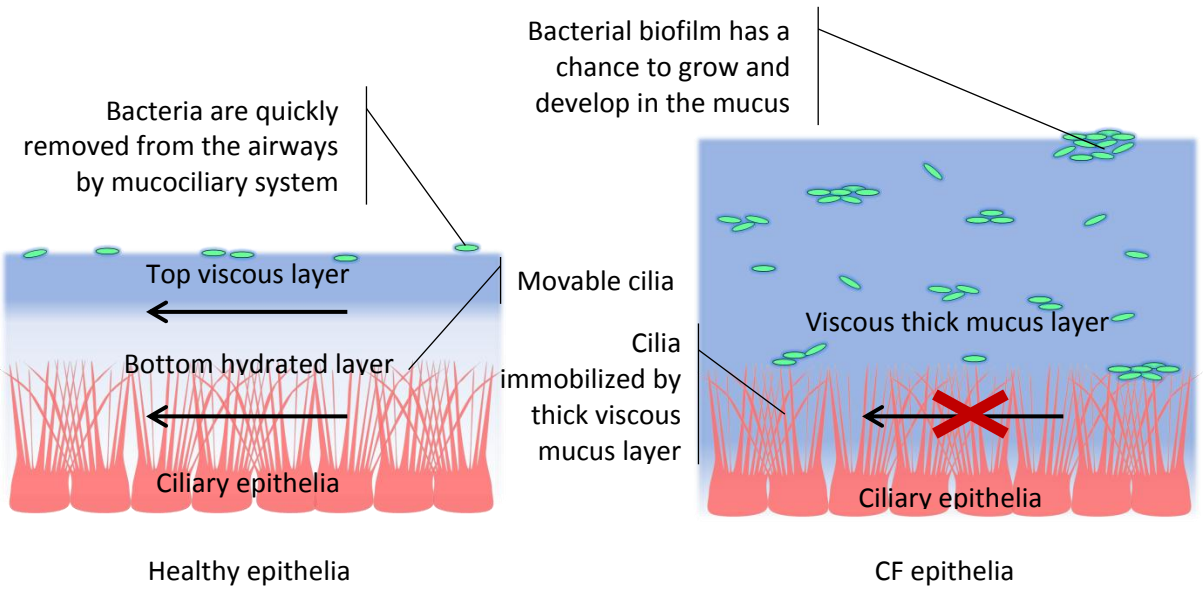

Figure 4. The mucociliary clearance mechanism in healthy individuals and CF patients (adopted from [26] and [29]).

4.5 Difference between infection clearance systems in conductive and respiratory zones

The mucociliary clearance mechanism is responsible for keeping the conductive zone of the human airways sterile. However, the respiratory zone lacks cilia and submucosal glands and the defence system against pathogens works in a different manner than the conductive zone. In order to facilitate gas exchange, the barrier between blood and air is very thin in the alveoli. Therefore, the immune system has a direct access to the surface of the epithelia in the respiratory zone and can efficiently eradicate most of the infections[34].

This difference between the conductive and respiratory zones also affects the treatment of an infection. The antibiotics administered intravenously or orally have better effects on treating the infections in the respiratory zone while being much less effective on the pathogens residing in conductive zone[35]. On the other hand, the nebulization of antibiotics allows to affect pathogens in the conductive zone in a much more efficient way than in the respiratory zone[36-38].

4.6 Infections associated with cystic fibrosis

Due to the impairment of the mucociliary clearance mechanism, CF patients are afflicted with frequent airways infections. The source of the infections is the upper respiratory tract. In healthy airways, the sterility of the lower respiratory tract is maintained by the fact that the invading germs adhere to the thin mucus layer, which is constantly cleared and renewed by the mucociliary system[32]. The mucus in the CF patients airways is very thick and viscous and the patient cannot clear the tracts[30].

The most common bacteria that colonise the airways of CF infants are *Haemophilus influenzae* and *Staphylococcus aureus[8]*. The simultaneous infection with both of these pathogens is not uncommon. In older patients (3 years old or more) *Pseudomonas aeruginosa* becomes the predominant pathogen[39-41]. Approximately 70% to 80% of CF patients are infected with this bacteria before reaching adolescence. This can be a result of the fact that *P. aeruginosa* is a common bacteria in the environment[42], which is spotted as an opportunistic bacteria in humans. Up to 20% of CF patients have their gastrointestinal tracts infected with *P. aeruginosa*[43]. This bacteria is also responsible for recurrent infections[44].

4.7 Biofilm formation of *P. aeruginosa* in CF lungs

Biofilms are communities of bacteria living in a complex extracellular matrix where cells are attached to each other or to a surface. This matrix consist mainly (approx. 75-89% of the composition) of proteins, exopolysaccharides[45] and additionally nucleic acids, lipids and phospholipids[46, 47]. Bacterial biofilms are very common in all kinds of environments including the human body[48], where the most commonly known is dental plaque[49].

The formation of a biofilm is probably due to the response against unfavourable conditions[50]. The first step of the biofilm formation is an initial attachment of a previously planktonic cell[2] (Figure 5 A) to the surface. If the cell does not leave the surface nor is cleared from it, the cell becomes irreversibly attached (Figure 5 B). The next generations of the cell stay on the surface. Bacteria will start to secrete the matrix, making the surface even more attractive to the following cells and the biofilm will grow and mature (Figure 5 C and D). If the conditions for the growth will aggravate, the biofilm will start to dissolve and the cells become planktonic once again in order to find a spot with more suitable conditions (Figure 5 E)[51].

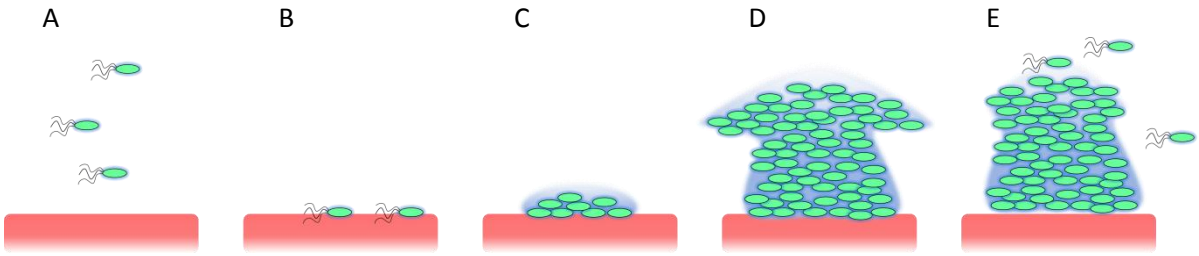

Figure 5. Biofilm formation and dissolution: (A) bacteria in the planktonic state, (B) attachment to the surface (C) biofilm growth, (D) mature biofilm, and (E) dissolution of the biofilm.

P. aeruginosa, as well as number of other bacterial and fungal species, can form biofilms. *P. aeruginosa* biofilms were found in the sputum[52, 53], freshly excised lung sections[50, 54] as well as in the *post mortem* explanted CF lungs[55]. However there is no consensus if the main form of *P. aeruginosa* exists in CF lungs as a biofilm[40].

[2] Cell which can float or swim in the aqueous media

4.8 Antibiotic resistance and tolerance of CF infections

Bacterial airway infections in patients with a normal mucosa are relatively easy to treat with antibiotics. This is unfortunately not the case for CF patients and the myriad of infections they acquire during their lifetime leave each patient with a high need for recurrent antibiotic treatments. This is a multifactorial phenomenon and a lot of theories that try to explain it have recently been published[56-59].

4.8.1 Antibiotic resistance and antibiotic tolerance

Antibiotic resistance needs to be distinguished from antibiotic tolerance. Antibiotic tolerance, unlike resistance, is not heritable by the tolerant cell progeny. It is rather connected to its decreased metabolic activity or the surrounding of the cells. Tolerant cells can still be non-resistant to antibiotic when its metabolic activity increases or its surrounding will change (Figure 6)[60].

Bacterial biofilms are much more tolerant to antibiotic treatment than planktonic cells. The minimum inhibitory concentration (MIC) and minimal bactericidal concentration (MBC) for the bacterial biofilms, especially for one cultivated for long time, can be 1000 times higher than for the planktonic form or the newly formed biofilm of the same species[50].

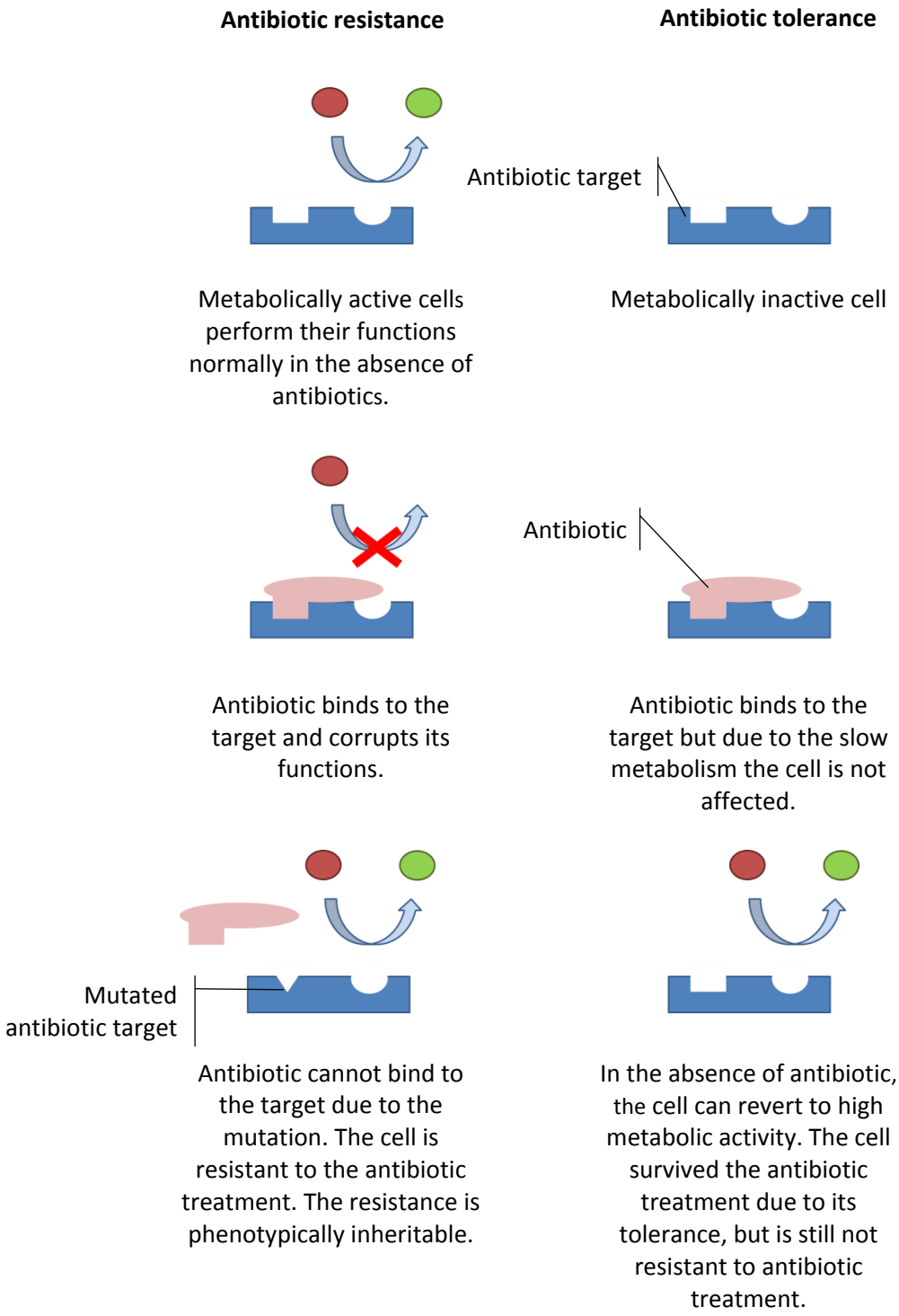

Figure 6. Antibiotic resistance and antibiotic tolerance.

4.8.2 Antibiotic diffusion through bacterial biofilm

The most obvious reason for a treatment failure in the CF airways is the hindered diffusion of the antimicrobial agent through the thick and viscous mucus layer. The transport is even more

obstructed if the agent needs to diffuse through the biofilm matrix[61, 62]. However, according to recent findings, the main reason may reside in limited oxygen availability in some parts of the airways[57, 63]. These highly different oxygen environments are due to the human physiology of the airways and furthermore endured by the oxygen consumption of epithelial and immune cells in the local surroundings.

4.8.3 Influence of oxygen tension on bacterial metabolism

As *P. aeruginosa* infections are almost inescapable in CF patients, especially in older patients, this makes *P. aeruginosa* an important organism for studies of "oxygen" phenomena[40].

P. aeruginosa is a facultative anaerobic bacteria[64] with reduced growth rate (paper IV) and metabolic activity[57] at low oxygen levels. Antibiotics such as tobramycin, ciprofloxacin, and tetracycline preferentially kill the physiologically active bacteria living at high oxygen levels (aerobic environment), while colistin is more effective on the physiologically inactive bacteria growing in anaerobic environment[65-67].

In the densely packed biofilm, the cells living at the biofilm surface have considerably different nutrients and oxygen accessibility than the cells inside the biofilm[57]. This affects the metabolism and growth of cells. The metabolically active and fast dividing cells at the biofilm surface are more susceptible for exposure to tobramycin, ciprofloxacin and tetracycline, while the cells inside the biofilm remain mostly unaffected. This renders the standard antibiotic monotherapy not suitable for biofilm infections. The mixture of at least two antibiotics that can target cells of different metabolic activity, e.g. colistin and ciprofloxacin, is usually needed to treat the infections in CF patients[68, 69].

4.8.4 Persister cells

Irrespectively of the environmental reasons, some bacterial cells are growing very slowly or even at some point cease to divide. This usually very small fraction of cells are called persisters[70-72] and are considered as dormant cells. Since the metabolism of these dormant cells is very slow the antibiotics that kill the metabolically active cells will not be able to clear the former. However, even some of the antibiotics that affects slow-dividing cells will not be effective for clearing the persister cells[73].

The exact way that leads a cell to its dormant state is not yet fully understood, but it seems to be connected with the toxin/antitoxin system present in most bacteria[74] [75-77]. This mechanism may

be connected with different functions of the bacterial cells, e.g. reaction to stress, maintenance of plasmids, programmed cell death and even biofilm formation[78-81].

4.8.5 *P. aeruginosa* biofilm resistance to antibiotics

The use of beta-lactams, from which penicillin was the first commonly used antibiotic, has a long history. The long time exposure and common overuse of antibiotics in general has allowed bacteria to develop specific resistance against them over time. The aggressive antibiotic treatment of CF infections has for instance allowed *P. aeruginosa* to quickly develop very efficient expression of the beta-lactam degrading enzyme beta-lactamase[82]. Moreover, the biofilm forming *P. aeruginosa* can secrete this enzyme into the intracellular matrix, making the antibiotics unable to reach the cells embedded into the matrix[83]. The use of beta-lactamase inhibitors[84] or beta-lactamase-stable antibiotics like meropenem[84] seems to be necessary for treatment of CF related infections with *P. aeruginosa*.

Some strains of biofilm forming *P. aeruginosa* have developed a specific antibiotic resistance mechanism, which is less active in planktonic cells, the so-called efflux pump[58]. The efflux pump can actively remove aminoglycosides such as tobramycin, gentamycin as well as ciproflaxin[85].

Another mechanism for *P. aeruginosa* resistance to tombramycin is the production of perismatic glucans which can bind this antibiotic[86]. Tobramycin, in order to be effective, needs to enter the cytoplasm and to bind to the 30S and 50S subunit of the bacterial ribosome. If most of the antibiotic is bound in the periplasm, much larger doses are needed in order to reach the cytoplasm and overcome this resistance mechanism.

4.8.6 The mucoid and non-mucoid phenotypes of *P. aeruginosa* in chronic infections of CF patience

The wild type strain of *P. aeruginosa* is a non-mucoid and is relatively easily treatable with antibiotics[87]. However, if the infection by this pathogen is not completely eradicated, the wild type non-mucoid strain can mutate into the mucoid strain. The mucus secreted by this strain contains very viscous alginate. The mucoid phenotype of *P. aeruginosa* is very hard and in some cases even impossible to treat with antibiotics and the patients can become chronically infected[88-90].

Recent findings[91] give hope for the treatment of mucoid *P. aeruginosa* strain with a mixture of nebulized colistin and gentamicin applied twice daily in a long-term manner. However, even this

harsh treatment allowed clearance of only 58% of the CF patients infected with the mucoid *P. aeruginosa* strain.

4.9 Airways damages caused by recurring infections in CF airways

As was described above, the mucociliary clearance mechanism physically removes pathogens from the conductive zone of the human airways and keeps and protects it from infections. The impairment of this system in CF patients leads to frequent and persistent infections, which escalates the response of the immune system and inflammatory defence mechanisms. These involve increased activity of the polymorphonuclear neutrophils[3] (PMN), which secrete reactive oxygen species (ROS)[92, 93]. This defence mechanism works well in compartments where the mucus is not present, e.g. in the alveolar sacks, however is not very effective in the conductive zone of the CF airways, which is covered with very viscous mucus. The concentration of ROS is high at the epithelia and brings damage to the tissues, but is not high enough in the mucus to kill the bacteria[34]. This effect of the immune system activity is responsible for inducing a mutation in the *P. aeruginosa mucA* gene, which leads to the transformation of the non-mucoid strain into the mucoid one. This mutagenic effect is likely due to the increased ROS concentration in the environment of the CF airways[94]. The alginate present in the biofilm of the mucoid phenotype protects the bacteria embedded in the extracellular matrix from the ROS[95]. Therefore, the mucoid phenotype of *P. aeruginosa* is not only tolerant for antibiotic treatment, but can also resist the immune system. Hence, the mucoid phenotype of *P. aeruginosa* which was not removed by the mucociliary clearance mechanism nor by the immune system response in the conductive airways, can now colonise the respiratory zone.

Recent findings show that the biofilm forming *P. aeruginosa* can protect themselves not only from ROS and antibiotics but also from other defence mechanisms, e.g. from phagocytosis[65]. The PMNs cannot reach the bacteria not only because of the physical barrier of extracellular matrix, but also because they are actively lysed (Figure 7). The factors that induce PMNs necrosis were identified as rhamnolipids, secreted by certain strains of *P. aeruginosa*[96].

[3] A type of white blood cells

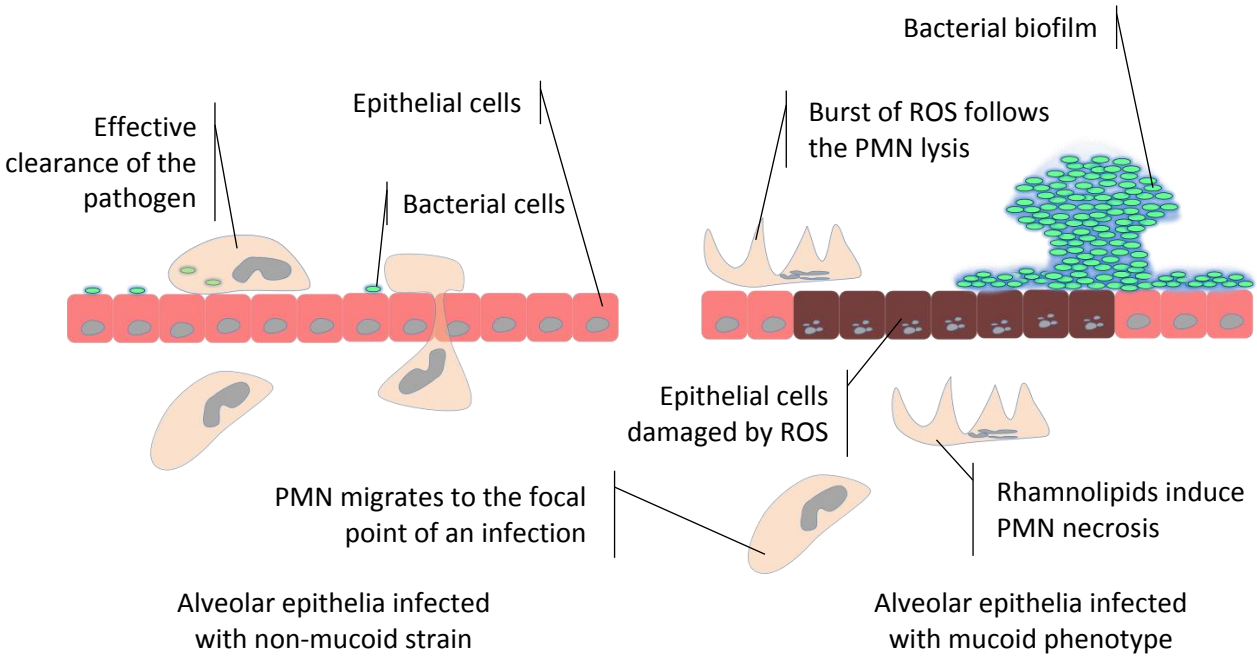

Figure 7. The damage in alveolar epithelia caused by the PMNs lysis induced by rhamnolipid expressing *P. aeruginosa* strains.

The secretion of these rhamnolipids has been connected to a quorum sensing (QS) mechanism, which allows bacterial cells to communicate[97]. The high concentration of the QS molecules gives a signal to the cells about their number, which controls the expression of virulence factors such as proteases, pigments, hemolysins and exotoxins[98].

In conclusion, the lysis of PMNs, further secretion of ROS, together with virulence factors lead to the escalation of the inflammatory mechanism and further damage to the tissues and impairment of the respiratory functions[99]. In the healthy person pulmonary function decline with the rate of approx. 1-2% per year[100], while this rate in CF patients is about 4 – 10%[101]. Considering the fact, that bacterial infections of CF patients are recurrent and very hard to treat, the damages to the tissues are eventually fatal.

4.10 *In vivo* models of the lung infections in CF patients

Animal models have proven to be useful in the study of different diseases, their mechanisms and possible treatment therapies. The recent advances in genetic manipulations, e.g. specific gene knock-outs or transgenic animals, have brought new tools for medical research[102]. A number of different animals have been tried as models for chronic infections in CF patients[103]. This includes rats[104-

106], guinea pigs[107], cats[108] and rhesus monkeys[109, 110]. However the most important animal model is today a mouse[111-114].

The main challenge in using the animal models that are not genetically modified has been to overcome their very effective mucociliary clearance mechanism. This was done by introduction of bacteria artificially embedded in gel matrix such as agar[111], alginate[104] or gastric mucin[115] or by suppressing their immune system[103]. However, the effects of these operations were usually not satisfying. The animals were either quickly clearing the infection or dying[116].

Mice with a CFTR gene knock-out[117] and, more recently, transgenic mice with differently mutated human CFTR[118] has brought a new quality to the research on CF related infections. However, the main challenge here is a very high fatality among the animals with a dysfunctional CFTR gene. The very low survival rate, which even can be below 5%, is mainly due to intestinal problems and not due to the respiratory failure[119]. Besides, the animal models of CF related infections are still not ideal, mainly because of the immune response differences of man and e.g. mouse, but also because the lung pathology after infection is very different in animals compared to humans[103]. The other disadvantage are the relatively high costs and growing concerns about ethical aspect of using animal models in research[120].

4.11 *In vitro* models of the lung infections in CF patients

The most commonly used and standardized devices for studying initiation and growth of bacterial biofilms are microtitre plates. They are especially useful for high-throughput screening of attachment of the bacteria to different substrates and initial response of the biofilms for chemotherapy[121, 122]. It is however very difficult to use these plates for long time observation of biofilms, even when one can use robots for automated culture media change.

So far, the most successful *in vitro* models for studying biofilm formation are different kinds of flow cell systems. These systems allow to observe the attachment of bacteria, biofilm formation and dissolution of the biofilm while nutrients and metabolites are constantly flowing into and out of the system[123].

The typical flow cell system is comprised of a culture media container, a multichannel pump, a flow cell and a waste container. During the constant flow of culture media, air bubbles can gather in the flow chambers and disrupt the biofilm. Therefore the flow cell systems are usually equipped with bubble traps (Figure 8)[124].

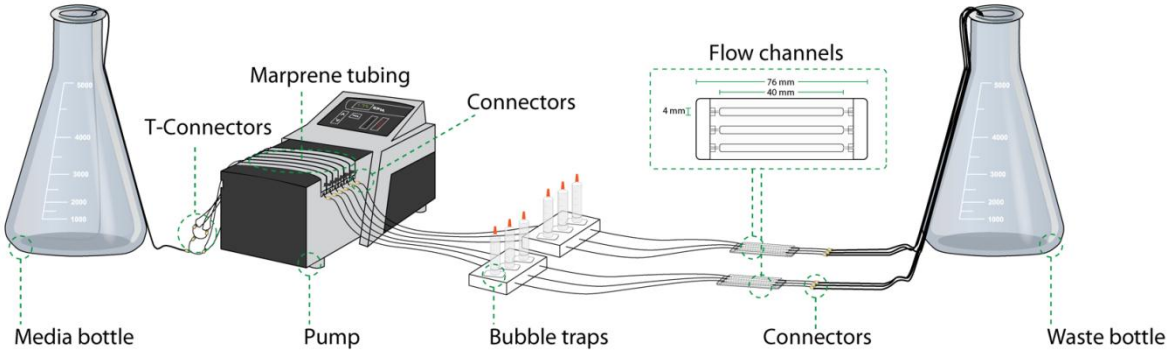

Figure 8. A flow cell system setup (reprinted with permission from[124]).

The flow cell systems allow to studying biofilms for an extended period of time, which is usually not feasible with biofilm formed in a microtitre well plate or in other standard culture vessels like tubes and petri dishes. Together with confocal laser scanning microscopy and specialized software for biofilm analysis like COMSTAT, the flow cell systems are powerful tools in studying bacterial biofilms[125]. These systems have successfully been used for determining spatial distribution of bacteria sensitive for different antibiotics[67, 126-128] as well as for the studying the distribution of motile and non-motile strains of *P. aeruginosa*[129]. The disadvantage of these systems is the quite complicated and time consuming assembly and lack of high-throughput capabilities in comparison to microtitre well plates[123, 124].

4.12 Summary

In most cases, CF patients suffer from infections caused by *P. aeruginosa*. This species can live in aerobic as well as in anaerobic conditions. These different conditions together with the mutagenic habitats caused by immunological response of the host make the bacteria highly changeable and adaptive to the environment. Together with its ability to form a biofilm, *P. aeruginosa* is extremely hard to eradicate from CF patients airways.

An antibiotic treatment can eventually seem successful, yet after a few months the very same bacteria which were responsible for the infection can reappear, possibly as a result of reinoculation from the anaerobic sinus[63, 130]. In this context the sinuses could very well serve as a reservoir for 'sinus' bacteria, which are difficult to treat with antibiotics and can cause the reinfection of otherwise cleared patients. *P. aeruginosa* infections will eventually become chronic and the pulmonary function will start to quickly deteriorate leading finally to the patient's death.

Therefore it seems to be crucial to better understand the differences in the metabolism, adaptation and genetic variability of bacteria living in the airways compartments with different oxygen tension. It is also very important to be able to mimic and observe the different environments of the human airways, the effect of infection treatment and the interaction between bacteria and tissues at the cellular scale. Thus, the microfluidic systems seems to be particularly useful to perform such studies.

5 Microfluidic devices as models of human organs

The use of animal models for studying different diseases and research on new pharmaceutics seems to be inescapable at present time[131]. However, there is a very strong pressure from public society, particular states and international organizations legislature, as well as from industry to replace, reduce and refine the research conducted with the use of animals[132, 133]. This strategy is known as the "3 Rs" principle[134, 135].

The development in cell culture as models of tissues and entire organs allowed to partially fulfil these expectations[136]. The main limitation of these substitutes is the lack of complexity of specific interactions between different tissues and organs in living organisms[137]. The recent advancement in tissue cultures, especially using microfluidic devices, give hope for overcoming some of these limitations[138-141].

The advancement in the micro- and nanofabrication and assembly as well as better understanding of microfluidics have allowed to develop devices for modelling different tissue organs. Thanks to these devices the control over the environment, relations and interactions between the cells and tissues at microscale and with high special and temporal resolution can be achieved[142, 143]. The yet small but fast growing number of the microdevices that can reassemble different and even entire organs have been reported. This includes blood vessels[144], bones[145], muscles[146], liver[147-150], brain[151], guts[152], kidneys[153, 154], endothelia[155] and blood-brain barrier[156].

In the field of mimicking the human airways, Huh *at al.*[157, 158] proposed a microfluidic device that can simulate injuries to the airways epithelia done by liquid plug flow. The same group proposed recently a model of the vacuoles in the lung[159]. In this work the phagocytosis of planktonic *Escherichia coli* cells by neutrophils on the epithelial surface was shown.

The silicon microfluidic device capable of exchanging gases form the blood stream has been recently shown by Hoganson et al.[160] This microfluidic device may be considered as a first step in developing a system for assisting patients with respiratory failure.

According to the author's best knowledge the microfluidic model of CF bronchi nor the model of different compartments of human airways, which would allow the observation of the influence of the microenvironment of these compartments on the development and clearance of bacterial infection, has not been reported previously.

Therefore, a model system that simulates the three compartments of the human airways is postulated (paper III and IV). The three sections of the human airways: the conductive airways (trachea, bronchi and bronchioles), which are considered micro-aerobic, the highly aerobic gaseous exchange compartments (the alveoli) and the compartments of the paranasal sinuses, which are basically anaerobic (Figure 9A), are reproduced in this Microfluidic Airways Model (MAM). It is realized by cell culture microchambers with different oxygen levels (Figure 9B). The microchamber with atmospheric air oxygenated media (aerobic environment) is connected by an additional channel to the microchamber with culture media, saturated below the atmospheric air saturation level (micro-aerobic environment). This chamber is consecutively connected to the chamber with deoxygenated media (anaerobic environment). The connections between the chambers as well as to the outlets can be closed and opened, and the actual oxygen level can be determined by using an oxygen probe.

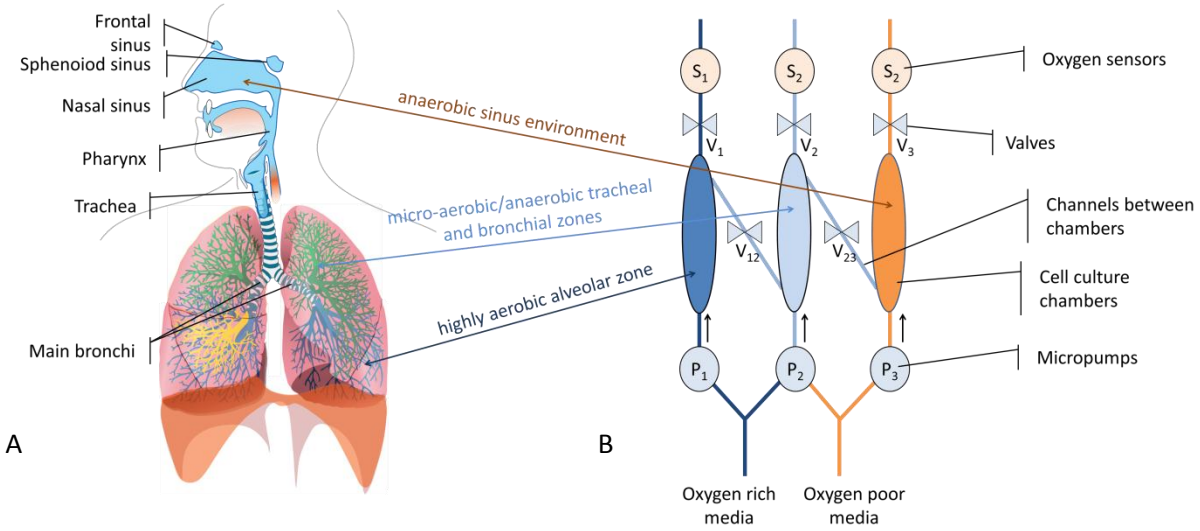

Figure 9. (A) Human airways system, (B) Microfluidic Airways Model (MAM).

The impairment of mucociliary clearance in CF bronchi seems to play very important role in developing chronic infections and reinoculation of the bacteria in the alveoli. Therefore a model of CF bronchi, was also proposed (paper VI and VII).

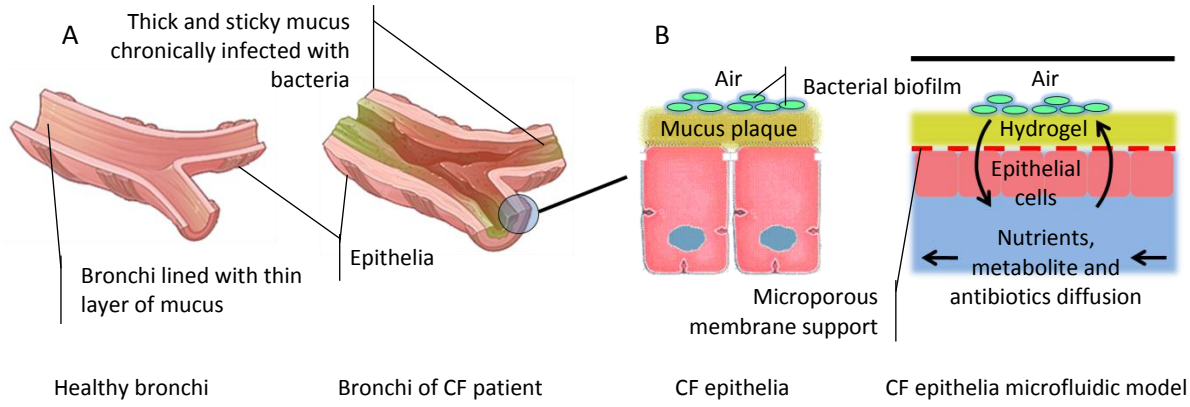

Figure 10. (A) Bronchi of the healthy individual and CF patient. (B) The microfluidic model of CF epithelia.

The microfluidic model of the CF bronchi consists of two microchannels separated by a microporous membrane (Figure 10). The membrane is a support for a hydrogel, which mimics the mucus layer in CF bronchi. The hydrogel can, in a similar way as in the mucus layer, be enriched with different components like DNA and proteins. The microchannel below the membrane simulates the artery, which supplies the nutrient containing media and transport of metabolites. These compounds are further supplied to the top channel by diffusion through the membrane and hydrogel. On the top part of the hydrogel the bacterial cells can be inoculated and cultured while at the bottom side of the membrane, epithelial cells are cultured. The top microchannel is enclosed with a cover slide, which allows observation and analysis of the biofilm growth by confocal microscopy.

6 Oxygen sensing and control in microfluidic biodevices

6.1 Oxygen permeability of different materials used for microfabrication of biochips

One of the most commonly used material for fabrication of microdevices used for biology is poly(dimethylsiloxane) (PDMS)[161-163]. PDMS is a chemically inert, biocompatible and optically transparent polymer[164] that is very commonly used for construction of microdevices[165, 166]. The most useful technique for microfabrication in PDMS is casting the not yet cross-slinked polymer against a mould.

These properties make PDMS a popular material for fast prototyping of microdevices particularly for cell culture purposes. Furthermore it can be utilised as a component in an active scheme of oxygen removal due to its high permeability for gases and vapours.

This high permeability of PDMS can in some cases be considered as a flaw, especially in applications where very small volumetric flows of aqueous media are involved. The high permeability to vapour means that the media can evaporate through the PDMS. This effect is particularly problematic in microdevices, where the surface to volume ratio is very high[167]. Other disadvantages of PDMS is the unspecific absorption of hydrophobic molecules[168]. This is due to the very high hydrophobicity of the material itself, connected with high solubility of hydrophobic species in loose PDMS chain networks. Moreover, the uncured short PDMS oligomers as well as the platinum based curing catalyst can leak out from the bulk of material[169, 170]. The high hydrophobicity also implies nonspecific adsorption of proteins to the PDMS surface[171].

The polymer of choice, when low gas permeability is required, would be poly(ether ether ketone) (PEEK). This material has very low oxygen permeability along with very high chemical and mechanical resistance[172], as well as exhibiting excellent biocompatibility[173, 174]. However the high price, challenging bonding, and lack of transparency makes it difficult to extensively use this polymer for constructing microdevices[175, 176]. Therefore the other thermoplastic polymers such as polystyrene (PS)[177], cyclic olefin copolymer (COC)[178], poly(methyl methacrylate) (PMMA)[179-181] (papers I-IV), polycarbonate (PC)[182] (papers V-VII) are more common in microdevice fabrication. These materials have a slightly higher oxygen permeability, but they are transparent and much easier for processing than PEEK. The use of thermoplastic polymers together with fabrication

techniques such as injection moulding allows to produce microdevices for industrial scale[178] (paper I). Table 1 contains oxygen permeabilities of different polymers calculated in commonly used units (the data was gathered from different sources including different vendor´s datasheets).

Table 1. Oxygen permeability of different polymers: PDMS - poly(dimethylsiloxane), FEP - fluorinated ethylene propylene, COC - cyclic olefin copolymer, PC – polycarbonate, PMMA - poly(methyl methacrylate), ETFE - poly(ethylene-co-tetrafluoroethylene), PEEK - poly(ether ether ketone).

Polymer	Oxygen permeability			
	Barrer	$cm^3 \cdot mil \cdot 100inch^{-2} \cdot 24h^{-1} \cdot atm^{-1}$	$cm^3 \cdot mm \cdot m^{-2} \cdot 24h^{-1} \cdot atm^{-1}$	$m^3 \cdot m \cdot m^{-2} \cdot s^{-1} \cdot Pa^{-1}$
PDMS	800.0	133 333	2 067 183	$6.00 \cdot 10^{-15}$
VITON®	14.0	2 333	36 176	$1.05 \cdot 10^{-16}$
FEP	4.5	748	11 600	$3.37 \cdot 10^{-17}$
COC	2.6	428	6 641	$1.93 \cdot 10^{-17}$
PC	1.8	302	4 677	$1.36 \cdot 10^{-17}$
PMMA	1.4	225	3 488	$1.01 \cdot 10^{-17}$
ETFE	0.6	100	1 550	$4.50 \cdot 10^{-18}$
PEEK	0.1	20	309	$8.97 \cdot 10^{-19}$

6.2 Control of dissolved oxygen concentration in microdevices

The first step to control the dissolved oxygen concentration in perfusion based cell culture chips is the choice of right construction material. However, in order to be able to steer the concentration, active removal or supply of oxygen is required.

The direct oxygen generation by electrolysis of water molecules has been proposed by Park at al[183]. This technique requires microelectrode fabrication and potentially can lead to small concentrations of hydrogen peroxide, generated in the same process. A different approach is to exploit the very high diffusivity and solubility of oxygen in PDMS[161-163].

Active removal of dissolved oxygen from a liquid at the macroscale can be achieved in many ways. These include bubbling liquid with nitrogen gas, electrochemical reduction of dissolved oxygen, biological consumption or chemical reaction with an oxygen scavenger[183-186]. At the microscale the first method would lead to extensive drying of the liquid, while the other two complicates the fabrication of the system.

There are a few recently published examples of the use of PDMS based microfluidic chips in which the authors are using nitrogen or nitrogen-oxygen gas mixtures to develop dissolved oxygen gradients[187-189]. The main advantage of such a solution is the possibility of reaching dissolved oxygen concentrations above the air saturation point (9.2 ppm at 293K and 1013.25 hPa)[163]. The main disadvantages are the complexity of the setup and the possibility of slowly drying out the chamber when a low liquid media flow is used.

6.3 Oxygen scavengers

The use of oxygen or other gas containers is difficult in cell culture labs, due to safety reasons and usually very confined space. Therefore, the application of a liquid oxygen scavenger is preferable over systems that rely on such gas containers in order to control the specific oxygen levels. Direct addition of an oxygen scavenging agent such as sulphite or pyrogallol to the cell culture media will alternate its chemical composition, which will have a heavy impact on the cultured organisms[190]. Therefore the technique which allows separating an oxygen scavenging liquid from the cell culture media is preferable. This can be achieved by using a gas permeable PDMS membrane. The control of the oxygen gradient across the cell culture microchamber can be realised by the combination of the diffusive and advective oxygen transport within the microchip (paper III, IV and V).

6.4 Oxygen sensing

It is crucial to be able to monitor the oxygen concentration at the microscale and here the classical amperometric method is not feasible because of the bulkiness of sensors and restriction to only point measurements. The most recent progress in miniaturization of the Clark electrode[191] allows one to build an electrode microarray[192, 193], which would allow monitoring gradients within microfluidic devices in the future. However, most widely used techniques for measurements of oxygen concentrations in microfluidic devices are based on optical methods, which involve photoluminescent dyes or polymer matrices doped with these probes[194, 195]. The basic phenomena responsible for oxygen sensing is dynamic quenching of the luminescence by molecular oxygen[196]. Most of the probes with very high quenching constants are based on either ruthenium complexes, such as tris(bipyridyl)ruthenium(II)[197] and Ru(II)-tris(4,7-diphenyl-1,10-phenanthroline)[198-200] or metalloporphyrins, mainly platinum(II) and palladium(II) octaethylporphyrin (accordingly PtOEP and PdOEP)[201-205] (paper IV) and platinum(II) *meso*-tetra

(pentafluorophenyl) porphyrin (PtTFPP)[202, 206, 207] (paper V). Other probes, like Erythrosin B[208] or pyrene[209], are also reported as suitable for oxygen sensing purposes.

The main advantage of the metalloporphyrin based sensors over complexes of ruthenium based sensors is the much higher sensitivity. This is especially important for sensing not pure oxygen, but atmospheric air saturated cell culture media, where the air saturation scale remains biologically relevant. Metalloporphyrins are non-soluble in water which is the main reason why mettaloporphyrins are usually embedded in polymers or silicone sol-gel matrices[202, 210]. Consequently, ruthenium complexes as water-soluble compounds can be added directly to the culture media[189], which definitely would simplify the task of sensing the dissolved oxygen concentration of the media. Such an addition would however lead to unspecified alterations in the metabolism of the cultured cells[163].

Therefore organically modified silica (ORMOSIL) are widely used as a sensor matrix[202]. The use of ORMOSIL is advantageous over direct dissolution of the sensing molecule in the culture media due to its chemical inertness[211] and the possibility of relatively easy surface modifications[59].

7 Fabrication techniques of polymer microfluidic devices

Initially, microfluidic devices were mainly fabricated in silicon. This was due to the well-known technology of microstructures fabrication developed for the electronic industry[212]. The use of the technologies for microfabrication in silicon brings, however, some major drawback. First of all, the costs of microfabrication in silicon are very high, especially for prototyping and small batch production. This is due to the requirements for using cleanroom facilities, long fabrication processes and expensive materials. Besides, the physical and chemical properties of silicon are not optimal for some applications, especially for microdevices used for cell culturing. Among these properties the minor issues are biocompatibility, lack of optical transparency in the UV and the visible range and chemical incompatibility with e.g. alkaline environment[213-215].

On the other hand, there is a wide range of choice of polymers. Such polymers as polystyrene, polycarbonate, poly(methyl methacrylate), poly(dimethylsiloxane), cyclic olefin copolymer and many others are relatively cheap, optically transparent and are for most biological application relatively biocompatible. The development of different microfabrication techniques for quick prototyping (micromilling, laser ablation, mould casting) as well as for mass production (injection moulding, hot embossing) allow to use polymer based microdevices in a wide range of applications[216-218].

7.1 Micromilling

Milling is a well known abrasive method for fabrication in polymers as well as in metal, alloys, wood and many others. Downscaling of the tools and components brings additional challenges to micromilling machines, micromilling and microdrilling tools. These tools have their diameters usually much below 1 mm. Up to date, the smallest end mills offered on the market have a diameter of 5 µm[219]. One of the important issues are small vibrations and excessive forces applied to the micromilling tools[220]. For the smallest tools it can be challenging to assess their integrity with a naked eye[221, 222].

Although the micromilling technique can be used for fabrication in a wide range of polymers, for some materials it can be challenging to obtain the desired structures without flaws. One of the most important issues is burrs formation[223]. Therefore, milling parameters such as feed rate, spin rate and use of coolant need to be carefully selected as well as the tool path and milling strategies need to be optimised for each material[224, 225]. Another disadvantage of micromilling is the relatively

high roughness of the machined surface. In order to decrease the surface roughness, mechanical or chemical polishing can be performed[226]. This is especially important for optical application of microdevices fabricated by milling.

The micromilling technique can be used for direct structures fabrication (paper I-VI). Due to the undoubted advantage in its flexibility, this technique is particularly useful for quick prototyping. However, for mass production purposes other techniques as injection moulding and hot embossing are usually a better choice. In this case micromilling can be used for fabrication of moulds and stamps[227-229].

7.2 Laser ablation

The other useful technique for fabrication of microstructures is laser ablation. This is a process in which the material is removed from a solid surface by a laser beam[230]. Two types of lasers: excimer laser and CO_2 laser are commonly used. In general, the excimer laser wavelengths are in the UV range (e.g. 196 nm for ArF laser and 248 nm for KrF laser) while the CO_2 laser operates with near infrared radiation (10.6 μm). The advantages of the CO_2 laser over the excimer laser are its cost-effectiveness[231, 232] and high speed of ablation while the main disadvantage is a relatively large beam diameter[233]. The Gaussian shape of the beam brings further constrains to the flexibility of this technique[234].

The CO_2 laser ablation has been shown particularly useful for quick prototyping of microstructures in PMMA[231-234]. Furthermore, it is possible to use this technique for fast and precise cutting of foils and membranes[235-239] (papers III-VII).

7.3 Mould casting

PDMS is one of the most commonly used materials for quick fabrication of microdevices, particularly for applications in life science. The most useful technique for forming the microstructures in this material is by casting the uncured mixture of the polymer, catalyst and curing agent against the mould[166](papers III-VI). In order to crosslink the polymer chains and to form a rubber, a thermal curing follows the casting. The mould is usually fabricated using either micromilling or photolithography techniques[142].

7.4 Bonding of microfluidic chip

Today's wide range of fabrication methods for microfluidic devices allows to reproduce almost any kind of shapes and dimensions in different materials. However, it still might be challenging, in some cases, to perform robust and reliable bonding between different chip layers. This is particularly problematic if one wants to integrate different materials in one functional microfluidic chip.

The microfluidic devices fabricated from thermoplastic materials such as PMMA, PC, COC, PS are relatively easy to bond using either thermal fusion bonding[240-242] or solvent assisted bonding[182, 243, 244].

The general rule for thermal fusion bonding of thermoplastics is to heat up the material near or above its glass transition temperature (T_g) and apply a pressure in order to increase the surface of contact[245]. It is possible to use this technique to bond different thermoplastics as long as the materials have similar T_g. Sometimes, the surfaces of the substrates need to be treated (e.g. with UV[246] or plasma[247]) before bonding. These treatments are used to locally lower the T_g of the materials and to enhance the bonding strength. Careful optimisation of the bonding parameters (temperature and pressure) as well as the possible pre-treatment is always needed.

The other way to bond the thermoplastics is to use solvent assisted bonding. This method can be employed even to bond materials with different T_g as long as the different materials have no tendency to separate from each other and are soluble in the used solvent[245]. Moreover, the exposition of the machined surface to the solvents vapours can reduce its roughness and be used as a polishing step[226]. This was one of the methods applied for bonding the devices described in papers V-VII.

In order to bond materials belonging to different groups like thermoplastics and elastomers (e.g. PC and PDMS) an intermediate adhesive layer is needed. The choice of the adhesive depends on the type of materials to be bonded. One of the easiest ways is to use a pressure activated adhesive transfer tapes[248]. These commercially available tapes can be die cut or laser cut to the desired size and shape. This method has been exploited to bond PDMS to thermoplastic substrates in papers III-V.

8 Publications

8.1 Paper I

Skolimowski, M., Tofteberg, T., Andreassen, E., and Geschke, O., *A novel passive micromixer suitable for mass production in polymers.* The 25th Annual meeting of The Polymer Processing Society, conference proceedings, 2009.

A novel passive micromixer suitable for mass production in polymers

Maciej Skolimowski[1*], Terje Tofteberg[2], Erik Andreassen[2] and Oliver Geschke[1]
[1] Technical University of Denmark, Department of Micro- and Nanotechnology, Produktionstorvet, Building 423/118, DK-2800 Kgs. Lyngby, Denmark
[2] SINTEF Materials and Chemistry, PO-Box 124 Blindern, 0314 Oslo, Norway

[*]maciej.Skolimowski@nanotech.dtu.dk, tel: +45 25 6887, fax: +45 4588 7762

Abstract: This paper presents a novel passive micromixer concept that creates direct lamination in a 2D channel. The principle is to make a controlled 90 degree rotation of the flow cross section followed by a splitting into several channels; the flow in each of these channels is rotated further 90 degrees before recombination. The 90 degree rotation is achieved by patterning the channel bed with ribs. The effect of the mixers has been studied using simulations and prototypes have been made using direct micromachining of polymer. Confocal microscopy has been used to study the mixing. The main advantage with the presented design is that the channels can be made in one part which only has to be sealed by a planar lid e.g. by laser welding or thermal bonding. The geometry and simplicity of this design made it suitable for mass production in various polymers using injection moulding techniques.

Keywords: micromixer, injection molding, polymers, computational fluid dynamics, microfabrication

Introduction: A mixing process, very well know at the macro level, is still a challenge to realise at microscale. This is especially important in mass production of polymeric devices with integrated micromixer units. The micromixers are usually divided into passive and active devices according to the source of energy that is used for mixing (Nguyen and Wu, 2005).
Active mixers, where the external source of energy is needed, are relatively complex and expensive to build. Still, due to very low Reynolds number in the microscale, active mixing by introducing turbulence is by far not as effective as at the macroscale.
What is a main cause of problems in the case of active micromixers is, in contrary, a strong advantage in case of passive micromixers. Small dimensions of the channels enable us to use diffusion as a driving force. Still, to achieve an effective mixing, lamination of the fluid is often employed.
The most straightforward solution is to divide two fluids that are going to be mixed into small streams and then join them alternately. Hinsmann et al. (2001) proposed a 3D structure device based on this idea. The device was fabricated in SU-8 epoxy-polymer with a procedure involving several photolithography and metal deposition steps. Slightly different devices were proposed by Cha et al. (2006). The authors used poly(dimethylsiloxane) (PDMS) as a main construction material. Fabrication by this process involves fabrication of silicon moulds and precise aligning of several PDMS layers.
Other solutions are based on the work of Stroock et al. (2002) where microstructures enable a fluid rotation in channels. Since then several micromixers based on these structures, called staggered herringbones have been proposed. The mixing usually takes place in the relatively long microstructured channels.
In this work the authors propose a novel approach to micromixing based on rotation, splitting and joining fluids in microchannels. The main goal was to develop an effective micromixer that can be easily and not expensively mass produced in polymer e.g. by injection moulding techniques.
Design and fabrication: Figure 1 shows the micromixer design with dimensions. The prototype of the device was fabricated by micromilling (Mini-Mill/3PRO, Minitech Machinery Corp., USA) in poly(methyl methacrylate) (PMMA, Röhm GmbH & Co. KG, Germany) and sealed with a lid using adhesive thin film (ARcare® 91005, Adhesive Research Ireland Ltd.). Alternatively thermal bonding and laser bonding were used. This particular fabrication strategy was chosen due to similarity with mould fabrication for injection moulding techniques. Other successfully tested fabrication processes involve direct laser ablation (48-5S Duo Lase carbon dioxide laser, SYNRAD Inc., USA) in PMMA.
Results: The lamination in one mixing module was investigated using 3D finite volume simulations in ANSYS CFX 11.0. We used a procedure similar to the one recommended by Mendels et al. (2008). The two fluids are treated as isothermal and incompressible Newtonian fluids following the Navier-Stokes equations. Fabricated prototype efficiency was analysed using scanning laser confocal microscopy (Zeiss LSM 510 Meta, Brock og Michelsen A/S, Denmark). Two fluorescent dyes: Fluorescein and Rhodamine B (Sigma-Aldrich Denmark A/S) were used. Figure 2 shows the high degree of conformity between the simulated and measured rotation of the fluids in the microdevice. Almost complete mixing was achieved after 3 modules as shown on Figure 3.

Discussion and conclusions: The presented device was proven to be an effective micromixer, yet relatively simple in fabrication. Moreover, the mixer can easily and efficiently be stacked on a limited surface as shown on Figure 4. The device can be fabricated in one single piece of substrate and does not need any alignment steps which is a substantial advantage over 3D devices known from the literature. Furthermore it can be produced from relatively inexpensive polymers like PMMA or polystyrene.

Results from the tests of the different fabrication strategies show that the microdevice can be produced in mass scale with techniques like injection moulding and laser ablation. This is especially important in applications such as medical diagnostics where cost effective, disposable micromodules are preferably used.

Acknowledgements: The idea for the mixer presented in this work originated at the Summer School *Micro mechanical system design and manufacturing* held at the Technical University of Denmark in summer of 2008. We would like to thank the organizers, especially Arnaud De Grave and all students participating for two instructive, hectic and utmost enjoyable weeks in Lyngby. We would also like to thank the Research Council of Norway and the Technical University of Denmark for funding.

References:

Cha, J.; Kim, J., Ryu, S.-K., Park, J., Jeong, Y., Park, S., et al., *J. Micromech. Microeng.*, **16**, 1778–1782, (2006)

Hinsmann, P.; Frank, J., Svasek, P., Harasek, M., and Lendl, B., *Lab Chip*, **1**, 16–21, (2001)

Mendels, D. A.; Graham, E. M., Magennis, S. W., Jones, A. C. and Mendels, F., *Microfluid. Nanofluid.*, **5**, 603-617, (2008)

Nguyen, N.-T., and Wu, Z., *J. Micromech. Microeng.*, **15**, R1–R16, (2005)

Stroock, A. D.; Dertinger, S. K. W., Ajdari, A., Mezic, I., Stone, H. A., and Whitesides, G. M., *Science*, **295**, 647–651, (2002)

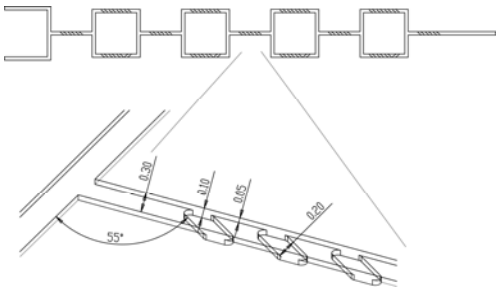

Fig.1: Above: Design showing four mixing modules. Below: Detailed view of the grooves with dimensions indicated [mm].

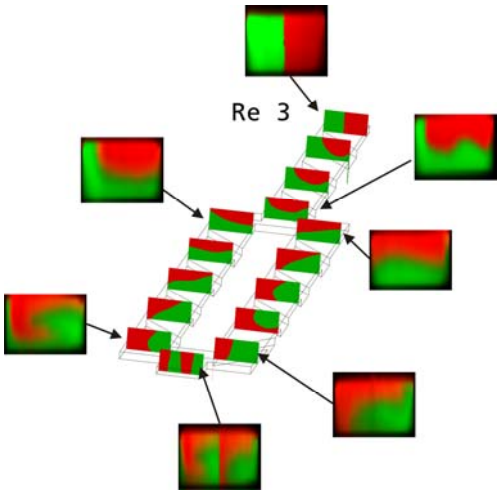

Fig 2: Simulated and measured concentration distributions within one mixing module

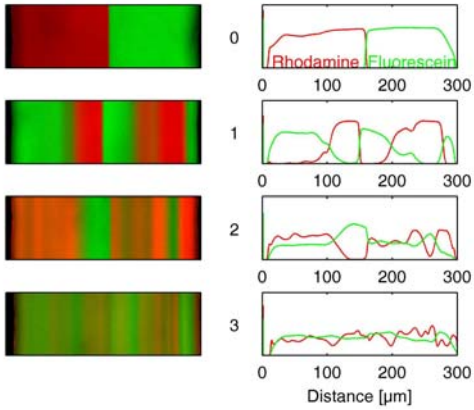

Fig 3: Left: Confocal microscopy images showing planes at z = h/2, where h is the channel depth. The images show the intensity after 0, 1, 2 and 3 full modules. Right: Normalized intensity of the two flourophores measured across the cross sections on the left.

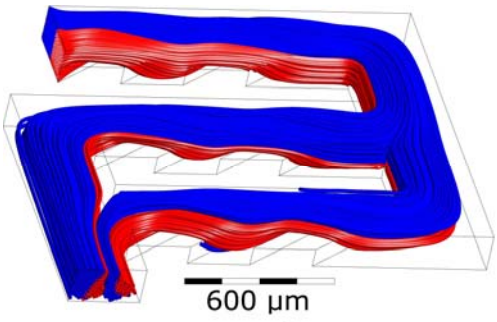

Fig 4: Simulated flow field in one compact mixing module showing lamination

8.2 Paper II

Tofteberg, T**., Skolimowski, M.**, Andreassen, E., and Geschke, O., *A novel passive micromixer: lamination in a planar channel system.* Microfluidics and Nanofluidics, 2010. 8(2): p. 209-215, DOI: 10.1007/s10404-009-0456-z.

Microfluid Nanofluid (2010) 8:209–215
DOI 10.1007/s10404-009-0456-z

RESEARCH PAPER

A novel passive micromixer: lamination in a planar channel system

Terje Tofteberg · Maciej Skolimowski · Erik Andreassen · Oliver Geschke

Received: 10 February 2009 / Accepted: 29 April 2009 / Published online: 26 May 2009

Abstract A novel passive micromixer concept is presented. The working principle is to make a controlled 90° rotation of a flow cross-section followed by a split into several channels; the flow in each of these channels is rotated a further 90° before a recombination doubles the interfacial area between the two fluids. This process is repeated until achieving the desired degree of mixing. The rotation of the flow field is obtained by patterning the channel bed with grooves. The effect of the mixers has been studied using computational fluid mechanics and prototypes have been micromilled in poly(methyl methacrylate). Confocal microscopy has been used to study the mixing. Several micromixers working on the principle of lamination have been reported in recent years. However, they require three-dimensional channel designs which can be complicated to manufacture. The main advantage with the present design is that it is relatively easy to produce using standard microfabrication techniques while at the same time obtaining good lamination between two fluids.

Keywords Passive mixer · Micromixer · Split-and-recombine mixer · Confocal microscopy · Micromilling · Simulations

T. Tofteberg (✉) · E. Andreassen
SINTEF Materials and Chemistry,
PO Box 124, Blindern, 0314 Oslo, Norway
e-mail: terje.tofteberg@sintef.no

M. Skolimowski · O. Geschke
Institute for Micro- and Nanotechnology,
Technical University of Denmark,
Building 423, 2800 Kgs Lyngby, Denmark

1 Introduction

At high Reynolds numbers (typically >2400) two fluids can readily be mixed by turbulence. In microchannels with cross-sections less than one millimeter, this becomes difficult to achieve. For water at room temperature, turbulence in such a channel would require a velocity of several meters per second, which, in most cases, is unfeasible. Mixing of two fluids can still be easily done if the Peclet number is small enough. The Peclet number is defined as the ratio between advection time and diffusion time as $Pe = uL/D$, where u is the characteristic velocity, L the characteristic length and D the characteristic diffusion coefficient. When Pe is small, diffusion is fast compared to advection, meaning that mixing can usually be left to diffusion alone, e.g. as in a T-type mixer (Wong et al. 2004). This will be the case if the channels are either very small or the diffusion coefficient is very large. In the domain where the Reynolds number is small and the Peclet number is large, mixing becomes difficult. In microchannels this typically occurs if the channel dimensions are between 1 and 1,000 μm for species with low diffusivity.

There are several principles already available to achieve mixing in microchannels. Nguyen and Wu (2005) presented an overview of some of the mixers available. The coarsest classification of mixers in their article is between active and passive mixers. Active mixers can, for example, utilize pressure field disturbances (Rife et al. 2000; Niu and Lee 2003) or ultrasonic devices (Yang et al. 2001) to mix fluids. If the fluids are electrolytes, time-dependent electric or magnetic fields (Bau et al. 2001; Glasgow et al. 2004) can be used. It is also demonstrated that moving magnetic beads in a changing magnetic field can efficiently mix fluids (Suzuki and Ho 2002).

In contrast to active mixers, passive mixers are stationary and do not require any external energy input apart from the pressure drop required to drive the flow. In general, this makes passive mixers simpler to fabricate and fewer external connections are needed. In the review by Nguyen and Wu, the passive mixers for microchannels are subdivided into five categories:

(1) Chaotic advection micromixers: the channel shape is used to split, stretch, fold and break the flow. One way of achieving this is to introduce obstructions to the fluid flow in the channel (Bhagat et al. 2007; Lin et al. 2007; Hsieh and Huang 2008). Another is to introduce patterns on the channel walls that rotate the flow field, as in the staggered herringbone mixer (Stroock et al. 2002).
(2) Droplet micromixers: droplets of the fluids are generated and as droplets move an internal flow field is generated within the droplet causing a mixing of fluids. The first such mixer was demonstrated by Hosokawa et al. (1999).
(3) Injection micromixers: a solute flow is splitted into several streams and injected into a solvent flow (Voldman et al. 2000).
(4) Parallel lamination micromixers: the inlet streams of both fluids are splitted into a total of n substreams before combination. For $n = 2$, this is the classic T-type mixer. By increasing n, the diffusion length can be decreased (Bessoth et al. 1999).
(5) Serial lamination micromixers: the fluids are repeatedly splitted and recombined in horizontal and vertical planes to exponentially increase their interfacial area. One well-known example is the Caterpillar mixer (Schönfeld et al. 2004) but other similar designs have also been proposed (Cha et al. 2006; Xia et al. 2006).

In this report we present a lamination mixer that is similar to the serial lamination mixers. However, whereas both the parallel and the serial lamination mixers described in the literature need out of plane channels to split and rejoin the streams, our mixer has all channels in one plane. This means that the mixer can be fabricated by just bonding a planar lid on the top of a structured channel. On the other hand, a three-dimensional channel will need at least two structured parts which have to be aligned precisely in the fabrication process. Thus, the main advantage of the present mixer when compared with active mixers and other lamination mixers is the ease of fabrication. The structures can easily be mass produced using polymer replication techniques such as injection molding or hot embossing.

To the authors knowledge this is the first time a mixer working on the principle of splitting and recombining in such a simple design is presented. In order to achieve the folding, the flows are rotated 90° between each splitting and rejoining. This helical flow pattern is achieved by patterning the channel bed. An illustration of a mixing module of this kind is shown in Fig. 1. In this figure, the simulated streamlines are colored according to their origin.

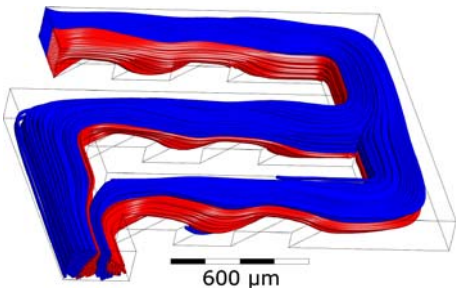

Fig. 1 Simulated flow field in one mixing module showing lamination in the Stokes flow regime ($Re < 5$). The two fluids enter in the *upper left* corner. The interfacial area between the two has approximately tripled at the exit in the *lower left* corner

The present mixer has been realized using several microfabrication techniques.

- Direct laser ablation of channels and grooves in poly(methyl methacrylate) (PMMA).
- Direct micromilling in polycarbonate (PC) and PMMA.
- Milling of the negative structure in aluminum and replication with injection molding in polystyrene (PS).
- Milling of the negative structure in PMMA and replication in polydimethylsiloxane (PDMS).

The results presented in this article relate to mixers milled directly in PMMA. We want to emphasize that the design, because of its open structure and lack of intricate details, can easily be realized using a range of microfabrication techniques.

2 Procedure

2.1 Microfabrication

As a main fabrication method micromilling (Mini-Mill/3PRO, Minitech Machinery Corp., USA) in PMMA (Röhm GmbH & Co. KG, Germany) was used. First, channels with depth of 50 µm and width of 300 µm (equal to the diameter of the tool) were milled. In the bed of the channels 200 µm wide grooves were fabricated using a ∅100 µm milling tool. This tool diameter was chosen to minimize the fillet radius on the corners of the grooves. Cut feed speed was 70 mm/min and spindle rotation was 4,000 RPM.

As an alternative fabrication method, laser ablation (48-5S Duo Lase carbon dioxide laser, SYNRAD Inc., USA) was used. The channels were obtained using a 10 W laser beam (wavelength 10.6 µm) and a focusing lens with

200 mm focal length (beam diameter 290 μm). The ablation velocity was adjusted to 300 mm/min. For ablation of 200 μm grooves, an 80 mm focal length lens was used (beam diameter 90 μm) and the power was reduced to 4 W. Ablated structures had a Gaussian-like cross-section as reported earlier (Klank et al. 2002).

The microdevice was sealed with a lid using a silicone adhesive thin film (ARcare® 91005, Adhesive Research Ireland Ltd.). Thermal bonding and laser bonding methods also gave good results.

2.2 Confocal laser scanning microscopy measurements

To investigate the performance of the designed micromixer two dyes were used: Rhodamine B and Fluorescein. The dyes were dissolved in phosphate buffered saline (pH 7.4) with 0.2% sodium dodecyl sulfate (SDS) (all from Sigma-Aldrich, Denmark A/S). Confocal laser scanning microscopy (Zeiss LSM 510 Meta, Brock og Michelsen A/S, Denmark) was done using a 40× Fluar oil immersion objective. A 488 nm Argon laser was used for exciting Fluorescein and a 543 nm HeNe laser for Rhodamine B. The pinhole was adjusted for approximately 5 μm z axis slice thicknesses. The solutions were pumped through the microdevice by a syringe pump (model 540060, TSE Systems GmbH, Germany) with flow-rate according to the desired Reynolds number.

2.3 Simulations

The mixing efficiency was investigated using 3D finite volume simulations in ANSYS CFX 11.0. The procedure adopted is similar to the one described by Mendels et al. (2008) where the fluids are treated as isothermal and incompressible Newtonian fluids following the Navier–Stokes equations.

$$\nabla \cdot \mathbf{u} = 0 \tag{1}$$

$$\rho\left[\frac{\partial \mathbf{u}}{\partial t} + \mathbf{u} \cdot \nabla \mathbf{u}\right] = -\nabla p + \eta \nabla^2 \mathbf{u} \tag{2}$$

Here $\mathbf{u}$ is the velocity vector, ρ the density, η the viscosity and t the time. To track the location of the interface between the two fluids an additional concentration variable c is transported through the domain by convection and diffusion.

$$\frac{\partial c}{\partial t} + \mathbf{u} \cdot \nabla c = D\nabla^2 c \tag{3}$$

Since the mixer works by lamination, the efficiency of the mixer was best evaluated in the absence of diffusion, therefore the diffusion coefficient, D, was set to 0 in the simulations.

At the inlet, a sharp step in c is prescribed, representing two completely separated fluids. Because of numerical diffusion, it is necessary to have a fine mesh at the interface between the two phases. This interface is not initially known and in order to define a fine mesh here, an adaptive meshing procedure was used. Equations 1–3 were first solved on a relatively coarse mesh. When convergence was obtained, the mesh was refined where the variation in c over an element edge exceeded a given value. This procedure was repeated six times with an increasingly finer mesh, until convergence in mesh size. The fluid properties in the simulations are the same as water at 20°C with $\eta = 1.002$ mPa s and $\rho = 998$ kg/m^3.

2.4 Validation

To validate the simulations, a channel was made using laser ablation. The channel has a cross-section of 300 μm × 50 μm, and 50 μm deep, 200 μm wide grooves inclined 55° relative to the channel axis. The shape of the grooves was measured using confocal microscopy and the measured geometry was used as a basis for simulations. The resulting rotation can be seen in Fig. 2. It can be seen that there is a good qualitative agreement between the simulated and measured rotations. Using this geometry, the closest thing to a 90° rotation occurs after three grooves. It can also be seen that after six grooves, a full 180° rotation is observed in the simulations. The experimental data indicates that this rotation is taking place already after five grooves. Note also the almost perfect match between the cross-section after the first and seventh grooves in the simulations, which is also seen after the first and sixth grooves in the experiments.

2.5 Design optimization

As can be seen in Fig. 2, the rotation after three grooves is not exactly a straight angle. There is also some deformation of the interface between the two tracers; it is no longer a straight line as was the case at the inlet. Three design parameters were varied in a full factorial design to see how a 90° rotation could best be achieved:

- the groove angle (45°–55°–65°),
- the depth of the grooves (50–100–200 μm),
- the depth of the channel (50–100–200 μm).

The channel width was fixed to 300 μm. The design optimization was performed using simulations in CFX of straight channels to find the configuration that gave a rotation of the flow as close to 90° as possible. The best results were obtained with a groove angle of 55°, a channel depth of 50 μm and a groove depth of 50 μm which are the parameters used in the following experiments. This optimal

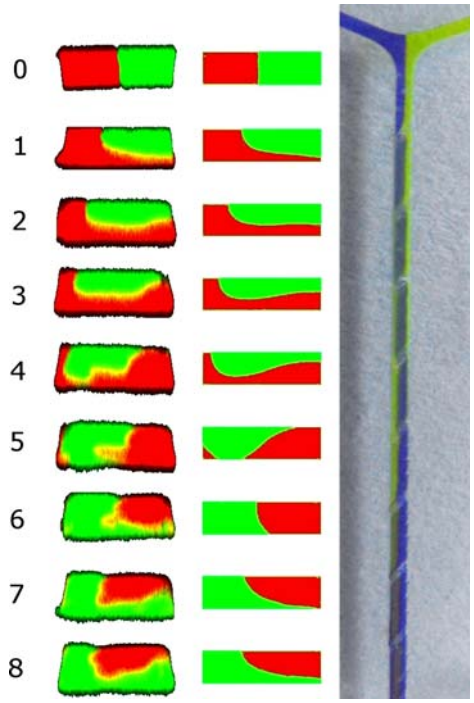

Fig. 2 Helical rotation of the flow field in a straight channel with grooves on the channel bed in the Stokes flow regime ($Re \sim 1$). *Left* confocal fluorescence microscopy measurements of the distribution of rhodamine (*red, left at the inlet*) and Fluorescein (*green, right at the inlet*). *Center* simulated flow field. *Right* photography showing a top view of channel. The *numbers* indicate the cross-section after a given number of grooves, which can be seen in the *right* image

design is shown with dimensions in Fig. 3. Note that this is not a global optimum but only the optimum within the limited space sampled. Other authors have studied the optimization of helical flow patterns by patterning the channel (Yang et al. 2005, 2008) and it is likely that further optimization of the structure is possible.

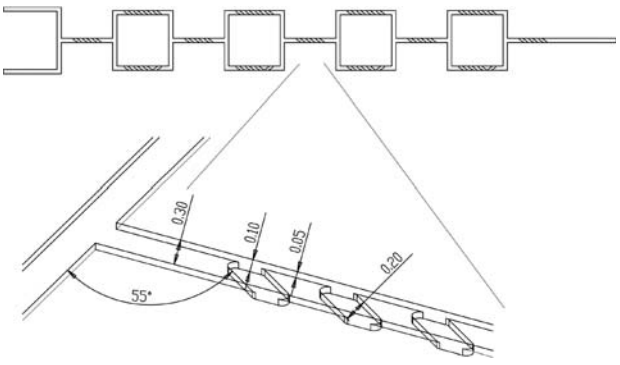

Fig. 3 Design showing four mixing modules (*above*). Detailed view of the grooves with dimensions indicated (in mm) (*below*). The main channel is 50 μm × 300 μm with 50 μm deep, 200 μm wide grooves, inclined 55° relative to the channel axis

3 Results and discussion

The lamination observed experimentally and in simulations, for one module, is shown in Fig. 4. There is a good agreement between the simulated and measured rotations of the flow field. It is also demonstrated that the mixer is able to laminate the flow field as desired.

The lamination, as measured with confocal microscopy, after one to four modules is shown in Fig. 5a. Note that after three modules the two fluids are mixed well. The different laminae can still be seen, demonstrating that it is the stretching and folding effect of the device that is mixing the fluids. The mixing efficiency will in general be dependent on the Peclet number, showing better mixing at lower Peclet numbers. The diffusion coefficients for Rhodamine B and Fluorescein alone in water are 3.6×10^{-10} and 4.9×10^{-10} m^2/s, respectively (Rani et al. 2005). Note that Rhodamine B is hydrophobic and is likely to form micelles with sodium dodecyl sulfate, increasing the diffusion coefficient. This increased diffusion coefficient was not measured. The Peclet number for Fluorescein in the setup shown in Fig. 5 is 9700. The effective Peclet number for Rhodamine B is probably larger than for Fluorescein because of the micelles. This is indicated by the fact that the evaluated degree of mixing for Rhodamine B rises slower than for Fluorescein as can be seen in Fig. 5c.

In the original staggered herringbone article by Stroock et al. (2002), the efficiency is evaluated by measuring the standard deviation σ in fluorescence at different locations. The distance required to achieve a reduction in standard

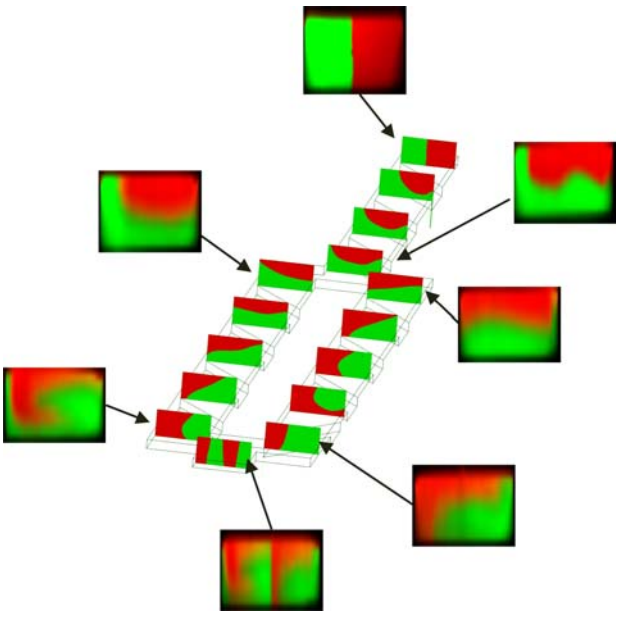

Fig. 4 Concentration distributions within one mixing module. The images on the geometry show the simulated distribution and the outer ones are confocal microscopy measurements

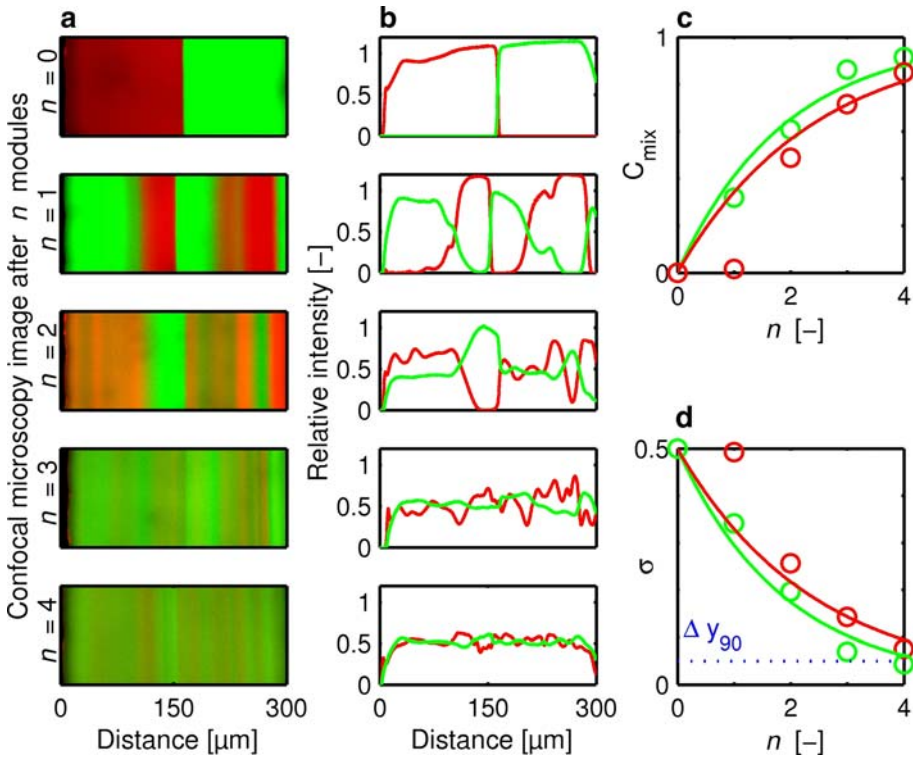

Fig. 5 **a** Confocal microscopy images showing planes at $z = h/2$, where h is the channel depth. The images show from the top the intensity at the entrance and after one to four full modules ($Re = 5$). The modules can be seen in Fig. 3. **b** Normalized intensity of the two fluorophores measured across the cross-sections in **a**. **c** The index of mixing evaluated using the variance in the data from **b**. **d** The standard deviation of the intensities from **b** including a line showing the criteria used for mixing

deviation by 90% relative to the inlet, Δy_{90}, is taken as an indication of the length of mixer required. This standard deviation for the present mixer is seen in Fig. 3d after one to four full modules and it can be seen that this criterion has been met for the fluorophore with the highest diffusivity, Fluorescein, after four modules. The larger, and slower diffusing rhodamine B is close to achieving this criterion. In Stroock et al. this criterion is met after between 3.5 ($Pe = 2000$) and 8.5 ($Pe = 2 \times 10^5$) rotation cycles. Note that the standard deviation measure for mixing will be dependent on the resolution of the confocal microscopy used and therefore these values for mixing efficiency are not directly comparable from study to study. They are still included here for an indication of the mixing efficiency.

To quantitatively evaluate the mixing efficiency, we define the index of mixing as in (Liu et al. 2004) as

$$C_{\text{mix}} = \frac{\sigma_{\text{inlet}} - \sigma}{\sigma_{\text{inlet}}} \tag{4}$$

where σ is the standard deviation of the fluorescence intensity. They use simulation to evaluate the mixers and sigma is the standard deviation in the concentration of a phase variable. They find that the index of mixing for the herringbone mixer when mixing solutions of glycerol and water is approximately 0.5 ($Pe = 1000$) after two full mixing cycles. The mixing index for the present mixer is shown in Fig. 5c.

3.1 Reynolds number dependence

The simulated lamination for two different Reynolds numbers is shown in Fig. 6. Up to a Reynolds number of 5 (flow rate 50 μl/min), changing the flow rate does not change the lamination process. The characteristic length, is in this case, taken as the hydraulic diameter of the channel (85 μm) and the characteristic velocity is the volume flow divided by the channel cross-section (300 μm × 50 μm) where no grooves are present. It can be seen that in the Stokes flow regime, almost perfect lamination is observed. As the momentum effects become more important,

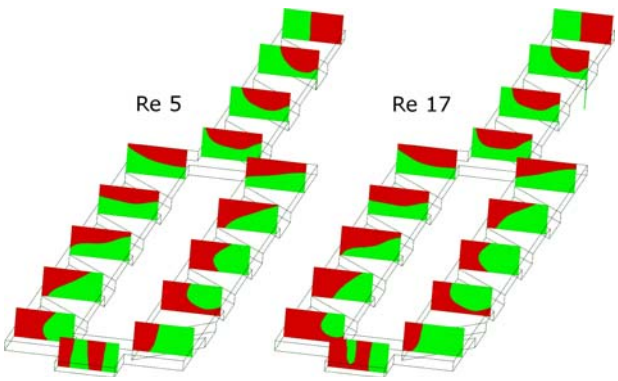

Fig. 6 Simulated lamination as a function of the Reynolds number. For $Re < 5$, the profiles are independent of Re to the accuracy of this graphical representation

however, the helical rotation of the flow field changes. The structure still works as a mixer, but since the helical rotation outside the Stokes flow regime is Reynolds number dependent, it is not given that the two substreams join each other after the designed 90° rotation for Reynolds number above five. For the staggered herringbone mixers, which also reliy on grooves on the channel bed to rotate the flow field, it has been reported that at high Reynolds numbers (>10) vortices form in the grooves which significantly reduce the rotation (Williams et al. 2008). Similar effects are also seen for three-dimensional mixers working on the split and recombine principle, for example, good lamination is only observed with the caterpillar mixers for low Reynolds numbers (<30, Schönfeld et al. 2004).

3.2 Stacking of design

In this report, the focus has not been on making the design as compact as possible. This can, however, be done when considering the layout in Fig. 1. By changing the direction of flow after each rotation of the flow field the overall shape of one mixer module is rectangular. The module shown measures 1.5 × 1.7 mm and the rectangular overall shape makes it easy to pack it densely on a chip device.

4 Conclusions

A new concept for a passive micromixer has been developed. It is shown that the combination of patterning the channel bed and splitting and recombining the streams can be used to make controlled lamination in a 2D channel system. This is shown using both numerical simulations and experiments with prototypes. The design can easily be realized using a range of microfabrication techniques and mass produced using, for example, injection molding.

In the design optimization used in this work only a small subset of the design parameter space was investigated. A further optimization of the design with respect to mixing efficiency on an area as small as possible should be carried out in the future. It is also possible to change the mixer to divide the flow into more than two substreams. Preliminary studies indicate that splitting into three or four substreams can be used to obtain better mixing on a smaller area. Further examination of this question should be made in the future.

Acknowledgments The idea for the mixer presented in this work originated at the Summer School *Micro mechanical system design and manufacturing* held at the Technical University of Denmark the summer of 2008. We would like to thank the organizers, especially Arnaud De Grave and all students participating for two instructive, hectic and utmost enjoyable weeks in Lyngby. We would also like to thank the Research Council of Norway and the Technical University of Denmark for funding.

References

Bau HH, Zhong J, Yi M (2001) A minute magneto hydro dynamic (MHD) mixer. Sens Actuat B Chem 79:207–215

Bessoth FG, de Mello AJ, Manz A (1999) Microstructure for efficient continuous flow mixing. Anal Commun 36:213–215

Bhagat AAS, Peterson ETK, Papautsky I (2007) A passive planar micromixer with obstructions for mixing at low Reynolds numbers. J Micromech Microeng 17:1017–1024

Cha J, Kim J, Ryu SK, Park J, Jeong Y, Park S, Park S, Kim HC, Chun K (2006) A highly efficient 3D micromixer using soft PDMS bonding. J Micromech Microeng 16:1778–1782

Glasgow I, Batton J, Aubry N (2004) Electroosmotic mixing in microchannels. Lab Chip 4:558–562

Hosokawa K, Fujii T, Endo I (1999) Droplet-based nano/picoliter mixer using hydrophobic microcapillary vent. In: 12th IEEE international conference on micro electro mechanical systems (MEMS 99), pp 388–393

Hsieh S-S, Huang Y-C (2008) Passive mixing in micro-channels with geometric variations through μPIV and μLIF measurements. J Micromech Microeng 18:065017

Klank H, Kutter JP, Geschke O (2002) CO2-laser micromachining and back-end processing for rapid production of PMMA-based microfluidic systems. Lab Chip 2:242–246

Lin Y-C, Chung Y-C, Wu C-Y (2007) Mixing enhancement of the passive microfluidic mixer with J-shaped baffles in the tee channel. Biomed Microdevices 9:215–221

Liu YZ, Kim BJ, Sung HJ (2004) Two-fluid mixing in a microchannel. Int J Heat Fluid Flow 25:986–995

Mendels DA, Graham EM, Magennis SW, Jones AC, Mendels F (2008) Quantitative comparison of thermal and solutal transport in a T-mixer by FLIM and CFD. Microfluid Nanofluid 5:603–617

Nguyen NT, Wu ZG (2005) Micromixers—a review. J Micromech Microeng 15:R1–R16

Niu X, Lee YK (2003) Efficient spatial–temporal chaotic mixing in microchannels. J Micromech Microeng 13:454–462

Rani SA, Pitts B, Stewart PS (2005) Rapid diffusion of fluorescent tracers into Staphylococcus epidermidis biofilms visualized by time lapse microscopy. Antimicrob Agents Chemother 49:728–732

Rife JC, Bell MI, Horwitz JS, Kabler MN, Auyeung RCY, Kim WJ (2000) Miniature valveless ultrasonic pumps and mixers. Sens Actuat A Phys 86:135–140

Schönfeld F, Hessel V, Hofmann C (2004) An optimised split-and-recombine micro-mixer with uniform 'chaotic' mixing. Lab Chip 4:65–69

Stroock AD, Dertinger SKW, Ajdari A, Mezic I, Stone HA, Whitesides GM (2002) Chaotic mixer for microchannels. Science 295:647–651

Suzuki H, Ho CM (2002) A magnetic force driven chaotic micromixer. In: 15th IEEE international conference on micro electro mechanical systems (MEMS 2002), pp 40–43

Voldman J, Gray ML, Schmidt MA (2000) An integrated liquid mixer/valve. J Microelectromech Syst 9:295–302

Williams MS, Longmuir KJ, Yager P (2008) A practical guide to the staggered herringbone mixer. Lab Chip 8:1121–1129

Wong SH, Ward MCL, Wharton CW (2004) Micro T-mixer as a rapid mixing micromixer. Sens Actuat B Chem 100:359–379

Xia HM, Shu C, Wan SYM, Chew YT (2006) Influence of the Reynolds number on chaotic mixing in a spatially periodic

micromixer and its characterization using dynamical system techniques. J Micromech Microeng 16:53–61
Yang Z, Matsumoto S, Goto H, Matsumoto M, Maeda R (2001) Ultrasonic micromixer for microfluidic systems. Sens Actuat A Phys 93:266–272
Yang JT, Huang KJ, Lin YC (2005) Geometric effects on fluid mixing in passive grooved micromixers. Lab Chip 5:1140–1147
Yang JT, Fang WF, Tung KY (2008) Fluids mixing in devices with connected-groove channels. Chem Eng Sci 63:1871–1881

8.3 Paper III

Skolimowski, M., Nielsen, M.W., Emnéus, J., Molin, S., Dufva, M., Taboryski, R., Sternberg, C., and Geschke, O., *Microfluidic biochip as a model of the airways of cystic fibrosis patients.* Proceedings of the Thirteenth International Conference on Miniaturized Systems for Chemistry and Life Sciences, p. 1091-1093, 2009.

MICROFLUIDIC BIOCHIP AS A MODEL OF THE AIRWAYS OF CYSTIC FIBROSIS PATIENTS

Maciej Skolimowski[1,2], Martin Weiss Nielsen[1,2], Jenny Emnéus[1], Søren Molin[2], Rafael Taboryski[1], Martin Dufva[1], Claus Sternberg[2] and Oliver Geschke[1]

[1]Technical University of Denmark, Department of Micro- and Nanotechnology, Ørsted Plads, Building 345east, DK-2800 Kgs. Lyngby, DENMARK;
[2]Technical University of Denmark, Department of Systems Biology, Matematiktorvet, Building 301, DK-2800 Kgs. Lyngby, DENMARK

ABSTRACT

Here we report work towards development of a microfluidic system that can simulate the aerobic and anaerobic conditions in the human airways. The main purpose of this device is to mimic habitats of bacteria that usually attack airways of cystic fibrosis (CF) patients. The presented system enables the study of formation, growth, and dissolution of the bacterial biofilms, which is the main cause of the massive pulmonary deficiency and eventually death of CF patients. The ultimate goal for the microdevice is to replace the existing animal models (mice) in the development of new drugs and new treatment strategies in CF.

KEYWORDS: biochip, cystic fibrosis, biofilm, airways, microsystem

INTRODUCTION

The airways consist of at least three independent compartments, the conductive airways (the trachea, bronchii and bronchioles), the oxygen exchange compartment (alveoles) and a third, less recognized compartment, the paranasal sinuses (maxillary sinuses, frontal sinuses and ethmoid sinuses). In the first and the last compartment the environment is essentially anaerobic while in the alveoles the environment is highly aerated.

THEORY

To simulate the environmental conditions, especially the oxygen level which is major parameters affecting biofilm growth in CF patients, we propose the microfluidic airways model (*Figure 1*). The model consists of microchambers for bacterial biofilm growth and microfluidic channels for providing oxygen-scavenging liquid or oxygen-rich liquid. To avoid any impact on the

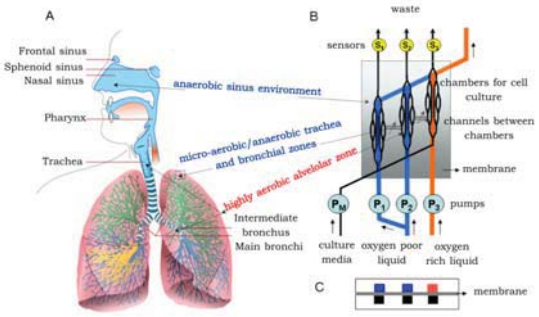

Figure 1. Human airways system, (B) top view sketch of Microfluidic Airways Model (MAM) and (C) cross-section view of MAM

978-0-9798064-2-1/μTAS2009/$20

growth of microorganisms from these liquids, the compartments are separated by an oxygen permeable membrane. All media and liquid flow is controlled by external pumps. The oxygen level in the chambers can be controlled by varying the flow rates (*Figure 3*). A sensing layer for oxygen concentration measurements was incorporated at the bottom of the chambers. To provide the possibility of tracking bacterial re-infections, the bacteria growth chambers exposed to different oxygen levels were interconnected with channels (Figure 1 B).

EXPERIMENTAL

The biochip (*Figure 2*) was fabricated by micromilling of inlets and outlets and laser ablation of the channels in poly(methyl methacrylate). Poly(dimethylsiloxane) (PDMS) was used as the oxygen permeable membrane. The oxygen permeability of PDMS is a well known property, and its use for supplying oxygen in microdevices has been reported [1,2]. However, to our knowledge, no applications comprising active removal of oxygen by means of utilizing concentration gradients below oxygen saturation has been reported. This mechanism mimics the physiological oxygen exchange in the airways compartments. The lid comprising the oxygen sensing layer was fabricated by doping uncured PDMS with platinum(II) octaethylporphyrin (PtOEP), diluted with THF and spincoated to a thickness of approx. 15 µm on a 100 µm thick glass lid followed by thermal curing. Substitution of the usually used sensor matrix (ORMOSIL) [3] with PDMS allows to perform biological experiments in a 100 µm deep microchamber that is constructed from uniform material. All layers were sealed by silicone adhesive tape.

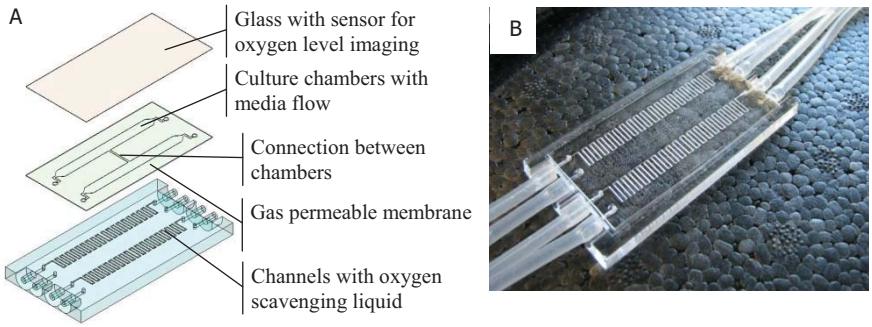

Figure 2: Designed (A) and fabricated (B) microdevice

To form the dissolved oxygen gradient in one of the culture chambers, oxygen scavenger (5% sodium sulphite water solution) was pumped through the corresponding microchannel situated beneath the membrane. The second channel was constantly flushed with oxygen saturated water.

RESULTS AND DISCUSSION

Formation of the oxygen concentration gradient inside the culture chamber was modelled, using numerical simulation with COMSOL 3.4 software (*Figure 3*), and experimentally confirmed by photoluminescence lifetime recordings on a multilabel reader Victor^2 (Perkin-Elmer Life Sciences) with the PtOEP sensing layer.

The microsystem was used for bacterial biofilm culture. A *Pseudomonas aeruginosa* strain, isolated from a CF patient (B54-1 WT-blue), was tagged with four different fluorescent proteins and inoculated. The experiment was carried out for 7 days. The biofilm was formed in 2 days and was not dissolving during the entire experiment. Confocal scanning laser microscopy was used for monitoring the biofilm formation (*Figure 4*).

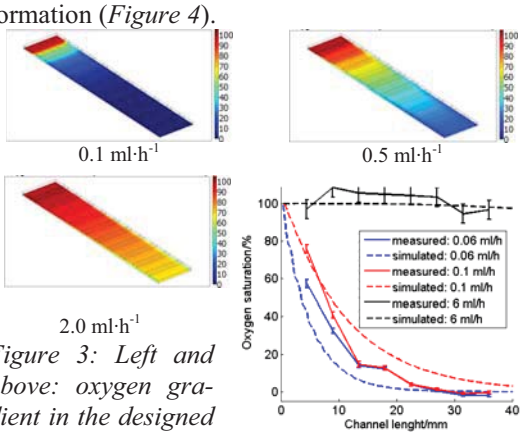

Figure 3: Left and above: oxygen gradient in the designed microdevice at various flow of the fluid in the chamber. Right: comparison between simulated and measured oxygen concentration

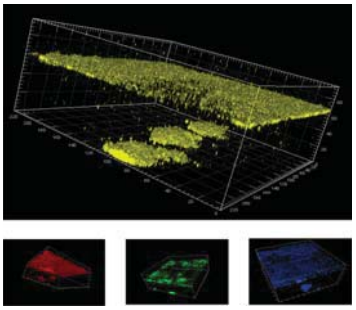

Figure 4: Confocal images of the bacterial biofilm formation in the microdevice. Cells express different fluorescent proteins (FP) (top: YFP, bottom from left to right: RFP, GFP, CFP).

CONCLUSIONS

The presented microfluidic chip was successfully used for generation of the oxygen gradient, which was easily regulated by altering the media flow rate and monitored by time-resolved photoluminescence measurements with integrated microsensor. Separation of the oxygen scavenger allows utilising the chip for cell culture.

The system was used for culturing of *Pseudomonas aeruginosa* biofilm. Future research will be focused on studies of the different antibiotic treatment strategies of bacterial biofilms.

ACKNOWLEDGEMENTS

We would like to aknowledge the founding of Ph.D. stipends by Technical University of Denmark together with DTU Nanotech, Department of Micro- and Nanotechnology and DTU BioSys, Department of Systems Biology.

REFERENCES

[1] L. Kim, et al., A practical guide to microfluidic perfusion culture of adherent mammalian cells, Lab on a Chip, 7, 681, (2007).

[2] G. Mehta, et al., Quantitative measurement and control of oxygen levels in microfluidic poly(dimethylsiloxane) bioreactors during cell culture, Biomedical Microdevices, 9, 123 (2007).

[3] B.J. Basu, Optical oxygen sensing based on luminescence quenching of platinum porphyrin dyes doped in ormosil coatings, Sensors and Actuators B, 123, 568, (2007).

8.4 Paper IV

Skolimowski, M., Nielsen, M.W., Emnéus, J., Molin, S., Taboryski, R., Sternberg, C., Dufva, M., and Geschke, O., *Microfluidic dissolved oxygen gradient generator biochip as a useful tool in bacterial biofilm studies.* Lab on a Chip, 2010. 10(16): p. 2162-2169, DOI: 10.1039/c003558k.

Microfluidic dissolved oxygen gradient generator biochip as a useful tool in bacterial biofilm studies

Maciej Skolimowski,†*[ab] Martin Weiss Nielsen,†[ab] Jenny Emnéus,[a] Søren Molin,[b] Rafael Taboryski,[a] Claus Sternberg,[b] Martin Dufva[a] and Oliver Geschke[a]

Received 24th February 2010, Accepted 29th April 2010
DOI: 10.1039/c003558k

A microfluidic chip for generation of gradients of dissolved oxygen was designed, fabricated and tested. The novel way of active oxygen depletion through a gas permeable membrane was applied. Numerical simulations for generation of O_2 gradients were correlated with measured oxygen concentrations. The developed microsystem was used to study growth patterns of the bacterium *Pseudomonas aeruginosa* in medium with different oxygen concentrations. The results showed that attachment of *Pseudomonas aeruginosa* to the substrate changed with oxygen concentration. This demonstrates that the device can be used for studies requiring controlled oxygen levels and for future studies of microaerobic and anaerobic conditions.

Introduction

The generation of concentration gradients of different chemicals in microfluidic biochips is a problem often addressed in the literature. Typically, for the water soluble components, these are generated by diffusive mixing in microchannels by splitting and merging streams with different concentrations of the molecules of interest.[1–6]

In this work we address the creation of controlled oxygen gradients in perfusion based cell culture chips. A few reports exist that involve *e.g.*, the direct oxygen generation by electrolysis of water molecules,[7] a technique that requires microelectrode fabrication and that potentially can lead to small concentrations of hydrogen peroxide, generated in the same process. A different approach is to exploit the very high diffusivity and solubility of oxygen in poly(dimethylsiloxane) (PDMS).[8–10] PDMS is a chemically inert, biocompatible and optically transparent polymer[11] that is very commonly used for fast construction of microdevices.[12,13] Its properties make it a popular material for construction of cell culture based microdevices. Furthermore it can be utilised as a component in an active scheme of oxygen removal due to its gas permeability.

Active removal of dissolved oxygen from a liquid at the macroscale can be achieved in many ways. These include bubbling liquid with nitrogen gas, electrochemical reduction of dissolved oxygen, biological consumption or chemical reaction with an oxygen scavenger.[7,14–16] At the microscale the first method would lead to extensive drying of the liquid, while the other two complicate the fabrication of such a system.

There are a few very recently published examples of the use of PDMS based microfluidic chips in which the authors are using nitrogen or nitrogen–oxygen gas mixtures to develop dissolved oxygen gradients.[17–19] The main advantage of such a solution would be the possibility of reaching dissolved oxygen concentrations above air saturation point (9.2 ppm at 293 K and 1013.25 hPa).[10] The main disadvantages are the complexity of the setup and the possibility of slowly drying out the chamber when a low liquid media flow is used.

The use of oxygen or other gas containers is difficult in cell culture labs, due to safety reasons and usually very confined space. Therefore, the application of a liquid oxygen scavenger is highly preferable over systems that rely on such gas containers in order to control the specific levels of oxygen gradients. Direct addition of an oxygen scavenging agent such as sulfite or pyrogallol to the cell culture media will alternate its chemical composition which will have a heavy impact on the cultured organisms.[20] Therefore, in this paper we propose the use of a gas permeable PDMS membrane to separate an oxygen scavenging liquid from the cell culture media. To control the oxygen gradient across the cell culture microchamber we rely on the combination of the diffusive and advective oxygen transport within the microchip. To the authors best knowledge, there is so far no scientific report on such a system applied in biological studies.

It is crucial to be able to monitor the oxygen concentration at the microscale and here the classical amperometric method is not feasible because of the bulkiness of sensors and restriction to only point measurements. The most recent progress in miniaturization of the Clark electrode[21] allows one to build an electrode microarray[22,23] which would allow monitoring gradients within microfluidic devices in the future. However, most widely used techniques for measurements of oxygen concentrations in microfluidic devices are based on optical methods, which involve photoluminescent dyes or polymer matrices doped with these probes.[24,25] The basic phenomena responsible for oxygen sensing is dynamic quenching of luminescence by molecular oxygen.[26] Most of the probes with very high quenching constants are based on either ruthenium complexes, such as tris(bipyridyl)ruthenium(II)[27] and Ru(II)-tris(4,7-diphenyl-1,10-phenanthroline)[28–30]

[a]*Technical University of Denmark, Department of Micro- and Nanotechnology, Ørsted Plads, Building 345east, DK-2800 Kgs. Lyngby, Denmark. E-mail: maciej.skolimowski@nanotech.dtu.dk; Tel: +45 4525 6887*
[b]*Technical University of Denmark, Department of Systems Biology, Matematiktorvet, Building 301, DK-2800 Kgs. Lyngby, Denmark*
† These authors contributed equally to this study.

or metalloporphyrins, mainly platinum(II) and palladium(II) octaethylporphyrin (accordingly PtOEP and PdOEP)[31–35] and platinum(II) *meso*-tetra (pentafluorophenyl) porphyrin (PtTFPP).[32,36,37] Other probes, like Erythrosin B[38] or pyrene,[39] are also reported as suitable for oxygen sensing purposes.

The main advantage of the metalloporphyrin based sensors over complexes of ruthenium based sensors is the much higher sensitivity. This is especially important for sensing not pure oxygen, but atmospheric air saturated cell culture media, where the air saturation scale remains biologically relevant. Metalloporphyrins are non-soluble in water which is the main reason why metalloporphyrins are usually embedded in polymers or silicone sol–gel matrices.[32,40] Consequently, ruthenium complexes as water-soluble compounds can be added directly to the culture media,[19] which definitely would simplify the task of sensing the dissolved oxygen concentration of the media. Such an addition would however lead to unspecified alterations in the metabolism of the cultured cells.[10]

Here we show the development of a microfluidic device that combines chambers for cell culturing, an oxygen gradient generator and an integrated optical sensor. This device was designed for high compatibility with hardware available in most laboratories. The system allows one to perform cell culturing without directly adding an oxygen scavenger or oxygen sensing compound to the culture media. This microfluidic system is applied as a useful tool for biological studies where oxygen niches are required and measurable.

Many bacteria experience fluctuating environmental changes in their living habitats. This is caused by changes in available nutritional factors and variation in oxygen concentrations which the bacteria will have to adapt to in order to become a successful colonizer.[41]

One such bacteria is the opportunistic pathogen *Pseudomonas aeruginosa* (*P. aeruginosa*) which is a recurrent and persistent cause of lung infections in patients with the genetic disease cystic fibrosis (CF).[42] Here we use *P. aeruginosa* as the model organism due to its history as a pathogen in highly diverting oxygenated milieus. In order for this pathogen to successfully colonize the human airways it needs to cope with varying nutritional and oxygen levels.[43] Differences in oxygen levels are generated within the viscous mucus layer of the CF airways and stress the bacteria to make a respiratory switch to cope with microaerobic or especially anaerobic conditions. Anaerobic growth of *P. aeruginosa* requires the presence of alternative electron acceptors as NO_3^-, NO_2^- or arginine in which the bacteria renders to generate profound biofilm.[44,45] Conditions of varying oxygen availability within the mucus layers of the CF respiratory system is a metabolic challenge for the bacteria and here we show a device that will be highly beneficial in future studies where controlled oxygen concentrations are needed.

Methods

Design and fabrication

The fabricated device is comprised of five layers (Fig. 1). The first two bottom layers (coloured red in Fig. 1A) are made of a very low oxygen permeable material (PMMA, Röhm GmbH & Co. KG, Germany, oxygen permeability: 1.35 barrers[46]). They contain inlets and outlets in order to connect the microchannel (300 μm width, 200 μm depth, 184 mm total length) and culture chamber. The microchannel and culture chamber were fabricated by laser ablation (48-5S Duo Lase carbon dioxide laser, SYNRAD Inc., USA). The third layer, the membrane, is made of 60 μm thick oxygen permeable material (PDMS, Dow Corning Corp., USA), obtained by spincoating (60 s, 800 rpm) uncured PDMS on an ETFE substrate (Tefzel® Fluoropolymer Film, 200LZ, DuPont de Nemours (Luxembourg) S.A., Luxembourg) followed by curing in 70 °C for 1 h. The ETFE substrate was used here as a temporary solid support for the membrane and was subsequently removed after integration of the membrane into the microchip. The fourth layer, a 150 μm thick cell culture chamber, was fabricated by laser ablation in the low oxygen permeable ETFE foil. The culture chamber was sealed with a glass slide covered with the oxygen sensing dye. The sensing layer was fabricated by doping uncured PDMS with PtOEP (Sigma-Aldrich Denmark A S^{-1}) diluted in THF. The solution was spincoated (60 s, 3000 rpm) to a thin film (thickness approx. 8 μm) on the 120 μm thick glass slide and cured at 70 °C for 20 min. All layers were sealed by silicone adhesive tape (ARcare® 91005, Adhesive Research, Inc., Ireland) and integrated with the base module which contains the milled (Mini-Mill/3PRO, Minitech Machinery Corp., USA) fluidic connectors (Fig. 1B). The microchip was designed to fit with outer dimensions to the microscope slide standard (76 × 26 mm).

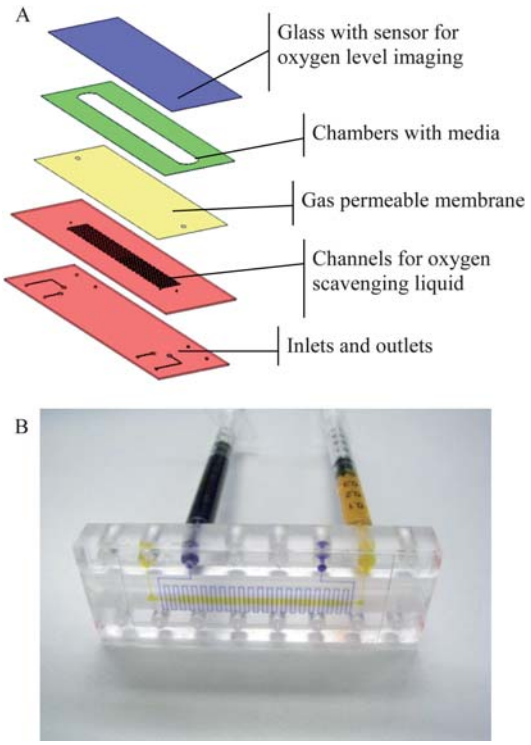

Fig. 1 Schematic presentation of the different layers of the device (A) and the fabricated microdevice (B). Here dyes are injected to visualize the microstructures of the assembled system (blue for channel and yellow for chamber).

Numerical simulations

The oxygen concentration gradients were numerically simulated in COMSOL Multiphysics 3.5a in accordance to the chamber geometry of the designed device. For the numerical simulation, the following conditions were assumed: the density and viscosity of the liquid are similar to water (1000 kg m^{-3} and 0.001 Pa s, respectively), a maximum concentration of oxygen in water (saturation point at standard conditions) of 0.281 mol m^{-3}, a diffusion coefficient of oxygen in water of 1.9×10^{-9} m^2 s^{-1}, a diffusion coefficient of oxygen in PDMS of 4.1×10^{-9} m^2 s^{-1}, oxygen solubility in PDMS 0.18 cm^3(STP) cm^{-3} atm.[8] The equilibrium between oxygen in water and in PDMS can be described by eqn (1). The rate constant of oxygen transport from water to PDMS (k_1 in eqn (1).) was set as 1.0×10^{-2} m s^{-1} [47] and the rate constant (k_2) for the reverse flux was set as 1.7×10^{-3} m s^{-1}.

$$O_2^{water} \underset{k_2}{\overset{k_1}{\rightleftharpoons}} O_2^{PDMS} \quad (1)$$

The ratio of these two rate constants, under steady state condition, is equal to the ratio of oxygen concentrations in water and in PDMS (2). This can otherwise be expressed as a partition coefficient (K_p) between the oxygen in PDMS and in the water phase. This implicates the linear correlation between oxygen concentrations in these two phases (3).

$$\frac{k_1}{k_2} = \frac{O_2^{PDMS}}{O_2^{water}} = K_p \quad (2)$$

$$O_2^{PDMS} = \frac{k_1}{k_2} O_2^{water} \quad (3)$$

The oxygen flux at the PDMS–water boundaries was modelled according to eqn (4). The signs at rate constants depend on the direction of oxygen diffusion.

$$flux_{O_2} = \pm k_2 \cdot C^{PDMS}{}_{O_2} \pm k_1 \cdot C^{water}{}_{O_2} \quad (4)$$

To simplify the simulation we additionally assumed a rapid reaction of the oxygen at the interface between the membrane and the oxygen scavenging liquid (0% oxygen concentration at this interface as a boundary condition) (Fig. 2). This condition can be achieved with an adequate flow of the scavenging liquid and the addition of a catalyst.[15] The liquid flow in the chamber varied from 1 μl min^{-1} to 500 μl min^{-1}, which corresponds to a Péclet number for dissolved oxygen from 0.6 (diffusive transport) to 290.4 (advective transport).

Photoluminescence lifetime measurements of the oxygen gradient

To form the gradient of dissolved oxygen in the growth chamber, an oxygen scavenger (10% sodium sulfite solution with 0.1 mM $CoSO_4$ as catalyst, both from Sigma-Aldrich Denmark A S^{-1}) was pumped by a syringe pump (model 540060, TSE Systems GmbH, Germany) through the microchannel situated beneath the membrane with a constant flow rate of 20 μl min^{-1}, while the growth chamber above the membrane was flushed with atmospheric air saturated water with varying flow rates according to the values used in the numerical simulations.

Photoluminescence lifetime measurements of the PtOEP based sensor were carried out on a multi-titre plate reader (Wallac Victor2, Perkin-Elmer Life Sciences, USA). The entire microchip was mapped to the sectors of a 384 well plate (Fig. 3). The excitation wavelength was 340 nm and the emission wavelength was 640 nm.

In order to correlate the photoluminescence lifetime measurements with the oxygen concentration, a two point calibration was made. The phosphorescence decay curves for the

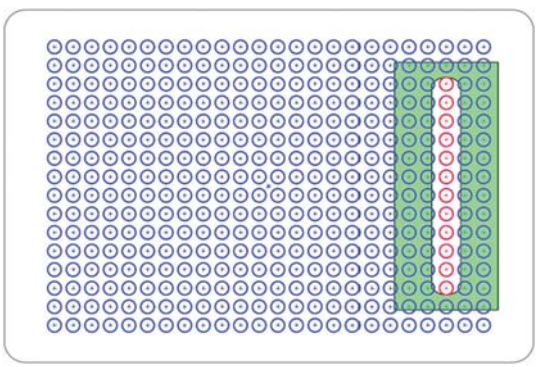

Fig. 3 The chamber mapped to the sector of a 384-wells microplate (the green area is the biochip, blue circles are the 384 microplate wells while the red circles are the oxygen gradient measurement points).

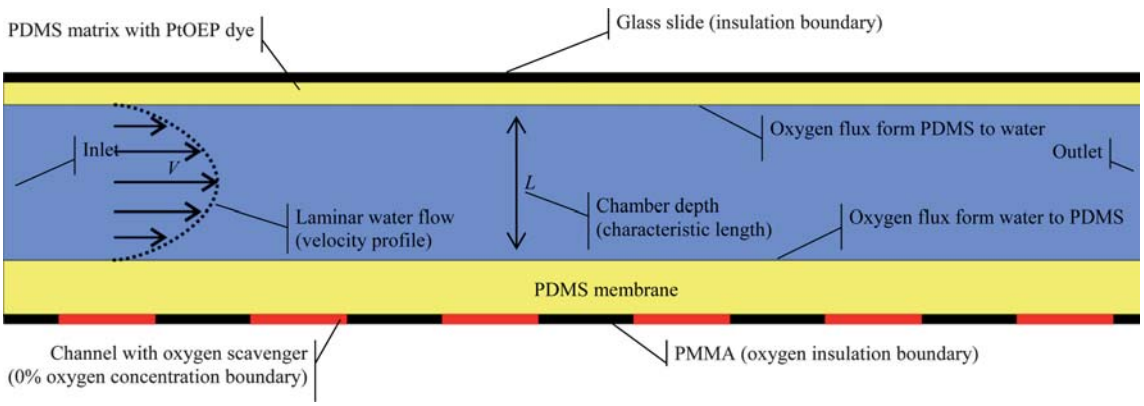

Fig. 2 Schematic model of the oxygen gradient generation in the microdevice.

sensing layer flushed with oxygen free and air saturated water were recorded.

For calculation of the oxygen gradient, in total 12 location points were used. For each measurement location, the decay of the phosphorescence curve was determined by reading the intensities after excitation pulses at 5, 10 15, and 20 μs and then with 10 μs intervals to 170 μs. In total, 20 points were used for the determination of each phosphorescence decay curve. The monoexponential model of the phosphorescence decay was assumed according to eqn (5), where $I(t)$ is the phosphorescence intensity at time t, I_0 is a pre-exponential factor and τ is the phosphorescence lifetime.

$$I(t) = I_0 \cdot e^{-\frac{t}{T}} \quad (5)$$

The data were fit to the model using MATLAB 2008a software and phosphorescence lifetime was determined for every location point. In order to convert the phosphorescence lifetime to the dissolved oxygen concentration, a two-point calibration was done by measuring phosphorescence lifetimes of oxygen free and atmospheric air saturated water.

Cultivation of *Pseudomonas aeruginosa*, PAO1 within the microfluidic chip

Pseudomonas aeruginosa strain PAO1[48] tagged with a green fluorescent protein (GFP)[49] was grown in the flow chambers of the device. The individual chambers were either set up with water in the channels as a control or with oxygen scavenging liquid. PAO1 biofilms were cultivated in chambers irrigated with FAB medium. For the initial attachment experiment the media was supplemented with 0.3 mM glucose and for the long term cultivation experiments with 10.0 mM sodium citrate. Several studies have demonstrated that FAB media supplemented with sodium citrate as the sole carbon source promote a carpet-like biofilm instead of microcolonies and mushroom-like structures. This generates a better possibility of quantitative comparison of the bacterial biomass developed under different oxygen environments.[50]

The flow chambers were inoculated by injecting 500 μl overnight culture diluted to an OD_{600} of 0.005 into each flow chamber. This inoculum ensured that the entire culture chamber was filled. To drive the growth of bacterial biofilm on the glass side the chip was turned upside down without flow for 1 h after inoculation. The media flow was subsequently started at the flowrate of 10 μl min^{-1} using a peristaltic pump (Watson Marlow 205S, Watson-Marlow Inc, USA), directly followed by detection of attached bacteria by confocal laser scanning microscopy (CLSM).

In order to illustrate biofilm development in different oxygen environments the long term cultivation of PAO1 was performed for 4 days using sodium citrate supplemented FAB media. All steps were carried out at 37 °C.

Microscopy and image analysis

Microscopic observations and image acquisitions were performed on a Zeiss LSM 510 CLSM (Carl Zeiss, Jena, Germany). Detectors and filter settings were set for monitoring GFP. Confocal images of the 1 h initial attachment was taken using the 63×/1.4. For each indicated time point 7 pictures were taken in random locations of the specific oxygen saturation point. For the long term experiments, pictures were taken at day 4 using the 40×/1.4 Plan-Neofluar oil objective. The first location for the long term biomass measurements was chosen at an oxygen concentration of 97%. Each consecutive measurement was performed in intervals of 1 mm down the oxygen gradient (see Fig. 8 and Fig. 9 later). All images were processed using the IMARIS software package (Bitplane AG, Zürich, Switzerland).

For quantification of biomass the COMSTAT software was used. COMSTAT defines biomass as a biomass volume divided by the substratum area (μm^3 μm^{-2}).[50]

Results

Description of the system

We have fabricated a multilayer system where we incorporated: a PDMS immobilised oxygen sensing probe, a culture chamber, a gas permeable membrane and a microfluidic channel for oxygen scavenging.

The purpose of the microfluidic channel is to constantly flush the PDMS membrane with an oxygen scavenging liquid. This allows oxygen transport across the membrane by diffusion from the growth chamber to the microchannel. Here the oxygen is irreversibly consumed in a rapid chemical reaction. The oxygen gradients generated within the chamber can be monitored by the oxygen sensing probe.

The culture chamber was used for *P. aeruginosa* cultivation in different dissolved oxygen environments.

Numerical simulations of the oxygen gradients

In order to verify the generation of dissolved oxygen gradients within the microdevice, numerical simulations were performed. The gradient can be observed in a horizontal as well as a vertical plane. Since PAO1 strain forms biofilm on the glass side of the chamber only the oxygen gradient from the top horizontal plane was taken into consideration (Fig. 4).

The oxygen gradients vary with the media flow rate (Fig. 4) due to changes in the ratio of advective and diffusive transport. This ratio can be described by the Péclet number (*Pe*) (see eqn (6) and Fig. 2 where L is the characteristic length, V is the velocity the media and D is the diffusion coefficient of oxygen in water). In the first case where the flow rate of the media is low

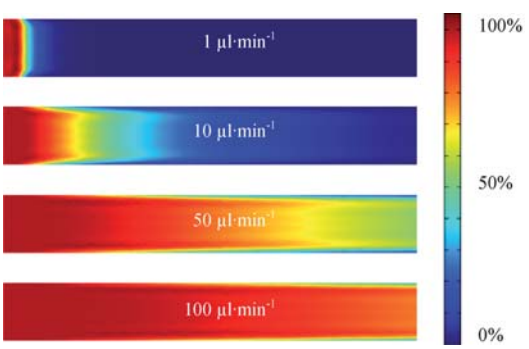

Fig. 4 Simulations of the oxygen saturation gradients in the growth chamber according to the various flow rates of culture media.

(1 μl min^{-1}, $Pe = 0.6$), only a very short horizontal distance within the chamber is needed to remove almost all the oxygen. When the flow rate within the chamber is increased, the oxygen saturation at the end of the chamber increases accordingly (2% at 10 μl min^{-1} ($Pe = 6$), 43% at 50 μl min^{-1} ($Pe = 29$), 63% at 100 μl min^{-1} ($Pe = 58$) and 88% at 500 μl min^{-1} ($Pe = 290$) (last not shown in Fig. 4)).

$$Pe = \frac{L \cdot V}{D} \quad (6)$$

Photoluminescence lifetime measurements of the oxygen gradients

A two point calibration of the PDMS immobilised oxygen probe was made to be able to calculate oxygen gradients generated within the microfluidic device. The determined phosphorescence lifetimes for oxygen free and atmospheric air saturated water were: 69.7 ± 0.4 μs and 8.2 ± 0.1 μs, respectively. These measurements allowed us to make a correlation between the photoluminescence lifetime and oxygen concentration (Fig. 5).

The comparison between the numerically simulated and measured oxygen concentration gradients were made in order to validate both the theoretical model and the experimental data (Fig. 6). The simulation curves were plotted as oxygen saturation in water from the middle chamber cross-section *versus* the length of the channel. For each curve, twelve measurement points were used according to the spots marked in Fig. 3.

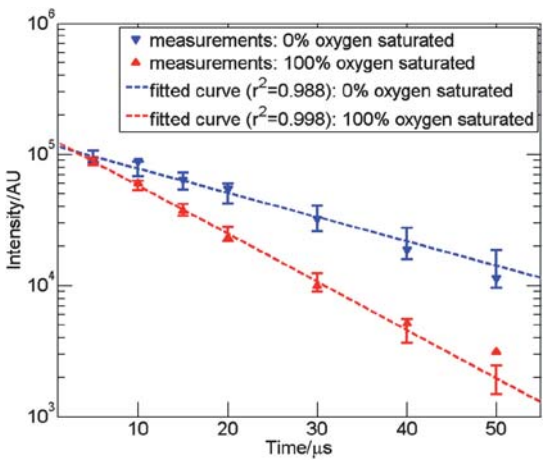

Fig. 5 Phosphorescence decay curve for oxygen free and atmospheric air saturated water (see equation 5).

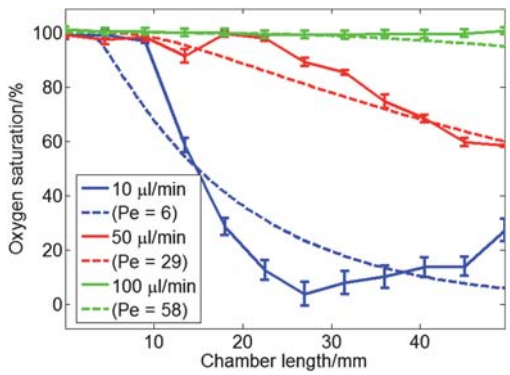

Fig. 6 Comparison between simulated (dashed lines) and measured (solid lines) oxygen concentration gradients in the culture chamber at different media flow rates.

The measured oxygen gradients follow the data obtained by the numerical simulations (Fig. 6). The variance coefficients between simulated and measured oxygen concentrations were 2.2%, 5.9% and 13.5% for, accordingly, 100, 50 and 10 μl min^{-1} media flow rates. The measured oxygen concentrations were slightly higher than the simulated ones at high flow rates and slightly lower at low flow rates. These differences can be explained by the flexibility of the PDMS membrane, which was not taken into consideration in the numerical simulations, for the sake of model simplicity, The membrane is slightly deflecting due to hydraulic pressure differences between the chamber and the channel with oxygen scavenger. This affects the chamber depth (L, Fig. 2), oxygen diffusion length and consequently the oxygen gradient.

According to both the numerical simulations and experimental measurements of the oxygen concentrations, we have shown that it is possible to control the oxygen gradient by merely alternating the media flow.

Reduced initial attachment and biofilm growth in the microdevice

To investigate the effect of the oxygen concentration on the growth of the *P. aeruginosa* PAO1, we cultivated this strain in the chip with a defined media known to support aerobic growth. We hypothesised that the lack of an alternative electron acceptor would affect the growth pattern of PAO1 under low oxygen concentrations. As a reference point for comparison purposes, we arbitrarily chose the culture chamber section with 20% of atmospheric air saturation (microaerobic conditions).

Following one hour of attachment under this low oxygen concentration, the attachment capacity of PAO1 to the PDMS surface was highly reduced. As shown in Fig. 7, PAO1 prefers to attach to the PDMS surface (shown 146.6μm × 146.6μm area) during conditions of higher air saturation. The attachment characteristics of PAO1 was furthermore investigated by time-lapse confocal microscopy. In a setup where the cells were allowed 1 h of initial attachment under atmospheric air saturated media, it was shown that the cells readily leave their attachment site after the media is reduced in oxygen concentration (data not shown).

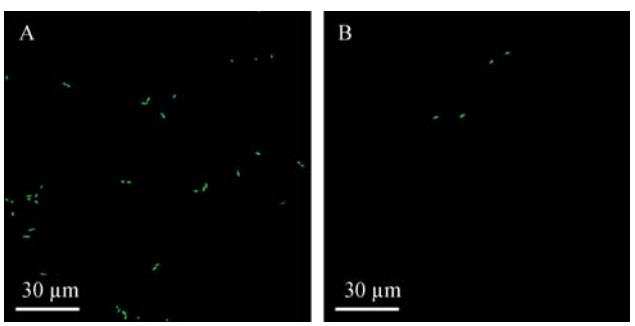

Fig. 7 Initial attachment of *P. aeruginosa* strain PAO1 at the end of microchambers recorded after 1 h of attachment: (A) media saturated with atmospheric air, (B) 20% of dissolved oxygen saturation.

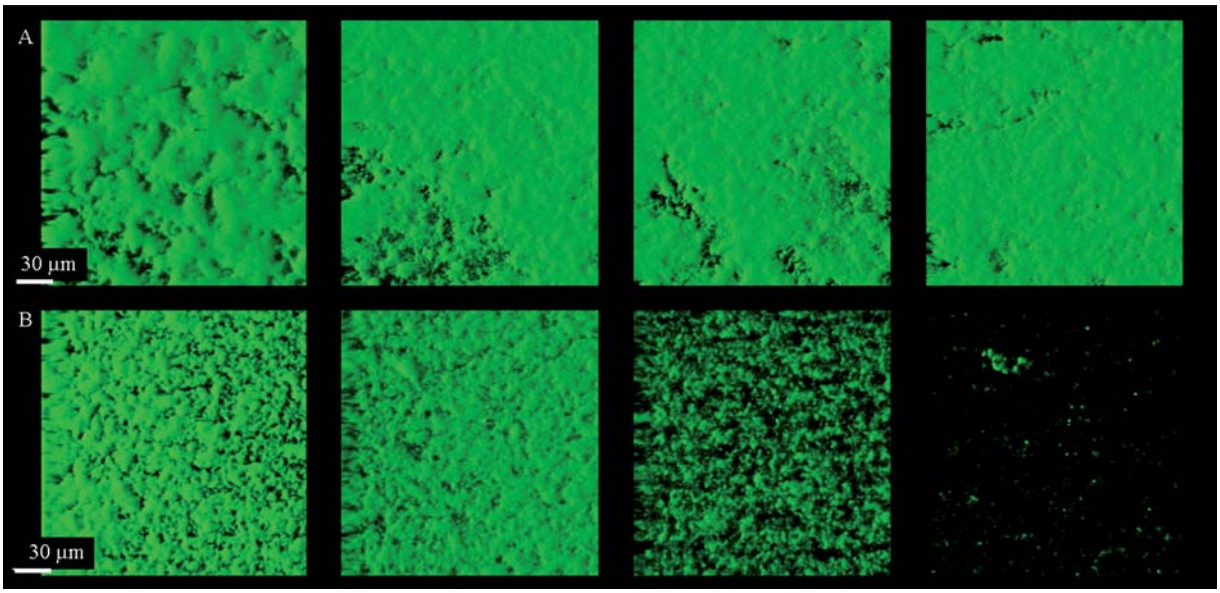

Fig. 8 Four day old biofilm of *P. aeruginosa* PAO1 cultivated in FAB media supplemented with 10 mM sodium citrate under: (A) atmospheric air saturation, (B) oxygen saturation (from left to right): 97%, 79%, 60% and 41%.

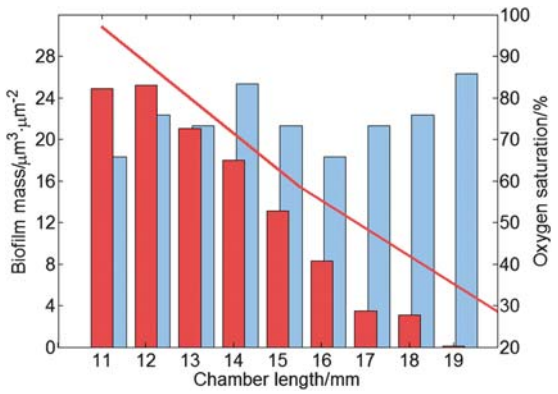

Fig. 9 Comparison of bacterial biomass developed in different oxygen environments. The red bars represent the PAO1 biomass within the culture microchamber under the oxygen gradient (red line). The blue bars represent PAO1 biomass produced in the atmospheric air saturated media.

In order to quantitatively compare the effect of different oxygen environments on PAO1 growth we used a FAB media supplemented with sodium citrate as the sole carbon source. We measured bacterial biomass formed after 4 days of cultivation in the microchambers. Under aerobic conditions (Fig. 8A) an even distribution of carpet-like biofilm is spread over the substratum. The drop in oxygen availability has a high impact on the cells ability to form a stable and evenly distributed biofilm (Fig. 8B). Fig. 9 shows clear correlation between PAO1 biomass and the oxygen gradient generated within the culture chamber.

Discussion

One of the main goals of our work was to design a device that was fairly easy to fabricate and handle. In order for a device to be a successful asset to a wide range of functional purposes in a laboratory, the need for complicated setups and supplies should be reduced as much as possible. In this paper we presented a developed system which easily produces controllable oxygen gradients within a culture chamber.

We exploit the advantages of an oxygen scavenging liquid over methods which involve flushing the channel with oxygen–nitrogen gaseous mixtures.[19] This significantly reduces the complexity of the setup and need of additional equipment.

Since PDMS is highly permeable, not only to O_2 and N_2 but also to water vapour, the use of pressurised gases would cause extensive drying of the culture media during long term experiments. In the case of low media flow rates, this could lead to severe changes in media osmolarity[51] and introduce bubbles within the culture chamber.[52]

The use of an oxygen tank in the laboratory is furthermore a serious safety threat to the personnel, therefore any solution which would eliminate it from the setup is highly desirable.

Furthermore we have produced a system which is cheap in expenses for oxygen scavenging due to very small amounts of chemicals needed.

The designed microfluidic system was integrated with a thin film sensor which was used for the detection of dissolved oxygen concentration gradients within the cultivation chamber. The oxygen concentrations were monitored by photoluminescence lifetime measurements. This specific way of monitoring oxygen concentration is compatible with several different detection methods as micro plate readers and fluorescence lifetime imaging microscopes.

Since bleaching of the oxygen probe by short excitation pulses, as used in time-resolved spectroscopy, is much lower than in the case of excitation with continuous light, the proposed thin film sensor can be used for long term experiments.

Prolonged exposition of the culture chamber to a strong light, used for oxygen probe excitation, would be harmful for the cultivated cells.[53] Therefore, the short excitation pulses used in

time-resolved spectroscopy techniques are preferable over continuous light excitation.

Furthermore, the choice of not using dissolved oxygen probes generate a system in which the influence of the probes on the cells[10] is completely eradicated. A significant advance over previous approaches,[19] where the authors created a system in which oxygen probes were present within their setup, is that we generated a highly biocompatible chip where the toxicity of the probes is eliminated.

For the making of the thin film sensor, we chose a PDMS matrix over the organically modified silica (ORMOSIL), which was widely used as a sensor matrix in previous works.[32] This substitution allows one to perform biological experiments without exposing the cultivated organism to two different environments (a hydrophilic glass-like surface in the case of ORMOSIL and a hydrophobic silicone rubber surface in the case of PDMS). Having these two surfaces with radically different properties could bias biological experimental data. This is especially important in studies of bacterial biofilm formation, where adherence will vary according to hydrophilicity of a specific surface.[54] However in other applications, especially for mammalian cell cultures, the use of ORMOSIL could be advantageous due to its chemical inertness[55] and the possibility of relatively easy surface modifications.[56]

Moreover, the cracking problem, reported for low molecular mass ORMOSIL precursors[40] is not present in PDMS films. Another advantage of the PDMS based matrix is the rapid fabrication time. The curing time for thin PDMS films is only 20 min while gelation and drying time of ORMOSIL based matrices, reported in the literature, can be as long as 2 weeks.[34]

The results from photoluminescence lifetime measurements of the dissolved oxygen gradients, which was generated within the culture chamber, correlated well with the results obtained from the numerical simulation. This does not only confirm the correctness of the mathematical model of the oxygen transport in the microfluidic system but also the reliability of time-resolved luminescence measurements done using the proposed PtOEP film sensor.

We consider that the discrepancies between simulated and measured oxygen concentrations observed at some media flow rates are due to deflection of the PDMS membrane. In order to include this effect in the numerical simulations one would need to incorporate one of the stress–strain models for a hyperelastic material. In the literature one can encounter a limited number of examples with numerical simulations of PDMS deflection.[57,58] However, to our best knowledge, there is no literature data describing how the gas permeability of PDMS is changing according to the strain.

When the only changes in dissolved oxygen levels are due to the chemical reaction with scavenger and diffusion–advection transport, the numerical simulations can predict the approximate shape of oxygen gradients within the chamber of the microchip. However, when this is not the case, *e.g.* when the chamber is used for cell culturing or when the material properties are not well characterised, a simple mathematical model cannot precisely predict the oxygen consumption. In such a case it will be necessary to use an integrated sensor.

The designed system was successfully applied to support growth of *P. aeruginosa* PAO1 biofilm. PAO1 responded to the low oxygen concentration environment by a reduced number of attached cells to the surface of the microchamber after the one hour adherence period. This indicates that the oxygen concentration within the microenvironment of the attachment site is highly important for PAO1 to effectively bind to this surface. The specific response to the low oxygen availability shows that PAO1 under flow conditions seems to lack the ability to effectively form an irreversible attachment.

In the CF lungs environment, the bacteria are living in a mucus matrix with the presence of DNA, proteins and other factors[59] which are highly diverting over the course of infection. This is currently not possible to fully grasp in the experimental conditions. However the most important factor in the chronically infected CF patients is the oxygen tension.[45] The presented device makes it possible to generate such differences in oxygen levels and is here proven to make an excellent platform for this kind of experimental setup.

Concluding remarks

In this paper we presented a novel approach for oxygen gradient generation within a microfluidic biochip. The system was successfully fabricated by micromilling, laser ablation and spin-coating techniques.

The simple layer-by-layer design allows the incorporation of several desirable elements as the integrated gas permeable membrane which we exploited by an oxygen scavenging liquid to produce the desired oxygen environments. The experimental data correlated as expected to the numerical simulations performed.

Stability and biocompatibility experiments were successfully performed over a long term biofilm culture, which proves the system as an excellent foundation for oxygen dependent studies.

We successfully made a system that does not rely on toxic dyes or difficult setups, but was built to be easy and safe to operate as well as highly mobile and compatible with common used biological laboratory equipment such as microscopes and multi-titre well plate readers.

In future CF biofilm studies, desired to be investigated in different oxygen environments, this platform could furthermore be used with the incorporation of other biologically important factors, like DNA and proteins. This would be a great advance towards mimicking the CF airways.

Acknowledgements

We would like to acknowledge the funding of PhD stipends by The Technical University of Denmark as well as the EU funded FP7 project EXCELL.

Notes and references

1 A. Tirella, M. Marano, F. Vozzi and A. Ahluwalia, *Toxicol. in Vitro*, 2008, **22**, 1957–1964.
2 M. Yamada, T. Hirano, M. Yasuda and M. Seki, *Lab Chip*, 2006, **6**, 179–184.
3 S. K. W. Dertinger, D. T. Chiu, N. L. Jeon and G. M. Whitesides, *Anal. Chem.*, 2001, **73**, 1240–1246.
4 M. Yang, J. Yang, C.-W. Li and J. Zhao, *Lab Chip*, 2002, **2**, 158–163.
5 M. A. Holden, S. Kumar, E. T. Castellana, A. Beskok and P. S. Cremer, *Sens. Actuators, B*, 2003, **92**, 199–207.
6 T. M. Keenan and A. Folch, *Lab Chip*, 2007, **8**, 34–57.

7 J. Park, T. Bansal, M. Pinelis and M. M. Maharbiz, *Lab Chip*, 2006, **6**, 611–622.
8 S. G. Charati and S. A. Stern, *Macromolecules*, 1998, **31**, 5529–5535.
9 T. C. Merkel, V. I. Bondar, K. Nagai, B. D. Freeman and I. Pinnau, *J. Polym. Sci., Part B: Polym. Phys.*, 2000, **38**, 415–434.
10 G. Mehta, K. Mehta, D. Sud, J. W. Song, T. Bersano-Begey, N. Futai, Y. S. Heo, M.-A. Mycek, J. J. Linderman and S. Takayama, *Biomed. Microdevices*, 2007, **9**, 123–134.
11 A. Mata, A. J. Fleischman and S. Roy, *Biomed. Microdevices*, 2005, **7**, 281–293.
12 L. Kim, Y.-C. Toh, J. Voldman and H. Yu, *Lab Chip*, 2007, **7**, 681–694.
13 J. C. McDonald, D. C. Duffy, J. R. Anderson, D. T. Chiu, H. Wu, O. J. A. Schueller and G. M. Whitesides, *Electrophoresis*, 2000, **21**, 27–40.
14 C. E. a. Aitken, R. A. Marshall and J. D. Puglisi, *Biophys. J.*, 2008, **94**, 1826–1835.
15 A. A. Shaikh and S. M. J. Zaidi, *React. Kinet. Catal. Lett.*, 1998, **64**, 343–349.
16 A. M. Shams el Din and R. A. Arain, *Corros. Sci.*, 1989, **29**, 445–453.
17 M. Polinkovsky, E. Gutierrez, A. Levchenko and A. Groisman, *Lab Chip*, 2009, **9**, 1073–1084.
18 A. P. Vollmer, R. F. Probstein, R. Gilbert and T. Thorsen, *Lab Chip*, 2005, **5**, 1059–1066.
19 M. Adler, M. Polinkovsky, E. Gutierrez and A. Groisman, *Lab Chip*, 2010, **10**, 388–391.
20 K.-A. M. P. J. Marianne Reist, *J. Neurochem.*, 1998, **71**, 2431–2438.
21 C.-C. Wu, T. Yasukawa, H. Shiku and T. Matsue, *Sens. Actuators, B*, 2005, **110**, 342–349.
22 J.-H. Lee, T.-S. Lim, Y. Seo, P. L. Bishop and I. Papautsky, *Sens. Actuators, B*, 2007, **128**, 179–185.
23 J. Park, J. J. Pak, S. Ahn and Y. K. Pak, *4th IEEE International Conference on Nano/Micro Engineered and Molecular Systems, NEMS 2009*, 2009, 1054–1057.
24 P. C. A. Jerónimo, A. N. Araújo, M. Conceição and B. S. M. Montenegro, *Talanta*, 2007, **72**, 13–27.
25 T. C. O'Riordan, A. V. Zhdanov, G. V. Ponomarev and D. B. Papkovsky, *Anal. Chem.*, 2007, **79**, 9414–9419.
26 E. R. Carraway and J. N. Demas, *Anal. Chem.*, 1991, **63**, 332–336.
27 P. A. S. Jorge, P. Caldas, C. C. Rosa, A. G. Oliva and J. L. Santos, *Sens. Actuators, B*, 2004, **103**, 290–299.
28 A. K. McEvoy, C. M. McDonagh and B. D. MacCraith, *Analyst*, 1997, **121**, 785–788.
29 l. Klimant and O. S. Wolfbeis, *Anal. Chem.*, 1995, **67**, 3160–3166.
30 S. B. Pieper, S. P. Mestas, K. L. Lear, Z. Zhong and K. F. Reardon, *Appl. Phys. Lett.*, 2008, **92**, 081915–081913.
31 T.-S. Yeh, C.-S. Chu and Y.-L. Lo, *Sens. Actuators, B*, 2006, **119**, 701–707.
32 B. J. Basu, *Sens. Actuators, B*, 2007, **123**, 568–577.
33 Y. Amao, T. Miyashita and I. Okura, *Analyst*, 2000, **125**, 871–875.
34 S.-K. Lee and I. Okura, *Analyst*, 1997, **122**, 81–84.
35 Y. Amao, T. Miyashita and I. Okura, *React. Funct. Polym.*, 2001, **47**, 49–54.
36 Y. Amao, T. Miyashita and I. Okura, *J. Fluorine Chem.*, 2001, 101–106.
37 E. Schmaelzlin, J. T. v. Dongen, I. Klimant, B. Marmodee, M. Steup, J. Fisahn, P. Geigenberger and H.-G. Loehmannsroeben, *Biophys. J.*, 2005, **89**, 1339–1345.
38 R. N. Gillanders, M. C. Tedford, P. J. Crilly and R. T. Bailey, *J. Photochem. Photobiol., A*, 2004, **163**, 193–199.
39 R. A. Dunbar, J. D. Jordan and F. V. Bright, *Anal. Chem.*, 1996, **68**, 604–610.
40 Y. Tang, E. C. Tehan, Z. Tao and F. V. Bright, *Anal. Chem.*, 2003, **75**, 2407–2413.
41 P. Stoodley, K. Sauer, D. G. Davies and J. W. Costerton, *Annu. Rev. Microbiol.*, 2002, **56**, 187–209.
42 S. Moreau-Marquis, B. A. Stanton and G. A. O'Toole, *Pulm. Pharmacol. Ther.*, 2008, **21**, 595–599.
43 D. J. Hassett, T. R. Korfhagen, R. T. Irvin, M. J. Schurr, K. Sauer, G. W. Lau, M. D. Sutton, H. Yu and N. Hoiby, *Expert Opin. Ther. Targets*, 2010, **14**, 117–130.
44 S. S. Yoon, R. F. Hennigan, G. M. Hilliard, U. A. Ochsner, K. Parvatiyar, M. C. Kamani, H. L. Allen, T. R. DeKievit, P. R. Gardner, U. Schwab, J. J. Rowe, B. H. Iglewski, T. R. McDermott, R. P. Mason, D. J. Wozniak, R. E. W. Hancock, M. R. Parsek, T. L. Noah, R. C. Boucher and D. J. Hassett, *Dev. Cell*, 2002, **3**, 593–603.
45 D. J. Hassett, M. D. Sutton, M. J. Schurr, A. B. Herr, C. C. Caldwell and J. O. Matu, *Trends Microbiol.*, 2009, **17**, 130–138.
46 C.-C. Hu, T.-C. Liu, K.-R. Lee, R.-C. Ruaan and J.-Y. Lai, *Desalination*, 2006, **193**, 14.
47 H. Shiku, T. Saito, C.-C. Wu, T. Yasukawa, M. Yokoo, H. Abe, T. Matsue and H. Yamada, *Chem. Lett.*, 2006, **35**, 234.
48 B. W. Holloway and A. F. Morgan, *Annu. Rev. Microbiol.*, 1986, 79–105.
49 M. Klausen, A. Heydorn, P. Ragas, L. Lambertsen, A. Aaes-Jorgensen, S. Molin and T. Tolker-Nielsen, *Mol. Microbiol.*, 2003, **48**, 1511–1524.
50 A. Heydorn, A. T. Nielsen, M. Hentzer, C. Sternberg, M. Givskov, B. K. Ersbøll and S. Molin, *Microbiology*, 2000, **146**, 2395–2407.
51 A. Blau, T. Neumann, C. Ziegler and F. Benfenati, *J. Biosci.*, 2009, **34**, 59–69.
52 L. Kim, T. Yi-Chin, J. Voldman and H. Yu, *Lab Chip*, 2007, **4**, 681–694.
53 M. Stangegaard, S. Petronis, a. M. Jorgensen, C. B. V. Christensen and M. Dufva, *Lab Chip*, 2006, **6**, 1045–1051.
54 M. Simões, L. C. Simões and M. J. Vieira, *LWT-Food Sci. Technol.*, 2010, **43**, 573–583.
55 J. Lin and C. W. Brown, *TrAC, Trends Anal. Chem.*, 1997, **16**, 200–211.
56 S. S. Jedlicka, J. L. Rickus and D. Zemlyanov, *J. Phys. Chem. C*, 2010, **114**, 342–344.
57 Y.-S. Yu and Y.-P. Zhao, *J. Colloid Interface Sci.*, 2009, **332**, 467–476.
58 A. Hoel and M.-C. Jullien, *Proceedings of the COMSOL Multiphysics User's Conference*, Paris, France, 2005.
59 C. B. Whitchurch, T. Tolker-Nielsen, P. C. Ragas and J. S. Mattick, *Science*, 2002, **295**, 1487.

8.5 Paper V

Skolimowski, M., Nielsen, M.W., Abeille, F., Skafte-Pedersen, P., Sabourin, D., Fercher, A., Papkovsky, D., Molin, S., Taboryski, R., Sternberg, C., Dufva, M., Geschke, O. and Emnéus, J, *Modular microfluidic system as a model of cystic fibrosis airways.* Submitted manuscript to Lab on a Chip, 2011.

Modular microfluidic system as a model of cystic fibrosis airways

*Maciej Skolimowski,[*a, b†] Martin Weiss Nielsen,[a, b†] Fabien Abeille,[a, b] Peder Skafte-Pedersen,[a] David Sabourin,[a] Andreas Fercher,[c] Dmitri Papkovsky,[c,d] Søren Molin,[b] Rafael Taboryski,[a] Claus Sternberg,[b] Martin Dufva,[a] Oliver Geschke[a] and Jenny Emnéus[a]*

[a] Technical University of Denmark, Department of Micro- and Nanotechnology, Ørsted Plads, Building 345B, DK-2800 Kgs. Lyngby, Denmark; Tel: +45 4525 6887; E-mail: maciej.skolimowski@nanotech.dtu.dk

[b] Technical University of Denmark, Department of Systems Biology, Matematiktorvet, Building 301, DK-2800 Kgs. Lyngby, Denmark

[c] University College Cork, Biochemistry Department, Cavanagh Pharmacy Building, Cork, Ireland

[d] Luxcel Biosciences Ltd., BioInnovation Centre, UCC, College Road, Cork, Ireland

† These authors contributed equally to this study

Abstract

A modular microfluidic airways model system that can simulate the changes in oxygen tension in different compartments of the cystic fibrosis airways was designed, developed and tested. The fully reconfigurable system comprise from modules with different functionalities: multichannel peristaltic pumps, bubble traps, gas exchange chip and cell culture chambers. We have successfully applied this system for studying the antibiotic therapy of *P. aeruginosa*, the bacteria mainly responsible for morbidity and mortality in cystic fibrosis, in different oxygen environments. Furthermore, we have shown the reinoculation of the bacteria form the anaerobic (CF sinuses) the aerobic compartments (lower respiratory tract) after the antibiotic treatment. This effect is hypothesised as the main reason for recurrent infections in CF patients.

1 Introduction

The human airways are complex multi-compartmental habitats for infectious bacteria. In healthy humans, the majority of the airways are essentially kept sterile as a result of highly efficient clearing mechanisms[1]. In cystic fibrosis (CF) patients, this clearing mechanism is severely impaired and bacterial infections inflict deteriorating health and becomes the major cause of mortality in these patients[2, 3].

The human airways consist of at least three independent compartments, the conductive airways (the trachea, bronchi and bronchioles), the oxygen exchange compartment (alveoli), and a third, less recognized compartment, the paranasal sinuses (maxillary sinuses, frontal sinuses and ethmoid sinuses). In the first and the last compartment, the environment is essentially anaerobic[4], while the alveoli are highly aerated.

In healthy individuals, the conductive airways are constantly cleared by mucociliary transport of entrapped microorganisms[5]. As a result, very few bacteria will ever reach the alveoli. Bacteria that do evade this clearing mechanism will rapidly be cleared by the actions of the immune system. The sinuses also have a mucociliary clearance mechanism although not as effective as the one found in the conductive airways. Large concentrations of bacteria can be found widely spread throughout the sinuses, in particular in cases of common colds, etc[6].

Cystic fibrosis patients suffer from a defect in the cystic fibrosis transmembrane conductance regulator (CFTR) gene. The affected gene codes for the CFTR protein, which is a chloride channel that is present in the epithelial cell membrane. Reduced or absent function of the CFTR will lead to highly reduced secretion of chloride and accordingly water over the cell membrane[7]. A direct consequence of this defect is that the mucus layer in the conductive airways becomes very viscous and the mucociliary clearance mechanisms are highly impaired[3, 8]. This results in frequent and recurrent infections of the CF airways, with the risk of pneumonia. As the bacteria infect the lungs in large numbers, the immune system tries to eradicate the infection but with a reduced effect since the bacteria are embedded in mucus and more or less recalcitrant to the cellular defence[9]. Instead the lung tissue is gradually damaged by the on-going immunological exposure, eventually leading to massive pulmonary deficiency and death[10]. In the clinic, the infections can be treated with cocktails of antibiotics, which can reduce or sometimes eradicate the infectious agents[11]

Bacterial airway infections in patients with a normal mucosa are relatively easy to treat with antibiotics. This is unfortunately not the case for CF patients and the myriad of infections they acquire during their lifetime leave each patient with a high need for recurrent antibiotic treatments. This is a multifactorial phenomenon and there are a lot of theories that try to explain this[12-14]. The most obvious reason for a treatment failure is the hindered diffusion of the antimicrobial agent through the thick and viscous mucus layer[15, 16]. However, according to recent findings, the main reason may reside in limited oxygen availability in some parts of the airways[17, 18]. These highly different oxygen environments are due to the human physiology of the airways and furthermore endured by the consumption from epithelial and immune cells in the local surroundings.

As *Pseudomonas aeruginosa (P. aeruginosa)* infections are almost inescapable in CF patients, especially in older patients, this makes *P. aeruginosa* an important organism for studies of “oxygen” phenomena[19]. *P. aeruginosa* is a facultative anaerobic bacteria[20] with reduced growth rate[21] and metabolic activity[18] at low oxygen levels. Antibiotics such as tobramycin, ciprofloxacin, and tetracycline preferentially kill the physiologically active bacteria living at high oxygen levels (aerobic environment), while colistin is more effective on the physiologically inactive bacteria growing in an anaerobic environment[10, 22].

An antibiotic treatment can seem eventually successful, yet after a few months the very same bacteria that were responsible for the infection can reappear, possibly as a result of reinoculation from the anaerobic sinus[6]. In this context the sinuses could very well serve as a reservoir for “sinus” bacteria, which are difficult to treat with antibiotics and can cause the reinfection of otherwise cleared patients.

The now classical ways of studying CF related bacterial infections, primarily *P. aeruginosa*, are either to use animal models or to grow the bacteria in flow-cell systems.

A number of different animals have been tried as models of chronic infections in CF patients[23]. This includes rats[24-26], guinea pigs[27], cats[28] and rhesus monkeys[29, 30]. However the most important animal model is a mouse[31-34]. The use of an animal models is expensive and rise ethical concerns[35, 36]. Besides, the animal models of CF related infections are still not ideal, mainly because of immune response differences between man and e.g. mouse, and because the lung pathology after infection is very different in animals compared to humans.

In flow-cell based systems, the bacteria are allowed to form a biofilm on a surface, as in the airways, and can then be monitored using a confocal microscope[11, 37]. However, this is not a suitable model for the human airways as they are subdivided into aerobic and anaerobic compartments.

The advancement in micro- and nanofabrication and assembly, as well as better understanding of microfluidics, has made possible the development of devices for modelling different tissue organs. Thanks to these devices, the control over the environment, relations and interactions between the cells and tissues at microscale with high spatial and temporal resolution can be achieved[38, 39]. The yet small but fast growing number of microdevices that can mimick different and even entire organs have been reported. These include blood vessels[40], bones[41], muscles[42], liver[43-46], brain[47], guts[48], kidneys[49, 50], endothelia[51] and blood-brain barrier[52].

In the field of mimicking the human airways, Huh *at al.*[53, 54] proposed a microfluidic device that can simulate injuries to the airways epithelia done by liquid plug flow. Recently, the same group proposed a model of the vacuoles in the lung[55]. In this work the phagocytosis of planktonic Escherichia coli cells by neutrophils on the epithelial surface was shown.

In our previous work[21] we have shown the possibility of using a poly(dimethylsiloxane) (PDMS) membrane and an oxygen scavenging liquid to control the oxygen gradient within cell culture microchambers. However, according to the authors' best knowledge, the microfluidic model of different compartments of the human airways that would allow to observe the influence of the microenvironment of these compartments on the recurrence of CF related infections has not been reported previously.

Therefore, the aim of this work was to make a model system, which simulates the three compartments of the airways to better understand the interplay between them. Using this artificial airways model, we can look into the bacterial details in the three compartments, their transmitting interaction, and the states of the bacterial inhabitants before, during and after antibiotic treatment.

2 Microfluidic Airways Model

The three sections of human airways: the conductive airways (trachea, bronchi and bronchioles), which are considered micro-aerobic, the highly aerobic gaseous exchange compartments (the alveoli) and the compartments of the paranasal sinuses, which are basically anaerobic (Fig. 1 A), are reproduced in this Microfluidic Airways Model (MAM). This is realized by constructing cell culture microchambers with different oxygen levels (Fig. 1 B). A microchamber with atmospheric air oxygenated media (aerobic environment) is connected by a channel to a microchamber with culture media saturated below the atmospheric air saturation level (micro-aerobic environment). This chamber is consecutively connected to a chamber with deoxygenated media (anaerobic environment). The connections between the chambers as well as outlets can be closed and opened

and the actual oxygen level in the compartments is determined by an oxygen probe. The entire system is actuated by peristaltic micropumps.

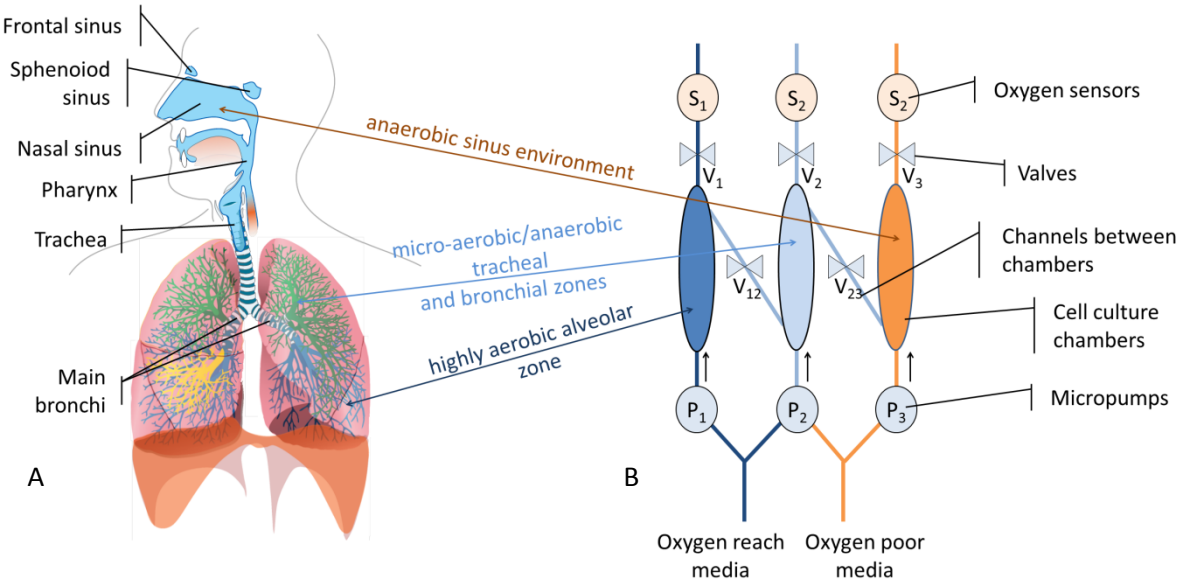

Fig. 1 (A) The human airways system and (B) the Microfluidic Airways Model (MAM)

3 Design

The above model was implemented, as a modular system comprised of the following distinct modules: a modified previously described multichannel microfluidic peristaltic pump[56, 57], a bubble trap, gas exchange and cell culture chambers (Fig. 2). The system allows to simultaneously cultivate cells in 8 chambers (3 of them facilitate aerobic environment, 2 micro-aerobic environment and 3 anaerobic environment).

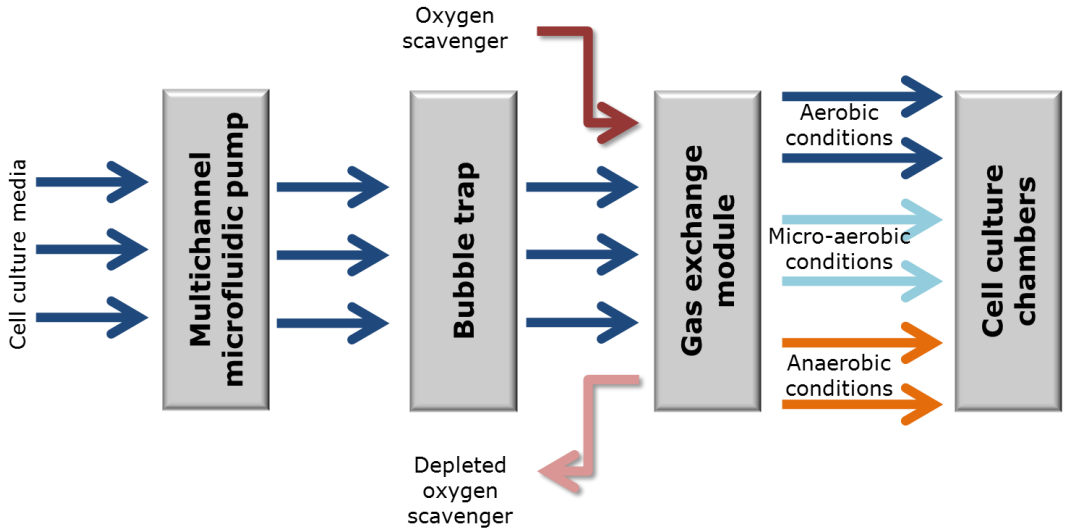

Fig. 2 Modular implementation of MAM

These modules can be attached to form a microfluidic platform. The detailed design of each of these modules and the platform is available in the electronic supplementary information (ESI) ‡.

4 Materials and methods

4.1 Microfabrication

The material of choice for most of the parts was polycarbonate (PC) (Nordisk Plast A/S, Denmark). This material exhibits low oxygen permeability (1.8 barrer[58]), very good mechanical and optical properties[59] as well as being resistant to alcohols and oils, which is important for sterilization and microscopy. The structures in PC were obtained by micromilling (Mini-Mill/3PRO, Minitech Machinery Corp., USA) followed by tetrahydrofuran vapour assisted bonding (50°C, 1.5 MPa).

PDMS inlays were fabricated by casting the silicone mixture (Sylgard 184, Dow Corning Corp., USA) against the milled mould. The PDMS parts were bonded to PC using silicone adhesive tape (ARcare® 91005, Adhesive Research, Inc., Ireland). The tape was cut into the desired shape using laser ablation (48-5S Duo Lase carbon dioxide laser, SYNRAD Inc., USA).

The gaskets used for sealing the modules to the platform, as well as check valves, were fabricated by milling in fluoroelastomer VITON A (J-Flex Rubber Products, UK).

4.2 Cultivation of *P. aeruginosa* strains

The P. aeruginosa laboratory strain PAO1 was used for all biofilm experiments. PAO1 was originally isolated from a burn wound [60]. PAO1 was fluorescently tagged at a neutral chromosomal locus with GFP or mRFP1 with miniTn*7* constructs as previously described[61]. A FAB medium[62] supplemented with 0.3 mM glucose and 65 mM KNO_3 (FAB-GN) was used for biofilm cultivation. All biofilms and batch cultures were grown at 37°C. PAO1 was pre-cultured overnight in Luria Bertani (LB) media and prepared for inoculation in FAB-GN media. The overnight culture was diluted to an OD_{600} of 0.01 and subsequently 100 µl was inoculated with a Gilson P200 pipette through the designed inlets. In order to visualise the bacteria migration, the anaerobic culture chambers were inoculated with the GFP tagged strain and microaerobic and aerobic chambers were inoculated with the mRFP1 tagged strain. The device was left upside down for an hour without media flow. Following the one hour incubation period, the media flow was started at 500 $\mu l \cdot h^{-1}$ per channel. After 48 hours of cultivation in the growth chambers the media was exchanged to media supplemented with 50 $\mu g \cdot ml^{-1}$ of the antibiotic, Ciprofloxacin (Sigma-Aldrich, Denmark A/S). 24 hours antibiotic treatment was followed by staining with 1 µM SYTOX® Blue dead cell stain (Molecular Probes, Invitrogen, Denmark). The chambers were left for 48 hours running on media without Ciprofloxacin. This was done in order to subsequently evaluate the cells ability to migrate between oxygen gradients. Interconnection was made between the chambers and cells were allowed to migrate for 24 hours before analysed with confocal laser scanning microscopy.

The interconnections between chambers were made with PVC tubing attached to PEEK connector plugs that were inserted into the specific chambers with different oxygen levels.

4.3 Dissolved oxygen level control

In order to control the dissolved oxygen levels in the cell culture media, one of the PDMS gas exchange module inlays was supplied with an oxygen scavenger (10% sodium sulphite solution with 0.1 mM $CoSO_4$ as catalyst, both from Sigma-Aldrich Denmark A/S). The second inlay was left open to atmospheric air.

Determination of the oxygen levels in the cell culture chambers was achieved using the phosphorescent oxygen-sensitive nanoprobe based on Platinum(II)- tetrakis-(pentafluorophenyl)

porphine (PtTFPP) dye[63] (Luxcel Biosciences, Ireland). The oxygen levels were determined by: (i) phosphorescence intensity and lifetime measurements on an Axiovert 200 wide-field microscope (Carl Zeiss, Germany) upgraded for phosphorescence lifetime imaging (LaVision Biotec, Germany), and (ii) phosphorescence lifetime measurements on a multi-label plate reader (Victor2, Perkin-Elmer Life Sciences, USA). The imaging experiments were performed as described in[64] using pulsed excitation with a 390 nm LED and emission collection at 655±50 nm. Plate reader measurements were performed as described in[63], using excitation at 340 nm and emission at 642 nm. For such measurements the device was inoculated with non-fluorescent *P. aeruginosa* laboratory strain PAO1, then maintained under a flow of medium, containing 0.01 mg.ml^{-1} of probe, for 12h and then washed with medium. Thus, biofilms stained with the phosphorescent probe were produced in the device, which can be used to monitor oxygenation and conduct biological experiments for several days.

The correlation between the phosphorescence intensity or photoluminescence lifetime and dissolved oxygen concentration was determined by two-point calibration: at 0% and 100% of atmospheric air oxygen saturation in the culture media. The 0% atmospheric air oxygen saturation was obtained by supplementing the glucose containing culture media with glucose oxidase (Sigma-Aldrich Denmark A/S). Each cell culture chamber was calibrated separately.

4.4 Confocal microscopy and image analysis

Confocal fluorescence images were taken with a Leica TCS SP5 microscope using a 50x/0.75W objective. 4 random pictures were taken from each chamber. Settings for visualization of the probes were: 514 nm excitation and 613-688 nm emission for mRFP1; 488 nm excitation and 517-535 nm emission for GFP; 458 nm excitation and 475-490 nm emission for SYTOX® Blue dead stain. All images were processed by the Imaris 7 software package (BITPLANE AG, Zürich, Switzerland).

5 Results

5.1 Integration of the modular microfluidic system

The microfluidic modules described in ESI‡ were successfully fabricated and assembled on a microfluidic platform (Fig. 3A). The system was integrated with 16-channel peristaltic micropump. The pump was actuated by two motors obtained from commercially available LEGO® Mindstorms® NXT 2.0 robotic kit[65] (The LEGO Group, Denmark) (Fig. 3B)[57].

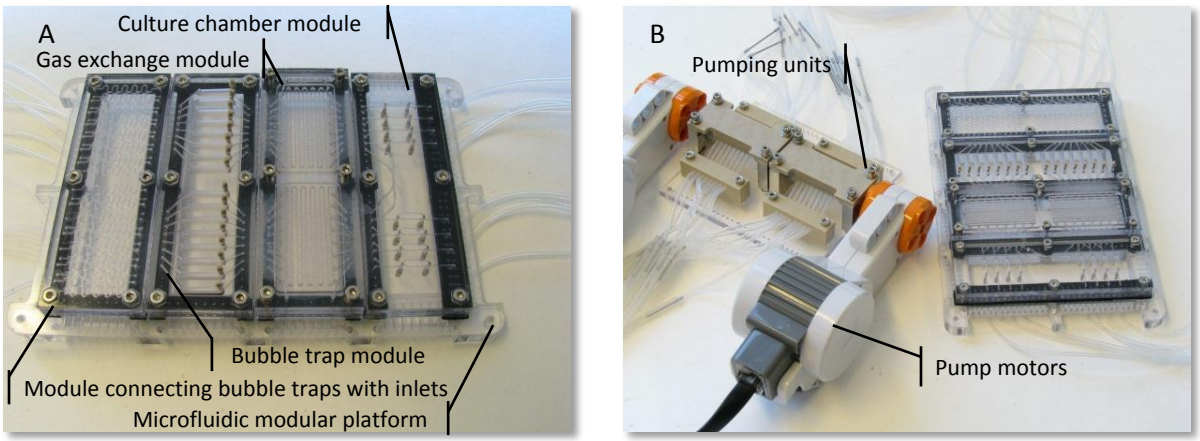

Fig. 3 (A) Microfluidic platform with modules and the peristaltic micropump (B).

5.2 Determination of the dissolved oxygen level

The correlation between the phosphorescence intensity of the *P. aerugionsa* biofilm stained with the PtTFPP nanoprobe in the aerobic and anaerobic environments was investigated in order to determine the oxygen removal efficiency from the culture media using the gas exchange module (Fig. 4). The phosphorescence intensity increased approximately two-fold in anaerobic conditions as compared with aerobic conditions.

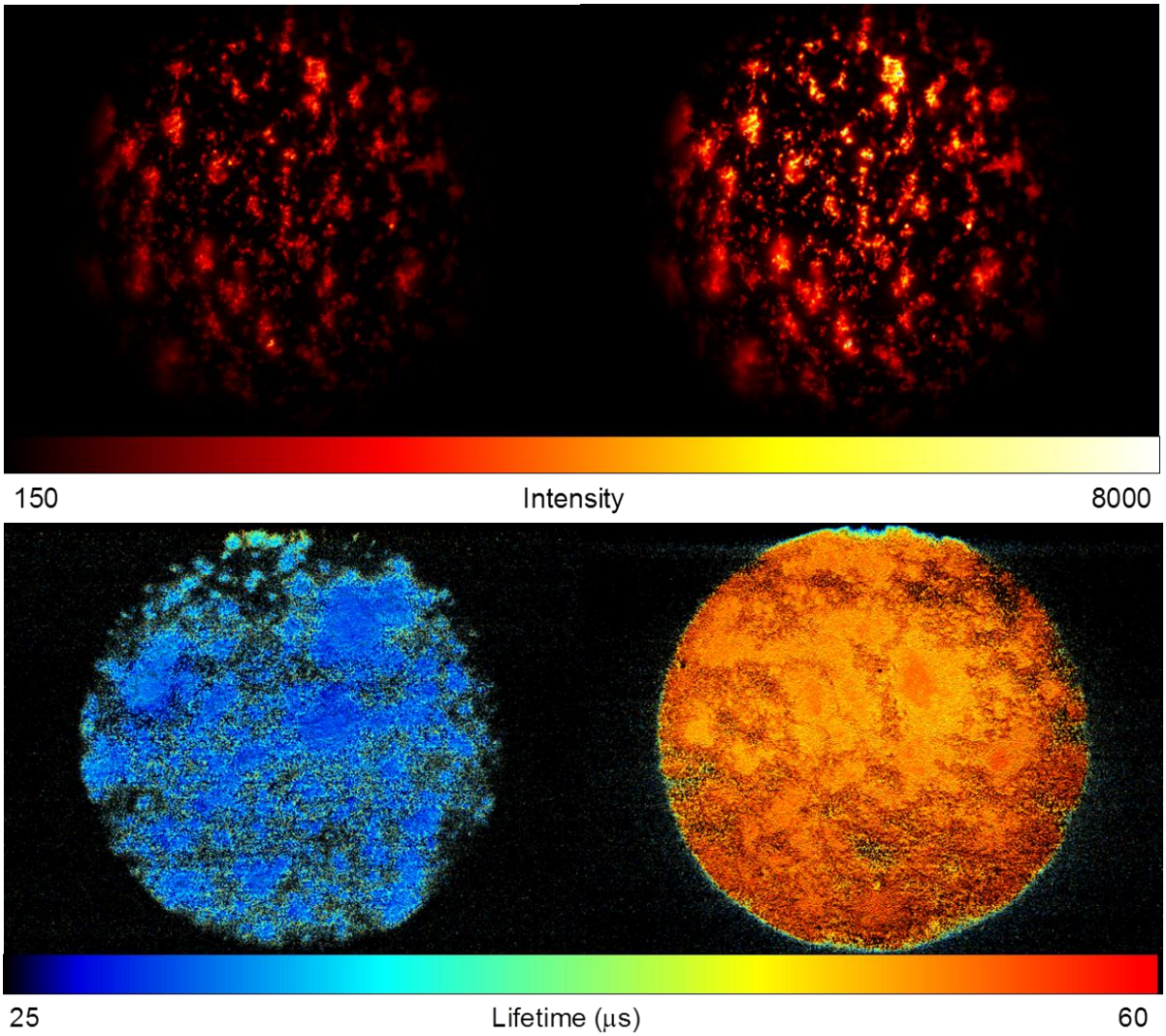

Fig. 4 Phosphorescence intensity (top panel) and lifetime (bottom panel) images of the *P. aeruginosa* biofilm stained with the PtTFPP nanoprobe in the culture chambers with high (left) and low (right) oxygen concentration.

A two step calibration curve was established by measuring The photoluminescence lifetime of the nanoprobe in oxygen free and atmospheric air-saturated media. The photoluminescence lifetime was determined to be 54.5±1.3 µs (oxygen free media) and 29.7±0.6 µs (and atmospheric air-saturated media). Oxygen concentration in atmospheric air-saturated media was determined to be 0.281 mM [66]. The measurements were performed at room temperature. Assuming a reversible collisional quenching model[67], the Stern-Volmer constant was determined to be 2.97 mM^{-1}.

The photoluminescence lifetimes of the nanoprobe in the chambers, resembling aerobic, micro-aerobic and anaerobic environments, were: 30.5 µs, 35.8 µs and 51.1 µs, respectively, which corresponds to 94.2%, 62.7% and 7.9% of atmospheric air-saturation of the culture media according to the two-point calibration curve.

5.3 Cultivation of *P. aeruginosa* strains in different oxygen environments

PAO1 biofilm formation was analysed after 24 hours after inoculation. In order to follow the trail of each specific population following each inoculation, we used differently fluorescently tagged versions of PAO1. The formation of the initial 24 hour biofilm under different oxygen environments in presence of nitrate as an alternative electron acceptor, gives rise to highly equivalent biofilm formations within the oxygen compartments.

The green 3D biofilm presentation (Fig. 5A) originates from GFP tagged bacteria and was cultivated under the lowest oxygen saturation. The red biofilm derives from mRFP1 tagged bacteria and was cultivated in microaerobic (Fig. 5B) and aerobic conditions (Fig. 5C). However, under the tested conditions in a minimal media, the biomass within first 24 hours of growth reached highly equivalent magnitudes of biomass regardless of oxygen tension. Under anaerobic conditions, supplemented with nitrate as electron acceptor, PAO1 has in LB media shown to develop 3 fold more biomass[68].

In order to evaluate the efficiency of the antibiotic ciprofloxacin on PAO1 biofilms under conditions on differentially lowered oxygen availability in a FAB-GN media, each chamber was challenged with the same ciprofloxacin concentration. After 24 hours of incubation each chamber received media supplemented with 50 $\mu g \cdot ml^{-1}$ of the antibiotic ciprofloxacin for a period of 24 hours. The treatment would present the differences in the effectiveness of the antibiotic in a developing PAO1 biofilm. Dead cells in the biofilms were visualized by staining each chamber with Sytox® blue dead cell stain (Fig. 5D-F). The effect of the ciprofloxacin on the PAO1 biofilm was highly dependent on the oxygen environment PAO1-GFP biofilm was much more susceptible to the antibiotic treatment than biofilm formed under higher oxygen concentrations. The antibiotic concentration was chosen to eradicate the majority of cells in the establishing biofilms, though low enough to allow surviving cells. PAO1 had in that sense been established enough to produce a healthy biofilm and represent a community associated environment.

Following the 24 h treatment with ciprofloxacin, the chambers were taken off the antibiotic containing media for 48 hours and connections between the different oxygen environments were made (Fig. 5G-I) (see connection details in the ESI). This enabled tracking of the bacteria in a novel way that has previously not been possible. We setup the system in a way to follow in which direction, if any, the surviving bacteria would move. As the ciprofloxacin treatment had been stopped the only difference between the chambers were the differences in oxygen concentrations. The small green clusters on Fig. 5H and I come from the GFP tagged bacteria. This proves that PAO1 moves from chambers with low oxygen tension (Fig. 5G) to microaerobic (Fig. 5H) and aerobic chambers (Fig. 5I).

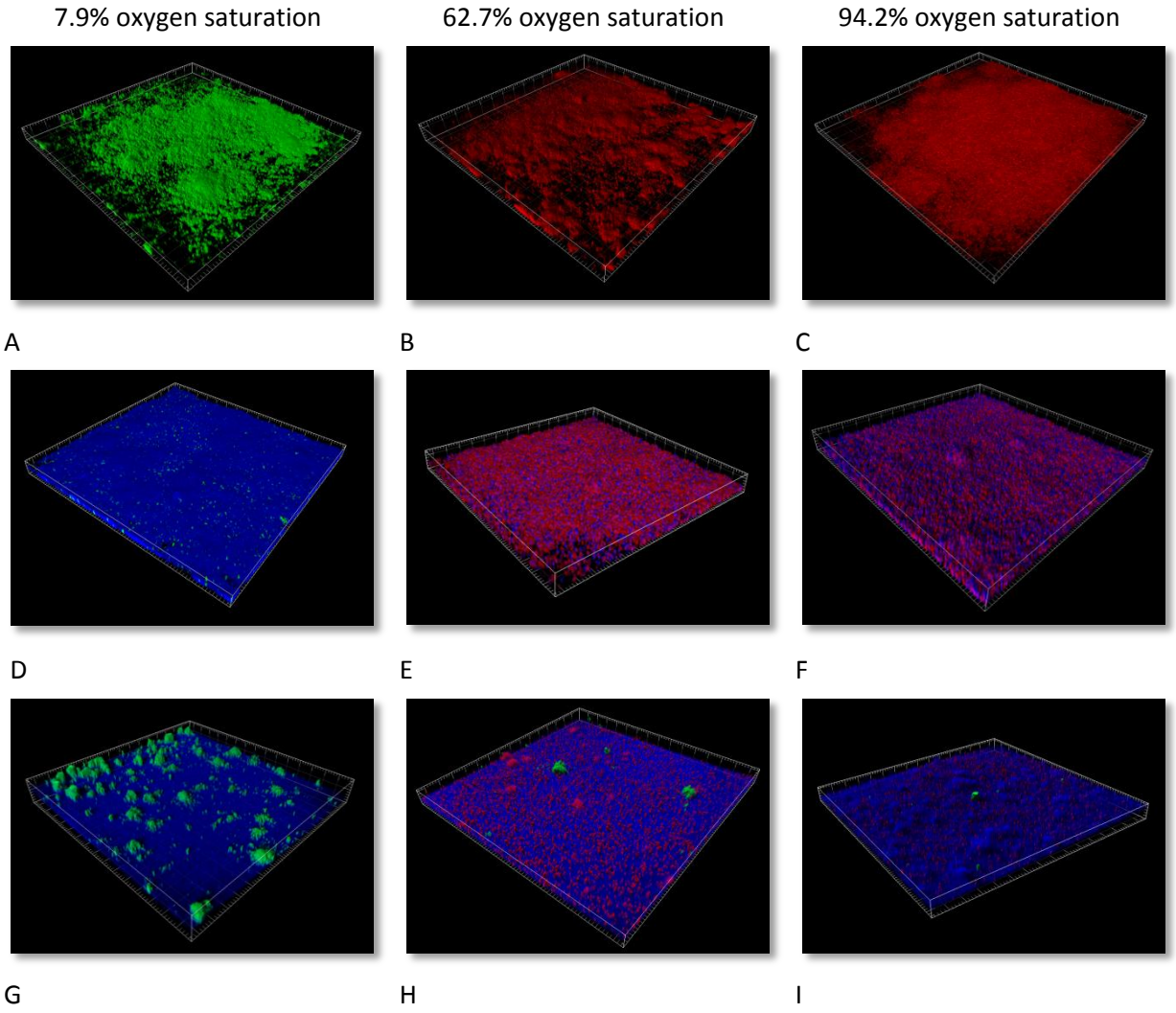

Fig. 5. 3D representation of the PAO1 biofilms at different oxygen saturation in FAB-GN media (minimal media supplemented with nitrate). PAO1 expresses either the fluorescent protein GFP or mRFP1. A-C: 24 hours old biofilms in FAB-CN media. D-F: 48 h after inoculation the cells were challenged with 50 µg·ml^{-1} Ciprofloxacin for 24 hours and then stained with dead stain SYTOX® Blue. G-I: Interconnected chambers of the different oxygen saturation environments.

6 Discussion and conclusions

In this paper we describe design, fabrication, working principle and application of a highly complex modular microfluidic system. Integration of different modules, bringing in such important functionalities as multichannel fluid control, bubble trapping, gas control - exchange and bacterial culturing on a microfluidic lab-on-a-chip system, has been shown to be successfully achieved. The modularity allows addition and removal of the different functionalities. The design permits easy reconfiguration and tailoring of the system to match particular needs. In case of malfunctions in a single module, the system benefits from its modular construction and allows uncomplicated exchange of the broken module without the need for fabrication of other essential parts of the system. This is particularly important in the field of life science microfluidic systems, in which not yet all of these components are suitable for mass production. Furthermore it allows quick prototype testing of different system configurations.

The microfluidic system in its present configuration enables comparison of changes between anatomically driven oxygen tensions in different compartments of the CF airways model, as well as full control and sensing of dissolved oxygen levels. By making the system compatible with common substrates such as microscope slides and multitier plates, it enables research staff to use standard laboratory equipment such as standard microscopes and multitier plate readers.

Furthermore, the microfluidic CF airways model permits to freely reconfigure connections between oxygen rich and oxygen depleted regions without bringing restrictions to the researcher in the design of experiments. It enables to mimic some different conditions and diseases in patients suffering from CF, such as clogging of the ostia in recurrent sinusitis[4, 69] or the development of mucus plugs[70] in the bronchioles. These experiments were not previously possible to perform in standard *in vitro* flow-cells models for biofilm studies. *In vivo* models will usually not allow precise control of such important conditions.

Moreover, the use of this microfluidic system, instead of a CF airways animal model, is cheaper, safer and easier to handle for researchers. Importantly, it furthermore does not raise any ethical concerns, which is the case for the use of animal models in medical research.

We demonstrated the application of our microfluidic airway model for studying *P. aeruginosa* PAO1 under different oxygen levels in response to treatment with ciprofloxacin. We have in this way explicitly shown that the system is an asset in reliable and controllable biofilm evaluations for treatment with antibiotics at reduced oxygen concentrations. Importantly, such a system allows testing of very small volumes thereby minimizing the use of large amounts of expensive antimicrobials. PAO1 survival was shown to be highly dependent on the amount of oxygen available during the antimicrobial treatment. This corresponds very well with previous studies where it was shown that higher metabolic rate, in nitrate supplemented media under anaerobic conditions, lead to a lower survival rate of the bacteria[71].

We have shown that PAO1 under lowered oxygen concentrations moves towards higher oxygen concentrations even in nitrate supplemented media. The effect of the presence of nitrate, which serves as final electron acceptor for anaerobic nitrate respiration (denitrification) utilized by *P. aeruginosa*, is not favoured in the presence of oxygen and drives the migration towards the higher oxygen gradient. The scenario can mimic the reinoculation of the lower respiratory tract, previously cleared with the antibiotic treatment from the sinuses. This effect is hypothesised as the main reason for recurrent infections in CF patients[17].

7 Acknowledgements

We would like to acknowledge for the funding of Ph.D. stipends by The Technical University of Denmark as well as the EU funded FP7 project EXCELL.

8 References

1. D. J. Smith, E. A. Gaffney and J. R. Blake, *Respir. Physiol. Neurobiol.*, 2008, **163**, 178-188.
2. V. L. Campodónico, M. Gadjeva, C. Paradis-Bleau, A. Uluer and G. B. Pier, *Trends Mol. Med.*, 2008, **14**, 120-133.

3. S. M. Moskowitz, J. F. Chmiel, D. L. Sternen, E. Cheng, R. L. Gibson, S. G. Marshall and G. R. Cutting, *Genet. Med.*, 2008, **10**, 851-868.
4. R. Aust and B. Drettner, *Acta oto-laryngologica.*, 1974, **78**, 264-269.
5. M. M. Norton, R. J. Robinson and S. J. Weinstein, *Phys. Rev. E: Stat., Nonlinear, Soft Matter Phys.*, 2011, **83**.
6. A. M. Hekiert, J. M. Kofonow, L. Doghramji, D. W. Kennedy, A. G. Chiu, J. N. Palmer, J. G. Leid and N. A. Cohen, *Otolaryngology - Head and Neck Surgery*, 2009, **141**, 448-453.
7. K.-Y. Jih, M. Li, T.-C. Hwang and S. G. Bompadre, *J Physiol*, 2011, **589**, 2719-2731.
8. M. Antunes and N. Cohen, *Curr Opin Allergy Clin Immunol*, 2007, **7**.
9. T. Leal, I. Fajac, H. L. Wallace, P. Lebecque, J. Lebacq, D. Hubert, J. Dall'Ava, D. Dusser, A. P. Ganesan, C. Knoop, J. Cumps, P. Wallemacq and K. W. Southern, *Clin. Biochem.*, 2008, **41**, 764-772.
10. T. Bjarnsholt, P. O. Jensen, M. J. Fiandaca, J. Pedersen, C. R. Hansen, C. B. Andersen, T. Pressler, M. Givskov and N. Hoiby, *Pediatr Pulmonol*, 2009, **44**, 547-558.
11. T. Bjarnsholt, in *Biofilm infections*, Springer, New York ; London :, 2010, ch. Different Methods for Culturing Biofilms In Vitro, p. 251.
12. J. W. Costerton, P. S. Stewart and E. P. Greenberg, *Science (New York, N.Y.)*, 1999, **284**, 1318-1322.
13. T. Bjarnsholt, in *Biofilm infections*, Springer, New York ; London :, 2010, ch. Antibiotic Tolerance and Resistance in Biofilms, p. 216.
14. S. S. Jedlicka, J. L. Rickus and D. Zemlyanov, *J. Phys. Chem. C*, 2010, **114**, 342-344.
15. K. Rasmussen and Z. Lewandowski, *Biotechnol. Bioeng.*, 1998, **59**, 302-309.
16. P. S. Stewart, *Antimicrob. Agents Chemother.*, 1996, **40**, 2517-2522.
17. K. Aanaes, L. F. Rickelt, H. K. Johansen, C. von Buchwald, T. Pressler, N. Høiby and P. Ø. Jensen, *Journal of Cystic Fibrosis*, 2011, **10**, 114-120.
18. M. C. Walters, F. Roe, A. Bugnicourt, M. J. Franklin and P. S. Stewart, *Antimicrob. Agents Chemother.*, 2003, **47**, 317-323.
19. S. Moreau-Marquis, B. A. Stanton and G. A. O'Toole, *Pulm. Pharmacol. Ther.*, 2008, **21**, 595-599.
20. A. M. Guss, G. Roeselers, I. L. G. Newton, C. R. Young, V. Klepac-Ceraj, S. Lory and C. M. Cavanaugh, *The ISME journal*, 2011, **5**, 20-29.
21. M. Skolimowski, M. W. Nielsen, J. Emnéus, S. Molin, R. Taboryski, C. Sternberg, M. Dufva and O. Geschke, *Lab Chip*, 2010, **10**, 2162-2169.
22. J. Kim, J.-S. Hahn, M. J. Franklin, P. S. Stewart and J. Yoon, *J. Antimicrob. Chemother.*, 2009, **63**, 129-135.
23. I. Kukavica-Ibrulj and R. C. Levesque, *Lab. Anim.*, 2008, **42**, 389-412.

24.S. S. Pedersen, G. H. Shand, B. L. Hansen and G. N. Hansen, *APMIS : acta pathologica, microbiologica, et immunologica Scandinavica*, 1990, **98**, 203-211.

25.H. A. Cash, D. E. Woods, B. McCullough, W. G. Johanson, Jr. and J. A. Bass, *The American review of respiratory disease*, 1979, **119**, 453-459.

26.A. Sato, H. Kitazawa, K. Chida, H. Hayakawa and M. Iwata, *Drugs*, 1995, **49 Suppl 2**, 253-255.

27.J. E. Pennington, W. F. Hickey, L. L. Blackwood and M. A. Arnaut, *The Journal of clinical investigation*, 1981, **68**, 1140-1148.

28.M. J. Thomassen, J. D. Klinger, G. B. Winnie, R. E. Wood, C. Burtner, J. F. Tomashefski, J. G. Horowitz and B. Tandler, *Infect. Immun.*, 1984, **45**, 741-747.

29.A. T. Cheung, R. B. Moss, A. B. Leong and W. J. Novick, Jr., *J. Med. Primatol.*, 1992, **21**, 357-362.

30.A. T. Cheung, R. B. Moss, G. Kurland, A. B. Leong and W. J. Novick, Jr., *J. Med. Primatol.*, 1993, **22**, 257-262.

31.J. R. Starke, M. S. Edwards, C. Langston and C. J. Baker, *Pediatr. Res.*, 1987, **22**, 698-702.

32.C. Morissette, E. Skamene and F. Gervais, *Infect. Immun.*, 1995, **63**, 1718-1724.

33.M. M. Stevenson, T. K. Kondratieva, A. S. Apt, M. F. Tam and E. Skamene, *Clin. Exp. Immunol.*, 1995, **99**, 98-105.

34.P. K. Stotland, D. Radzioch and M. M. Stevenson, *Pediatr Pulmonol*, 2000, **30**, 413-424.

35.S. Creton, R. Billington, W. Davies, M. R. Dent, G. M. Hawksworth, S. Parry and K. Z. Travis, *Toxicology*, 2009, **262**, 10-11.

36.C. F. M. Hendriksen, *Expert Rev Vaccines*, 2009, **8**, 313-322.

37.M. Weiss Nielsen, C. Sternberg, S. Molin and B. Regenberg, *Journal of visualized experiments.*, 2011.

38.G. M. Whitesides, E. Ostuni, S. Takayama, X. Jiang and D. E. Ingber, *Annu. Rev. Biomed. Eng.*, 2001, **3**, 335-373.

39.J. El-Ali, P. K. Sorger and K. F. Jensen, *Nature*, 2006, **442**, 403-411.

40.M. Shin, K. Matsuda, O. Ishii, H. Terai, M. Kaazempur-Mofrad, J. Borenstein, M. Detmar and J. P. Vacanti, *Biomed. Microdevices*, 2004, **6**, 269-278.

41.K. Jang, K. Sato, K. Igawa, U. I. Chung and T. Kitamori, *Anal. Bioanal. Chem.*, 2008, **390**, 825-832.

42.M. T. Lam, Y. C. Huang, R. K. Birla and S. Takayama, *Biomaterials*, 2009, **30**, 1150-1155.

43.A. Carraro, W. M. Hsu, K. M. Kulig, W. S. Cheung, M. L. Miller, E. J. Weinberg, E. F. Swart, M. Kaazempur-Mofrad, J. T. Borenstein, J. P. Vacanti and C. Neville, *Biomed. Microdevices*, 2008, **10**, 795-805.

44.P. J. Lee, P. J. Hung and L. P. Lee, *Biotechnol. Bioeng.*, 2007, **97**, 1340-1346.

45. M. J. Powers, K. Domansky, M. R. Kaazempur-Mofrad, A. Kalezi, A. Capitano, A. Upadhyaya, P. Kurzawski, K. E. Wack, D. B. Stolz, R. Kamm and L. G. Griffith, *Biotechnol. Bioeng.*, 2002, **78**, 257-269.
46. S. R. Khetani and S. N. Bhatia, *Nat. Biotechnol.*, 2008, **26**, 120-126.
47. J. W. Park, B. Vahidi, A. M. Taylor, S. W. Rhee and N. L. Jeon, *Nat. Protoc.*, 2006, **1**, 2128-2136.
48. M. L. Shuler, G. J. Mahler, M. B. Esch and R. P. Glahn, *Biotechnol. Bioeng.*, 2009, **104**, 193-205.
49. R. Baudoin, L. Griscom, M. Monge, C. Legallais and E. Leclerc, *Biotechnol. Prog.*, 2007, **23**, 1245-1253.
50. K. J. Jang and K. Y. Suh, *Lab Chip*, 2010, **10**, 36-42.
51. J. W. Song, W. Gu, N. Futai, K. A. Warner, J. E. Nor and S. Takayama, *Anal. Chem.*, 2005, **77**, 3993-3999.
52. S. G. Harris and M. L. Shuler, *Biotechnol. Bioprocess Eng.*, 2003, **8**, 246-251.
53. D. Huh, H. Fujioka, Y. C. Tung, N. Futai, R. Paine, 3rd, J. B. Grotberg and S. Takayama, *Proc. Natl. Acad. Sci. U. S. A.*, 2007, **104**, 18886-18891.
54. H. Tavana, C. H. Kuo, Q. Y. Lee, B. Mosadegh, D. Huh, P. J. Christensen, J. B. Grotberg and S. Takayama, *Langmuir : the ACS journal of surfaces and colloids*, 2010, **26**, 3744-3752.
55. D. Huh, B. D. Matthews, A. Mammoto, M. Montoya-Zavala, H. Y. Hsin and D. E. Ingber, *Science*, 2010, **328**, 1662-1668.
56. P. Skafte-Pedersen, D. Sabourin, M. Dufva and D. Snakenborg, *Lab Chip*, 2009, **9**, 3003-3006.
57. D. Sabourin, D. Snakenborg, P. Skafte-Pedersen, J. P. Kutter and M. Dufva, *Proceedings of the Fourteenth International Conference on Miniaturized Systems for Chemistry and Life Sciences*, 2010, 1433-1435.
58. S.-H. Chen, R.-C. Ruaan and J.-Y. Lai, *J. Membr. Sci.*, 1997, **134**, 143-150.
59. D. Ogonczyk, J. Wegrzyn, P. Jankowski, B. Dabrowski and P. Garstecki, *Lab Chip*, 2010, **10**, 1324-1327.
60. B. W. Holloway, *J Gen Microbiol*, 1955, **13**, 572-581.
61. M. Klausen, A. Heydorn, P. Ragas, L. Lambertsen, A. Aaes-Jorgensen, S. Molin and T. Tolker-Nielsen, *Mol. Microbiol.*, 2003, **48**, 1511-1524.
62. S. J. Pamp and T. Tolker-Nielsen, *J Bacteriol*, 2007, **189**, 2531-2539.
63. A. Fercher, S. M. Borisov, A. V. Zhdanov, I. Klimant and D. B. Papkovsky, *ACS Nano*, 2011.
64. A. Fercher, T. C. O'Riordan, A. V. Zhdanov, R. I. Dmitriev and D. B. Papkovsky, *Methods Mol. Biol.*, 2010, **591**, 257-273.
65. LEGO® Mindstorms® NXT 2.0, http://mindstorms.lego.com/en-us/default.aspx.
66. G. Mehta, K. Mehta, D. Sud, J. W. Song, T. Bersano-Begey, N. Futai, Y. S. Heo, M.-A. Mycek, J. J. Linderman and S. Takayama, *Biomed. Microdevices*, 2007, **9**, 123 - 134.

67.D. B. Papkovsky, in *Methods Enzymol.*, eds. K. S. Chandan and L. S. Gregg, Academic Press, 2004, vol. Volume 381, pp. 715-735.

68.S. S. Yoon, R. F. Hennigan, G. M. Hilliard, U. A. Ochsner, K. Parvatiyar, M. C. Kamani, H. L. Allen, T. R. DeKievit, P. R. Gardner, U. Schwab, J. J. Rowe, B. H. Iglewski, T. R. McDermott, R. P. Mason, D. J. Wozniak, R. E. W. Hancock, M. R. Parsek, T. L. Noah, R. C. Boucher and D. J. Hassett, *Dev. Cell*, 2002, **3**, 593-603.

69.C. Carenfelt and C. Lundberg, *Acta Otolaryngol*, 1977, **84**, 138-144.

70.B. L. Odry, A. P. Kiraly, C. L. Novak, D. P. Naidich, J. Ko and M. C. B. Godoy, *Proceedings of SPIE--the international society for optical engineering*, 2009, **7260**, 72603B-72608.

71.T. A. Major, W. Panmanee, J. E. Mortensen, L. D. Gray, N. Hoglen and D. J. Hassett, *Antimicrob. Agents Chemother.*, 2010, **54**, 4671-4677.

Electronic Supplementary Information (ESI)

1 Detailed design of the microfluidic modules

1.1 Multichannel peristaltic micropump

The design of the multichannel peristaltic micropump was based on a previously reported system[1, 2] with two major changes. In the new design (Fig. 1), the previously used poly(dimethylsiloxane) (PDMS) inlays were exchanged with thin-walled poly(vinyl chloride) (PVC) tubing with 0.63 mm internal diameter (medical grade, Thoma Fluid, Reichelt Chemietechnik GmbH + Co, Germany). The module (Fig. 2A) was equipped with two separate micropumping units (Fig. 2B). Each unit (Fig. 2B) is capable of actuating up to 8 channels. In this way the capacity of each module is a total of 16 individual channels. The replacement of the PDMS inlays with PVC tubing allows us to skip the laborious process of the inlay moulding. Besides, PVC is a much more durable material than PDMS which makes the entire system more reliable. PVC is also known to be far more resistant to organic solvents and does not absorb hydrophobic agents from aqueous media as PDMS does.

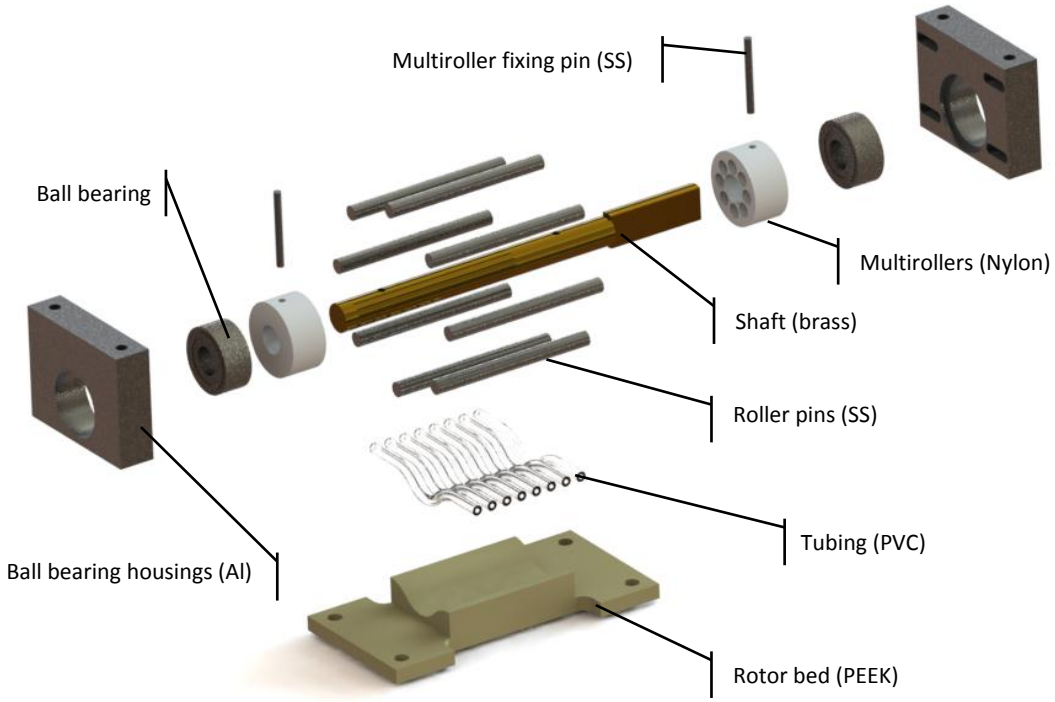

Fig. 1 Exploded view of the multichannel peristaltic micropump. The type of material for each fabricated part is indicated in parenthesis, the acronyms stands for: SS – stainless steel, Al –aluminium, PEEK – poly(ether ether ketone), PVC - poly(vinyl chloride), PC – polycarbonate.

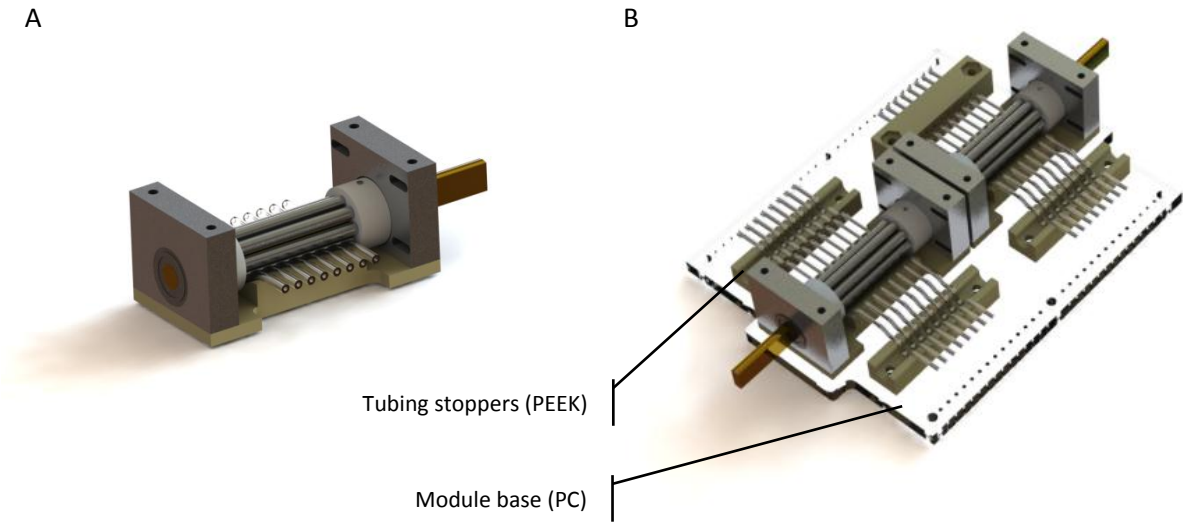

Fig. 2 Multichannel peristaltic micropump: (A) assembled micropumping unit, (B) module with two micropumping units facilitating 16 channels.

1.2 Bubble trap module

The array of bubble traps was designed according to previously reported work[3]. The entire module was made in polycarbonate (PC). Each bubble trap has a volume of 56 mm^3 and is equipped with a tapered opening on the top which serves as a vent. It can be closed or opened with the plug in order to release entrapped air bubbles (Fig. 3).

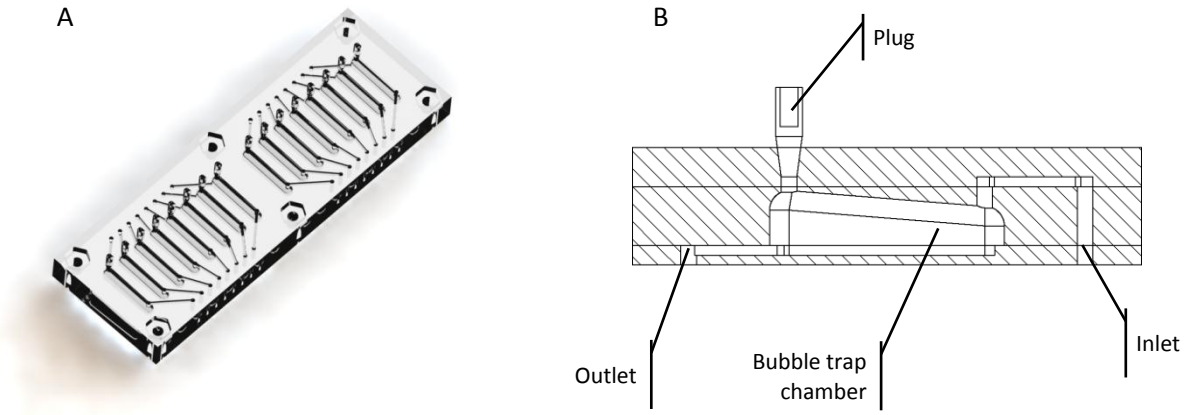

Fig. 3 Scheme of the bubble trap module: (A) image of the module, (B) cross-section of the bubble trap.

1.3 Gas exchange module

The gas exchange module allows oxygen saturation or desaturation of a desired culture media. The working principle of the module was communicated in our previous report[4]; here described briefly. It is based on the oxygen diffusion through gas permeable membranes made from PDMS. The culture media flows through the channels fabricated in PDMS. The channels were patterned with groves, similar as reported in our previous work[5], in order to improve mixing of the media. The oxygen can diffuse from the culture media through the integrated membrane to the channel filled with oxygen scavenging liquid. The scavenger (sodium sulphite) reacts with the available oxygen. In

the case, where the channels are filled with atmospheric air, the media is ensured to be saturated with oxygen. The PDMS inlays are enclosed in low gas permeability scaffold, made form PC, in order to separate the permeable material from the atmosphere (Fig. 4).

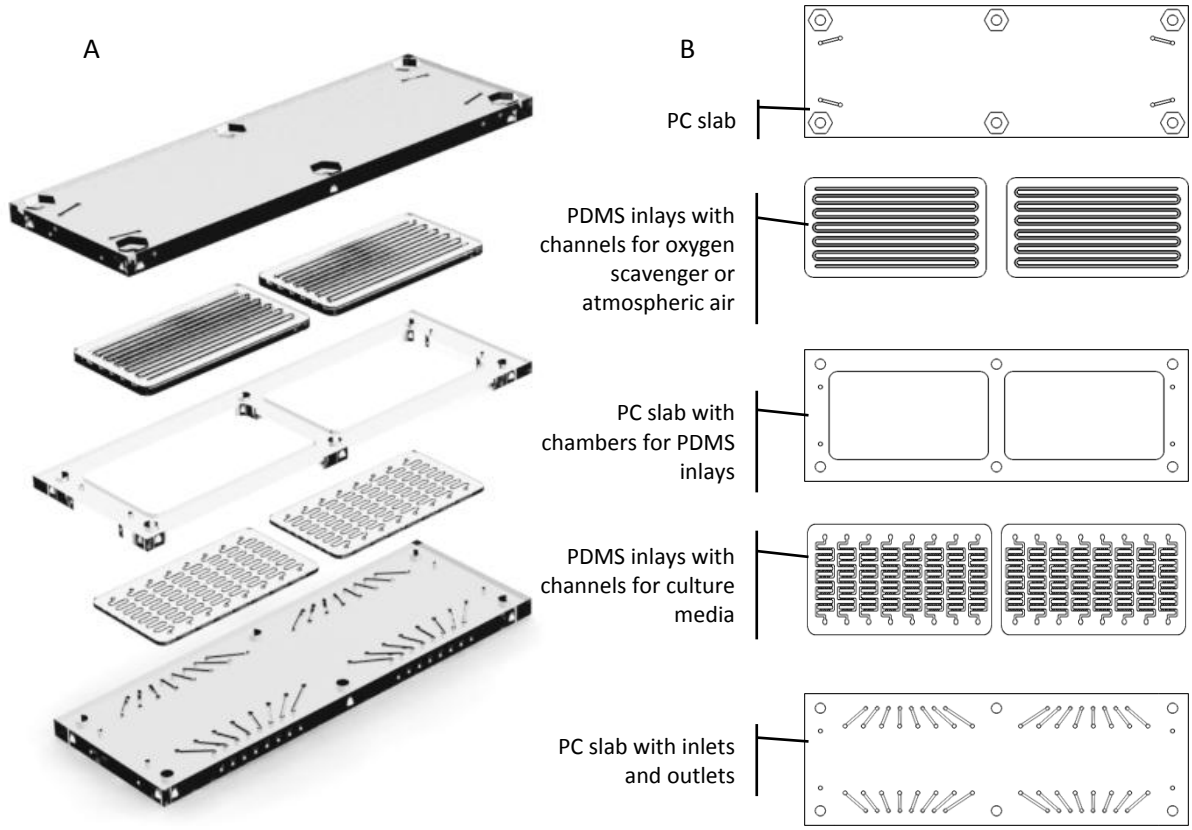

Fig. 4 Scheme of the gas exchange module: (A) exploded view of the module, (B) top view for on the module layers.

1.4 Culture chambers module

The culture chambers were designed to implement three different oxygen saturation environments (Fig. 5). The module consists of 8 chambers that can be interconnected by detachable PVC tubing. The volume of each chamber is 4.2 µl and the area for cells attachment equals to 12.7 mm^2. Each chamber has additional tapered openings: one near its inlet and the other near its outlet (Fig. 6). The opening near the inlet of the chamber is used as the inoculation site. It can be opened and closed with a plug in the same manner as the vents in the bubble trap module. Instead of plugs, these openings can be equipped with fittings and tubing in order to interconnect two chambers with different oxygen environments.

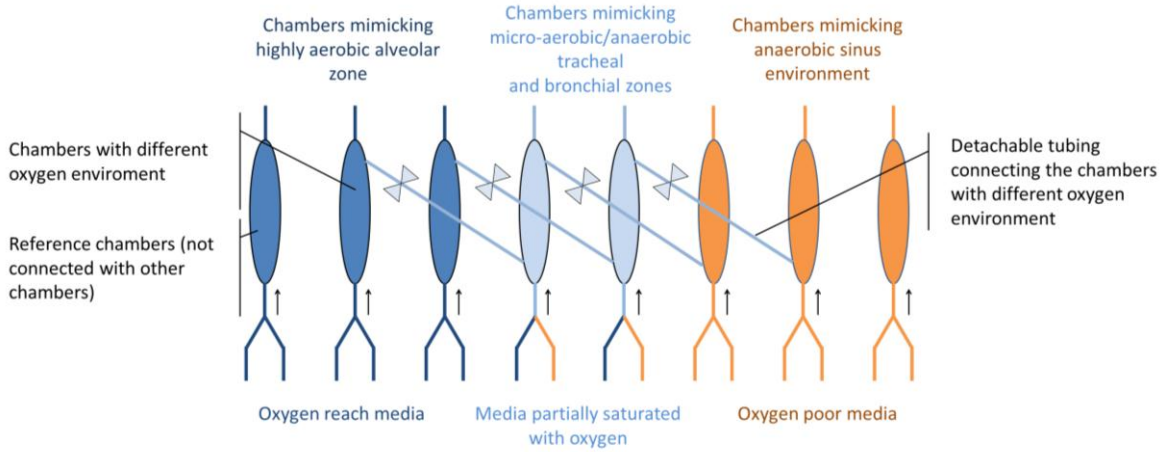

Fig. 5 The scheme of the cell culture chamber module facilitating different oxygen environments.

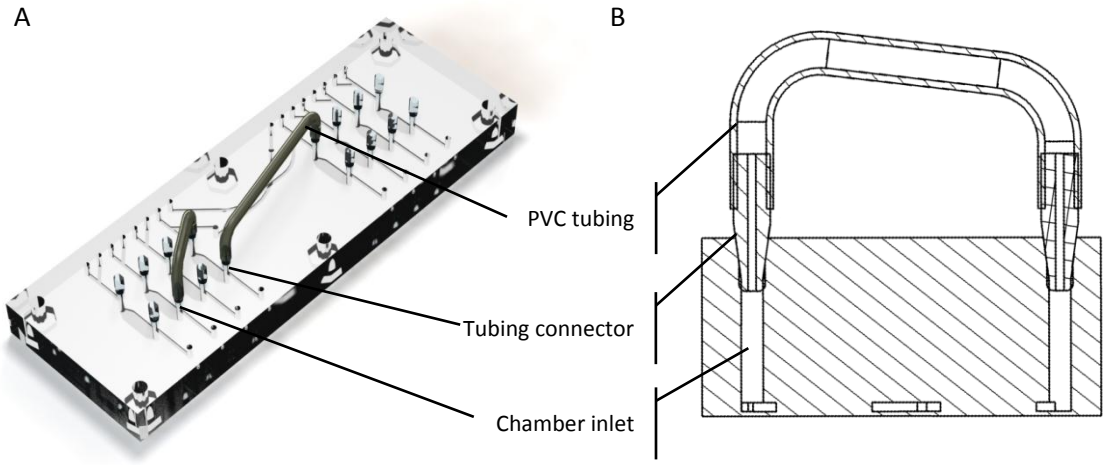

Fig. 6 Cell culture chamber module: (A) scheme of the module with plugs and tubing interconnecting different chambers (for clarity of the image, only two interconnections are shown), (B) cross-section of the fitting and tubing.

1.5 Check microvalve

The working principle of the designed check microvalve was based on a previous report[6]. An array of 28 check microvalves was fabricated in 1 mm thick fluoroelastomer (Fig. 7A), the same material that was used to fabricate the seals. The microvalves are clamped in-between the microfluidic modules and the platform. Each microvalve has a chamber with a 150 µm thick membrane (Fig. 7B). In the membrane there are two holes with Φ = 500 µm spaced 1.59 mm from each other (centre to centre). Such spacing is large enough to cover the holes of the microfluidic modules when the membrane is in a relaxed state. Membrane deflection is only possible inward the chamber thereby only allowing media flow in one direction (Fig. 7B).

The purpose of the microvalve is to stop the backflow from the outlet tubing while allowing the user to inoculate the system using standard laboratory micropipettes. The membrane thickness, as well as the size and spacing between the holes, was optimised in order to get the opening pressure low enough enabling the use of a micropipette (typically below 1 kPa).

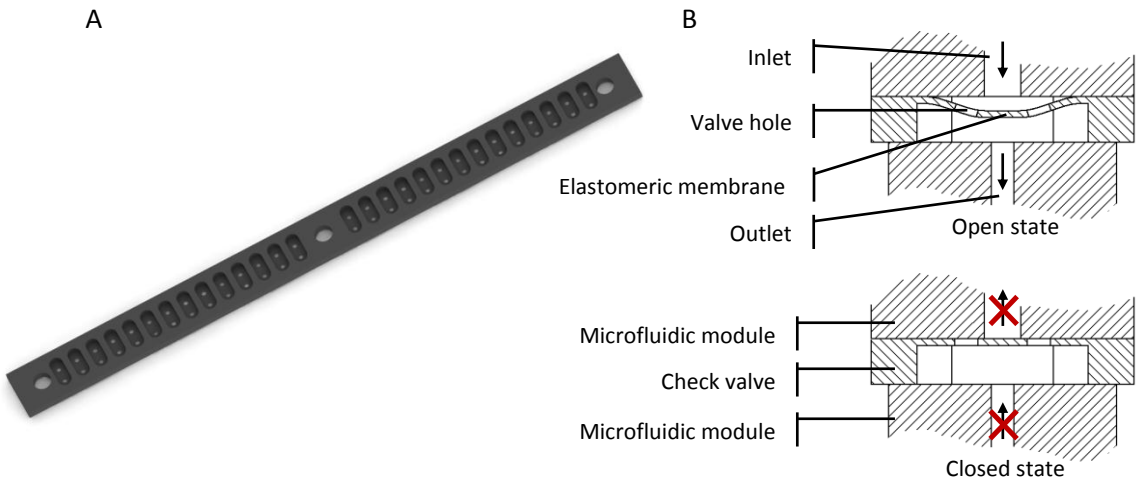

Fig. 7 Check microvalve: (A) scheme of the module with 28 independent microvalves, (B) the working principle of the valve

1.6 Modular platform

The platform was designed to comply with the microplate footprint standards[7, 8]. This allows the device to be used together with a broad range of commonly used laboratory equipment such as microtitre plate readers and microscopes. The platform can be equipped with up to 4 modules with a microscope slide size (76x26 mm). Modules can be serially interconnected by 28 independent channels at the long edges of a module. Additionally, each module has 8 inlets/outlets at each of the short edges. The platform has 28 independent inlets and the same amount of outlets (Fig. 8A).

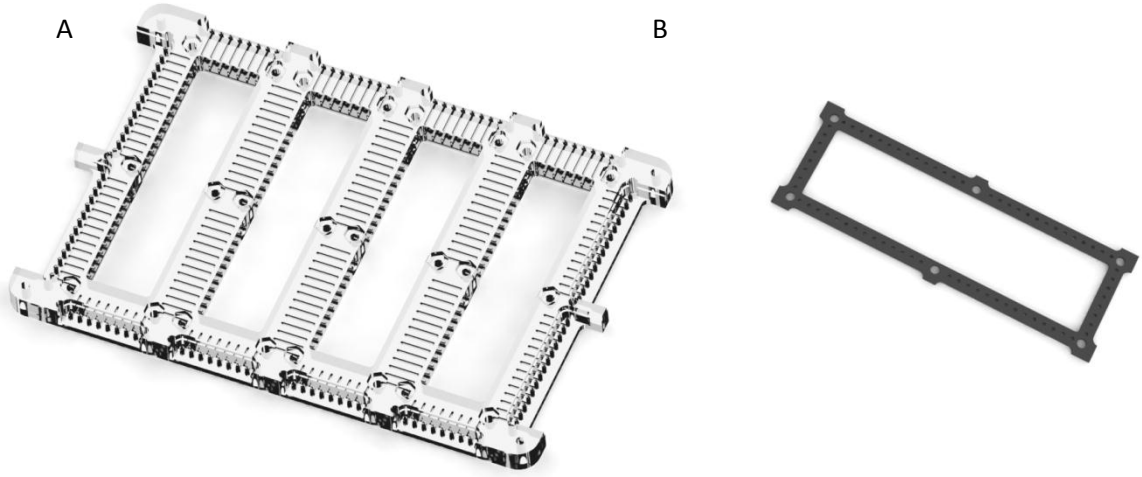

Fig. 8 (A) Microfluidic modular platform, (B) gasket used to seal the modules with the platform

Modules are attached to the platform by screws and nuts (Fig. 9) and all the microfluidic connections between the modules and platform are sealed by gaskets made from fluoroelastomer (Fig. 8B).

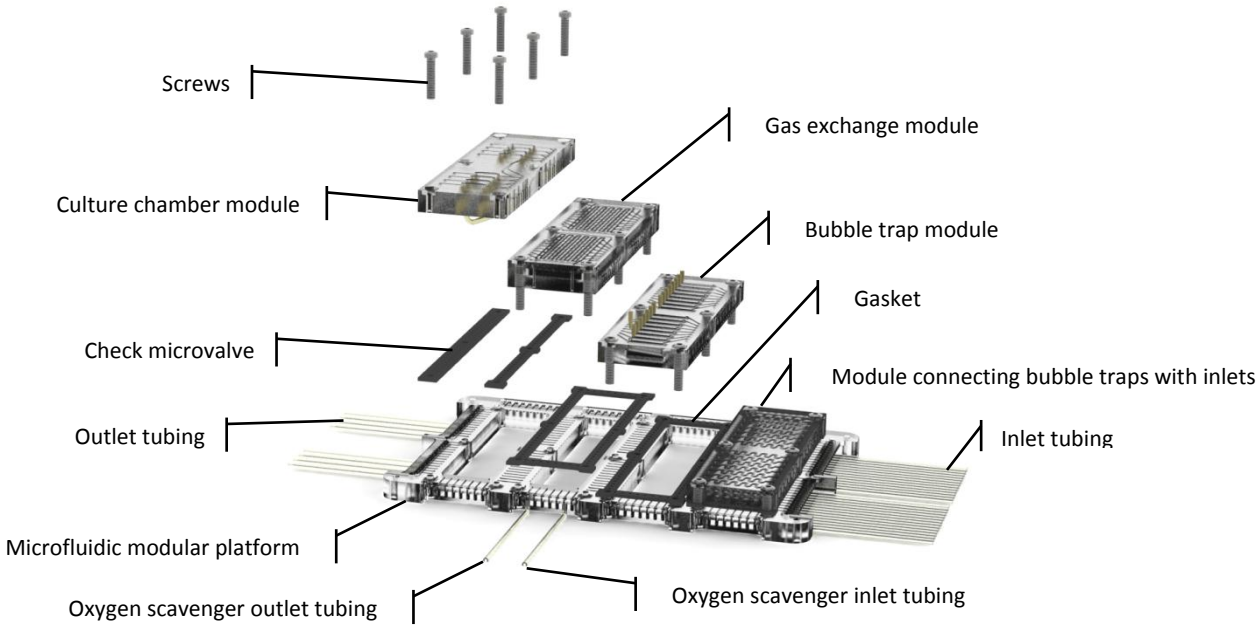

Fig. 9 Exploded view of the microfluidic platform with modules

2 References

1. P. Skafte-Pedersen, D. Sabourin, M. Dufva and D. Snakenborg, *Lab Chip*, 2009, **9**, 3003-3006.
2. D. Sabourin, D. Snakenborg, P. Skafte-Pedersen, J. P. Kutter and M. Dufva, *Proceedings of the Fourteenth International Conference on Miniaturized Systems for Chemistry and Life Sciences*, 2010, 1433-1435.
3. W. Zheng, Z. Wang, W. Zhang and X. Jiang, *Lab Chip*, 2010, **10**, 2906-2910.
4. M. Skolimowski, M. W. Nielsen, J. Emnéus, S. Molin, R. Taboryski, C. Sternberg, M. Dufva and O. Geschke, *Lab Chip*, 2010, **10**, 2162-2169.
5. T. Tofteberg, M. Skolimowski, E. Andreassen and O. Geschke, *Microfluidics and Nanofluidics*, 2010, **8**, 209-215.
6. D. Snakenborg, H. Klank and J. P. Kutter, *Microfluidics and Nanofluidics*, 2011, **10**, 381-388.
7. Microplates – Footprint Dimensions [ANSI/SBS 1-2004], http://www.sbsonline.com/msdc/pdf/ANSI_SBS_1-2004.pdf.
8. Microplates – Height Dimensions [ANSI/SBS 2-2004], http://www.sbsonline.com/msdc/pdf/ANSI_SBS_2-2004.pdf.

8.6 Paper VI

Skolimowski, M., Nielsen, M.W., Abeille, F., Lopacinska, J., D., Molin, S., Taboryski, R., Sternberg, C., Dufva, M., Geschke, O. and Emnéus, J., *Microfluidic model of cystic fibrosis bronchi.* Accepted for Proceedings of the Fifteenth International Conference on Miniaturized Systems for Chemistry and Life Sciences, 2011.

MICROFLUIDIC MODEL OF CYSTIC FIBROSIS BRONCHI

M. Skolimowski[1,2*], M. W. Nielsen[1,2], F. Abeille[1,2], J. Lopacinska[1], S. Molin[2], R. Taboryski[1], O. Geschke[1], C. Sternberg[2], M. Dufva[1] and J. Emnéus[1]

[1]*Technical University of Denmark, Department of Micro- and Nanotechnology, DENMARK*

[2]*Technical University of Denmark, Department of Systems Biology, DENMARK*

ABSTRACT

In this paper we report a microfluidic model to simulate the bronchi of a cystic fibrosis (CF) patient. The biochip is comprised of two cell culture chambers separated by a membrane. On top of the membrane an alginate hydrogel is formed in order to simulate the thick mucus layer spotted in a CF bronchi. In the bottom chamber a monolayer of epithelial cells are cultured to simulate the bronchi tissue. By inoculating the *pseudomonas aeruginosa* PAO1 strain to the hydrogel layer one can simulate bacterial infections commonly subjected to the CF patient, and the system can be applied for the studies on antibiotic treatment of bacterial infection related to CF.

KEYWORDS: cystic fibrosis, bronchi, model, microfluidic, microfabrication

INTRODUCTION

Here we report work towards a microfluidic system that simulates the cystic fibrosis (CF) bronchi and the impact of the mucus layer on the treatment of bacterial infections. The classical way of studying CF related bacterial infections, primarily *Pseudomonas aeruginosa*, is by growing them in flow-cell systems [1,2]. In these flow cells bacteria are capable of forming biofilm, as in the airways, and can then be monitored using confocal microscopy [3]. However, the bacteria in CF patient bronchi are not subjected to a constant flow of nutrients as in flow-cell based systems. Instead they embed in the mucus that covers the bronchi epithelia through which the nutrients and metabolites are diffusing (Figure 1A). Moreover, the content of the mucus highly affects bacterial attachment and biofilm growth. Consequently, the biological response for biofilm drug treatments can be altered by changes in the mucus [4].

THEORY

While the human primary bronchi have a relatively large lumen diameter (order of magnitude of centimetres), the respiratory bronchioles are about 1 mm in diameter. Therefore, in order to be able to mimic it as closely as possible to the *in vivo* conditions, a microfluidic system is required. The presented microfluidic model of the CF bronchi consists of two chambers separated by a microporous membrane (Figure 1B). The membrane is the underlying support for a hydrogel, which mimics the mucus layer in the CF bronchi. The chamber below the membrane simulates the artery and supplies the media with nutrients and transports the metabolites. These compounds are provided further to the top chamber by diffusion through the membrane and hydrogel. On the bottom side of the membrane epithelial cells are cultured while on the top part of the hydrogel the bacteria cells are inoculated. In order to simulate antibiotic treatment, the media in the bottom channel can be supplemented with drugs. This supplementation can be performed in cycles, which would mimic drug dosage to CF patients. The introduction of the human sub-bronchial gland cell line (Calu-3) without the layer of hydrogel can simulate the normal bronchi while the same system but with the hydrogel can simulate the bronchi of CF patients.

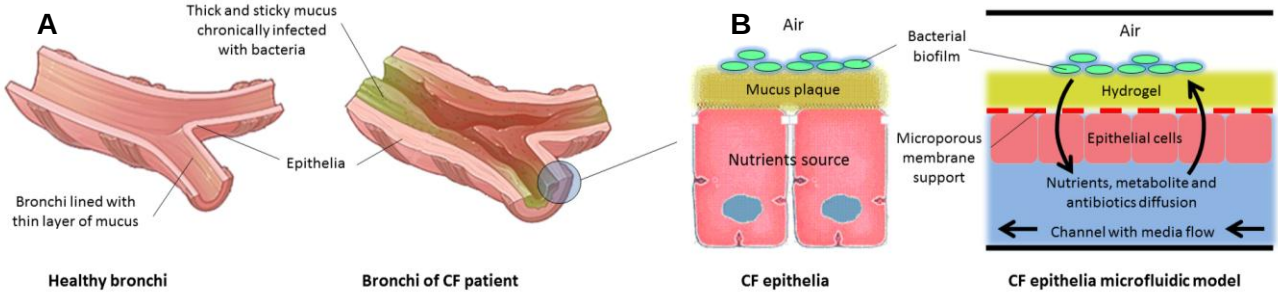

Figure 1: (A) Bronchi of the healthy individual and CF patient. (B) The microfluidic model of CF epithelia.

EXPERIMENTAL

The biochip (Figure 2) was fabricated in polycarbonate (PC) by micromilling (Mini-Mill/3PRO, Minitech Machinery Corp., USA). The PC membrane with 0.45 µm pores was inserted between the milled parts and bonded (tetrahydrofuran vapours assisted bonding, 3.5 MPa, 50°C).

The hydrogel layer was formed by introduction of 0.3% sodium alginate to the top chamber and 0.1 M $CaCl_2$ solution to the bottom chamber. The thickness of the hydrogel was controlled by focusing the sodium alginate stream with PBS (Figure 3). In order to visualise the hydrogel thickness, the sodium alginate was stained with 6-aminofluorescien according to the receipt by Strand *et al*. [5].

The biochip was thoroughly washed with PBS followed by cell culture media (DMEM, 10% FBS). Calu-3 cells with a density of $5 \cdot 10^5$ cells/ml were seeded on the membrane in the bottom chamber.

The inoculum (OD_{600} = 0.01) of the *P. aeuruginosa* PAO1 strain tagged with GFP was introduced into the upper chamber to mimic the bronchi infection (Figure 5). The culture was performed for 3 days in the incubator (5% CO_2, 37°C) (HERAcell incubator, Heraeus, Germany) with perfusion of culture media through the lower chamber with flow rate 0.3 $ml \cdot h^{-1}$.

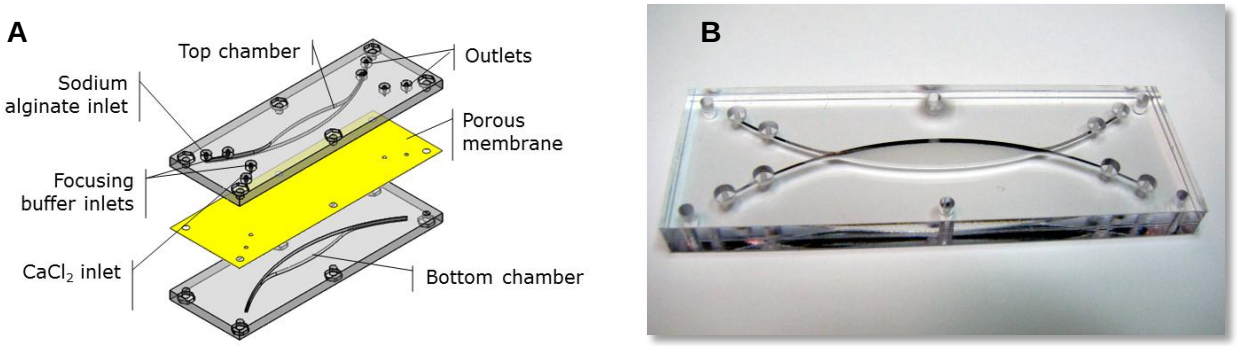

Figure 2: (A) The 3D model of the biochip consist from 3 layers. (B) Fabricated and bonded biochip.

RESULTS AND DISCUSSION

The obtained thickness of the hydrogel layer in the top chamber was 270±20 µm (Figure 4). The focusing buffer was actively pushing the sodium alginate through the membrane, therefore a thin (below 100 µm) layer of hydrogel was formed on the other side of the membrane. The vertical transport of the calcium ions through the membrane was purely diffusional.

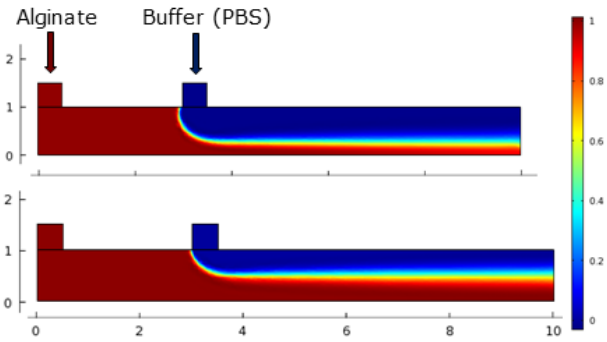

Figure 3: Numerical simulation of the formation of hydrogel layer in the top chamber. The thickness of the layer can be controlled by changing the ratio between the sodium alginate and focusing buffer flow rates.

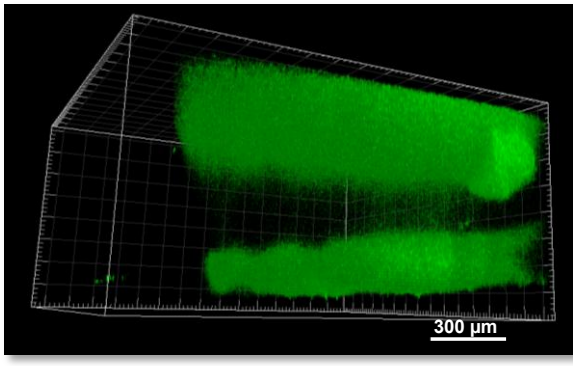

Figure 4: Confocal image of the hydrogel formed in the biochip. Green fluorescence represents calcium alginate and the gap between is the porous PC membrane. The alginate was stained according to [5].

The Calu-3 cells were cultured in the bottom chamber of the system. After reaching the 70% of confluency (3rd day of culture) the *P. aeruginosa* PAO1 strain was inoculated to the upper chamber. The bacteria were allow to form biofilm in the hydrogel for 3 days (Figure 5A). The Calu-3 cells were stained with live/dead stain (Calcein AM/PI) in order to visualise the viable and necrotic epithelia (Figure 5B).

The future application of the presented CF bronchi model lies in simulation of antibiotic treatment of CF related bacterial infection. The simulation of the treatment can be performed by supplementation of the culture media with drugs. The results expected from this should be a better understanding of the problems in the treatment of the chronically infected CF patient.

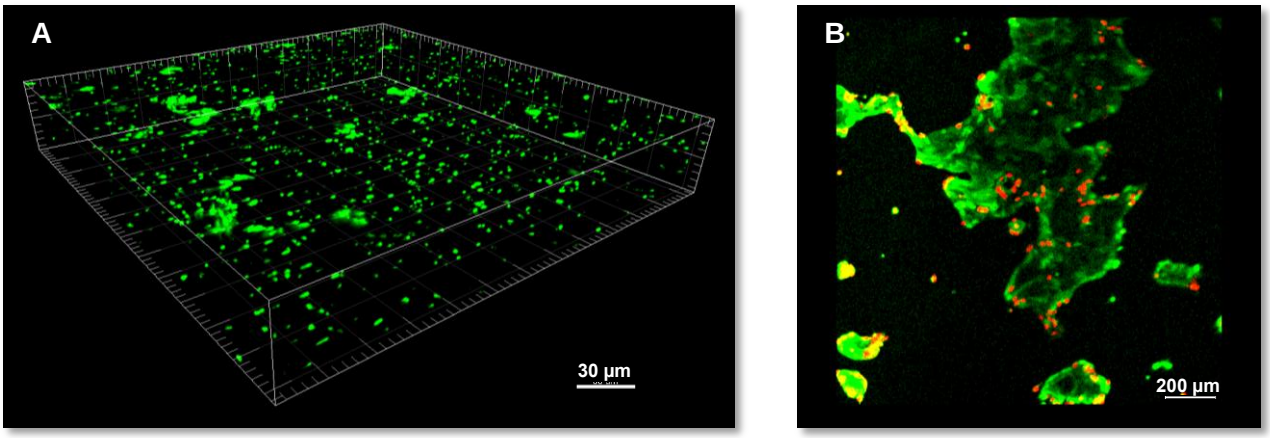

Figure 5: (A) Confocal image of the P. aeruginosa PAO1 strain tagged with the GFP growing in the hydrogel. (B) Fluorescence image of Calu-3 cells stained with live/dead stain (Calcein AM/PI) growing below the hydrogel.

CONCLUSION

We have successfully designed and fabricated a microfluidic biochip which can be used as a model of the CF bronchi. The co-culture of the Calu-3 cells and *P. aeruginosa PAO1* strain using the constructed biochip was shown. By alternating the thickness of the hydrogel layer, the presented model can be used in the future for comparative studies of the antibiotic treatment of bacterial infections in normal and CF patients. This system is a significant advancement in the mimicking of the airways function on the chip reported earlier [6].

ACKNOWLEDGEMENTS

We would like to acknowledge for the funding of PhD stipends by the Technical University of Denmark. Furthermore, we would like to thank Betinna Dinitzen, Maria Læssøe Pedersen and associate professor Hanne Mørck Nielsen from the Faculty of Pharmaceutical Sciences at the University of Copenhagen, for their help and supply of the Calu-3 cell line.

REFERENCES

[1] T. Bjarnsholt, P.O. Jensen, et al., "Pseudomonas aeruginosa tolerance to tobramycin, hydrogen peroxide and polymorphonuclear leukocytes is quorum-sensing dependent", Microbiology,vol. 151, pp. 373-383, 2005.
[2] B.B. Christensen, C. Sternberg, et al., "Use of molecular tools in physiological studies of microbial biofilms", Methods in Enzymology,vol. 310, pp. 20-42, 1999.
[3] M. Weiss Nielsen, C. Sternberg, et al., "Pseudomonas aeruginosa and Saccharomyces cerevisiae biofilm in flow cells", Journal of visualized experiments., pp., 2011.
[4] J.-H. Ryu, C.-H. Kim, et al., "Innate immune responses of the airway epithelium", Molecules and Cells,vol. 30, pp. 173-183, 2010.
[5] B.L. Strand, Y.A. Morch, et al., "Visualization of alginate-poly-L-lysine-alginate microcapsules by confocal laser scanning microscopy", Biotechnology and Bioengineering,vol. 82, pp. 386-394, 2003.
[6] D. Huh, B.D. Matthews, et al., "Reconstituting organ-level lung functions on a chip", Science,vol. 328, pp. 1662-1668, 2010.

CONTACT

*M. Skolimowski, tel: +45 4525 6997; maciej.skolimowski@nanotech.dtu.dk

8.7 Paper VII

Abeille, F.**, Skolimowski, M.**, Nielsen, M.W., Lopacinska, J., D., Molin, S., Taboryski, R., Sternberg, C., Dufva, M., Geschke, O. and Emnéus, J., *Microfluidic system for in vitro study of bacterial infections in cystic fibrosis bronchi.* Manuscript in preparation, 2011.

Microfluidic system for *in vitro* study of bacterial infections in cystic fibrosis bronchi

Abeille, F. *, Skolimowski, M. *,**, Nielsen, M.W. **, Lopacinska, J. *, Molin, S. **, Taboryski, R. *, Sternberg, C. **, Dufva, M. *, Geschke, O. * and Emnéus, J. *

* Technical University of Denmark, Department of Micro- and Nanotechnology, Ørsted Plads, Building 345B, DK-2800 Kgs. Lyngby, Denmark;
Tel: +45 4525 6887 ; E-mail: maciej.skolimowski@nanotech.dtu.dk

** Technical University of Denmark, Department of Systems Biology, Matematiktorvet, Building 301, DK-2800 Kgs. Lyngby, Denmark

Abstract

Here we present our work on a microfluidic device that mimics the bronchi in people suffering from cystic fibrosis. To imitate the mucus of the diseased bronchi, a 200 µm thick hydrogel is formed in a controlled manner on the top of a microporous membrane. This membrane is also the support for the attachment of the epithelial cells, to mimic the bronchial tissue. In the hydrogel, *P. aeruginosa* are inoculated to recreate the scenario of bacterial infections. Compared to flow- or static cell culture systems our microdevice allows better imitation of the nutrient supply through the bronchial bio-layers.

Eventually, nutrient driven development of bacterial growth and the viability of the epithelial cells are characterized by confocal laser scanning microscopy.

Introduction

Cystic fibrosis

Many severe infections in humans affect the airways. Different types of pneumonia are major causes of morbidity and mortality in patients with various immuno compromising conditions. Ineffective anti-microbial therapies often fail to remove the infecting microbes. One of the most severe genetic diseases affecting the human airways, is cystic fibrosis (CF) [1].

CF patients suffer from a genetic defect in the CFTR (Cystic Fibrosis Transmembrane Regulator) gene that hinders the salt transport over the cell membranes [2]. This leads to high salt concentration in the epithelia and low concentration in the mucus, which stops water from rehydrating it [3]. The mucociliary clearance mechanism is impaired and results in frequent infections in the CF airways with increased risk of pneumonia[4]. Since the bacteria can infect the airways unhindered and thrive in the CF mucus, the immune system tries to eradicate the increasing infecting populations. The success of the immunological battery is highly reduced since the bacteria are embedded in mucus and more or less recalcitrant to the attacks [5]. Instead the lung tissue is gradually damaged by the ongoing immunological exposure [6], eventually leading to massive pulmonary deficiency and death.

Several works exist on the mimicking of the human airways using microsystems: some focused on the reproduction of the mechanical function of the alveoli [7-9] while others were more oriented on the regulation of mucin production by NCI-h292 epithelial cells [10]. *Huh et al.* [7] proposed recently a model of the vacuoles in the lung. In this work the phagocytosis of planktonic *Escherichia coli* cells by neutrophils on the epithelial surface was shown. However, according to the author's best knowledge there is no system that mimics the bacterial habitats in the CF bronchi.

Microfluidic model of the cystic fibrosis bronchi

The classical way of studying CF related bacterial infections, primarily *Pseudomonas aeruginosa*, is by growing them in flow-cell systems [11-13] or static ones [14]. In the static cell systems, the amount of nutrients provided to the cells is decreasing in time as the consequence of bacterial consumption. Consequently, in such a system the media have to be renewed regularly but render a system with higher throughput than the flow-cell based systems. In the flow cells, nutrients and waste are constantly being exchanged to the biofilm forming bacteria. However, the bacteria in CF bronchi are not subjected to a constant flow of nutrients. Instead they are embedded in the mucus that covers the bronchi epithelia through which the nutrients and metabolites are diffusing (Fig. 1).

While the human primary bronchi have relatively large lumen diameter (order of magnitude of centimeters), the respiratory bronchioles can be less than 1 mm in diameter [15]. Therefore, in order to respect this order of dimension a microfluidic system is required.

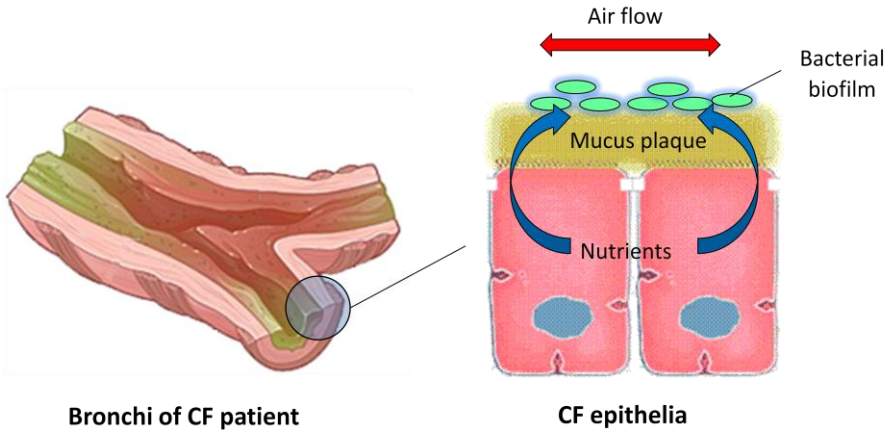

Fig. 1. Bronchus of CF patient. Cross section and microfluidic dynamic of the CF bronchi

Materials and methods

Design

The *in vitro* CF bronchus consists of a chamber divided into two parts (bottom chamber - top chamber) by a porous membrane (Fig. 2). The membrane is used as a solid support for a hydrogel on top and for attachment of epithelial cells beneath. The hydrogel mimics the mucus residing inside the bronchi and epithelial cells the bronchial epithelial tissue. In the top chamber, bacteria can be inoculated to simulate a bacterial infection taking place in chronically infected CF patients [16]. The bottom chamber mimics an artery, provides media with nutrients and transports the metabolites. These compounds are supplied further to the top chamber by diffusion through the epithelia layer, the membrane and the hydrogel.

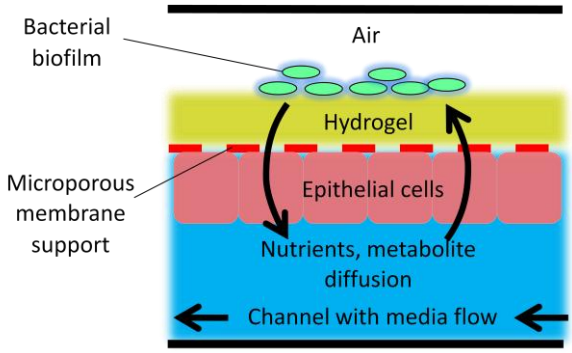

Fig. 2. Model for the mimicking of the CF bronchi.

Procedure

The reproduction of the *in vitro* bronchus model as described above followed a specific procedure:

To ensure the sterility inside the device, the entire system is flushed for 30 minutes with 70% ethanol and then flushed for another 30 minutes with 5% hydrogen peroxide (Sigma Aldrich A/S, Denmark).

The hydrogel (calcium alginate) was formed by a chemical reaction on top of the membrane. Following the formation of the desired thickness of alginate gel, epithelial cells were injected in the bottom chamber as described below in the "Epithelial cell culturing" section. Here the cells were allowed to adhere to the membrane as the device was orientated in an upside down position (top chamber down and bottom chamber up) for 24 hours. Once the bronchial cells reached a confluence of 90%, the 2nd day after seeding, bacteria were inoculated in the top chamber to recreate the scenario of a bacterial infection.

Fabrication of the microfluidic chip

The main feature of the chip is the chamber in the center where the CF bronchus is mimicked. It has an elliptic shape with a perigee of 2 mm, an apogee of 21 mm and a thickness of 2 mm. This shape enables to easily remove the bubbles that may get inside the device. The membrane dividing the chamber is a hydrophilic poly(tetrafluoroethylene) (PTFE) membrane (BCGM 000 10, Millipore A/S, Denmark). It is 50 µm thick with pores of 0.4 µm diameter. Two inlets and two outlets of 0.5 mm in diameter are connected to the upper chamber by a 1 mm thick and 0.5 mm wide channels, the same for the bottom chamber (Fig. 3). The different inlets are used to inject different solutions (see the "Hydrogel formation" section). In practice only one of the outlets from each channel is useful but for a symmetry matter more of them are created.

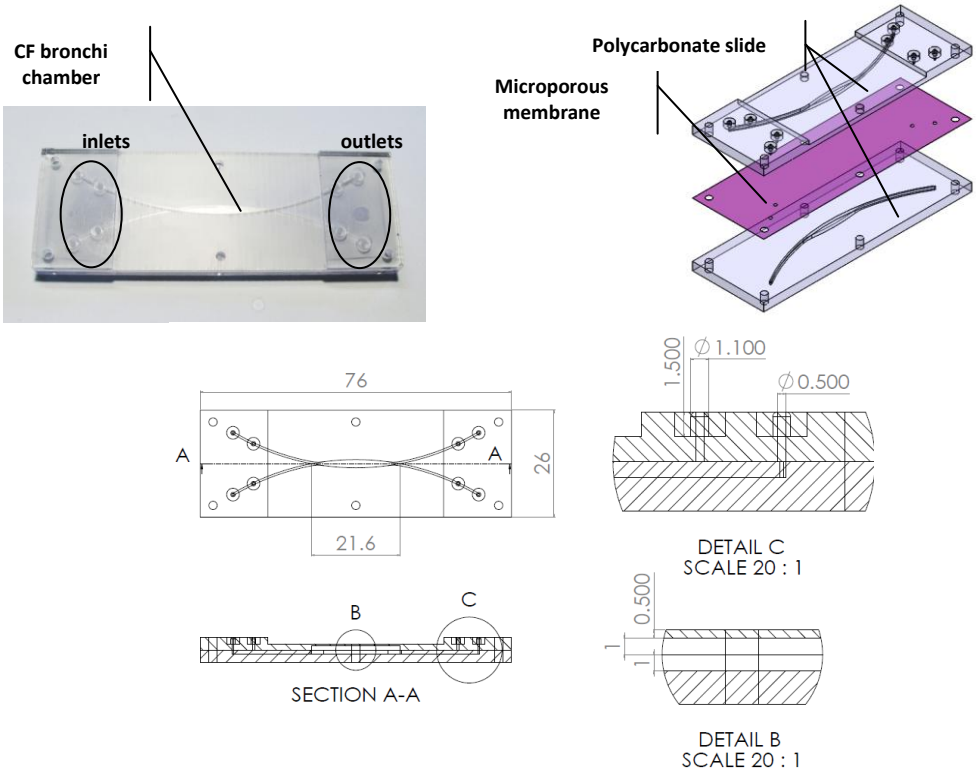

Fig. 3 Top left: Picture of the microfabricated device. Top right: Exploded view of the microfluidic chip. Bottom: Sketches of the top and side and view of the microfluidic chip.

Each chamber with inlets, outlets and channels (except for the porous membrane) were fabricated by micromilling (Mini-Mill/3PRO, Minitech Machinery Corp., USA) in two polycarbonate (PC) slides (Nordisk Plast A/S, Denmark). Each of the slides has the dimensions of a microscope slide (76x26 mm) and a thickness of 3 mm.

The polycarbonate constituting the cover of the chamber is milled down to 0.5mm in thickness to allow the use of high magnification microscope objectives for bacteria observation within the culture chamber (top chamber). Both sides of the PTFE membrane were exposed to air plasma (70 W, 6 mbar) for 30 s to later facilitate the attachment of the epithelial cells. The PC slides were exposed to tetrahydrofuran (THF) vapors for 5 min. Eventually, the PTFE membrane was inserted between the two polycarbonate slides followed by thermal bonding (using bonding press PW 10 H, P/O/Weber, Germany) at 50°C with 4 MPa for 30 min.

Hydrogel formation

A 100 mM $CaCl_2$ solution (Sigma-Aldrich Denmark A/S) was used to cross-link a 0.5% (w/v) solution of sodium alginate (Sigma-Aldrich Denmark A/S) in order to form the calcium alginate hydrogel. A phosphate buffer saline (PBS) solution (Sigma-Aldrich Denmark A/S) was used as buffer.

The hydrogel formation within the chamber was performed in the following order (Fig. 4):

Flush of both chambers with the PBS solution for 6 min at a flow rate of 10 ml·h^{-1}. This ensures that all chemicals previously used for sterilization are washed out.

Sodium alginate is sent to the top chamber at a flow rate of 5 ml·h^{-1}. In the bottom chamber PBS is kept at the same flow rate of 5 ml·h^{-1}. This procedure is carried out for 6 min.

The flow of PBS is stopped in the bottom chamber, instead $CaCl_2$ is sent with a flow rate of 5 ml·h^{-1} for 10 min. Calcium ions diffuse through the membrane and react with the sodium alginate to form the gel.

After the 10 min, the flow of Sodium alginate is stopped and instead PBS is sent through the chamber at 5 ml·h^{-1} for 10 min. The diffusion of calcium ions strengthens the hydrogel and the weakly cross-linked alginate is flushed out.

The chambers are subsequently flushed with PBS at a flow rate of 1 ml·h^{-1} for 30 min.

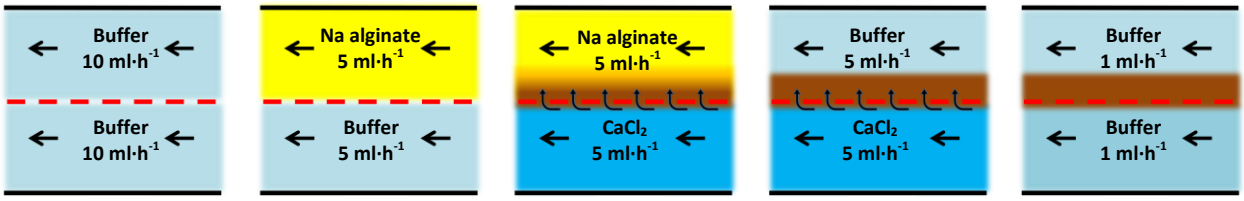

Fig. 4. Process for the hydrogel formation.

In order to determine the thickness of the hydrogel, experiments with stained sodium alginate were conducted. Aminofluorescein was covalently bound to the α-L-guluronate residues constituting the alginate by following a particular staining technique [17]. However, no stained alginate was used in the system while cell culturing was performed inside the device.

Epithelial cell culturing

Calu-3 cells were cultured in 25 cm² tissue culture flasks (Sarstedt Inc., USA) with DMEM (Dubelcco's Modified Eagle Medium) supplemented with 10% (v/v) Fetal Bovine Serum (FBS) , 50 µg·ml^{-1} of Gentamicin and 100 U·ml^{-1}/100 µg·ml^{-1} of Penicillin/Streptomycin. The media was changed every second day. Once the cells reached a stage of 90% confluence they were passaged by using Trypsin-EDTA solution for 10 min at 37°C.

From the harvested cells a concentration of $8 \cdot 10^5$ cells·ml^{-1} was prepared for seeding inside the chip. Cells were inoculated in the bottom chamber where the cells were allowed to adhere to the membrane. This was done by placing the device in an upside down position (top chamber down and bottom chamber up) for 24 hours in a cell culture incubator (5% CO_2, 37°C) (HERAcell incubator, Heraeus, Germany). Eventually, the microfluidic chip remained in the incubator with a continuous media flow of 0.3 ml·h^{-1} for both chambers until a cell confluence of about 90% was obtained.

Calu-3 viability was checked by using a 40 nM concentration of Calcein AM to stain living cells and a 1.5 µM concentration of Propidium Iodide (PI) to stain dead cells. Calcein and PI respectively stain the cells with a green and red fluorescence as shown in Fig. 6.

All chemicals, unless stated otherwise, were purchased from Sigma-Aldrich Denmark A/S.

Bacteria cell culture

The *P. aeruginosa* laboratory strain PAO1 was used all experiments involving bacterial cultivation or co-cultivation [18]. PAO1 was grown at 37°C in shaken conditions to stationary phase overnight in Luria Bertani (LB) media. Preparation for inoculation was done by diluting to an OD_{600} of 0.01 in 0.9% NaCl. 500 µL was inoculated in the top chamber and the cells were allowed to attach without any media flow delivered through the system for an incubation period of 1 hour. Following the incubation the flow was resumed at 0.3 $ml \cdot h^{-1}$ in DMEM media with 10% of FBS without antibiotics.

PAO1 was expressing the green fluorescent protein (GFP) tagged by the miniTn7 insertion method [19].

Microscopy and data analysis

A confocal laser scanning microscope (CLSM) (Leica TCS SP5 from Leica Microsystems A/S, Denmark) was used to acquire images of cells and hydrogel. Detectors and filters were set for monitoring Calcein-, GFP- and PI fluorescence. Images of Calu-3 cells and hydrogels were performed with a 10x/0.3 air objective. Bacteria were imaged with a 63x/0.70 air objective.

In order to evaluate the thickness of the hydrogel, the pixels with an intensity higher than 25% of the maximum intensity value were taken into consideration.

All the pictures were treated and analyzed by using the Imaris 7.1.1 software package (BITPLANE AG, Zürich, Switzerland).

Results

Hydrogel layer

The thickness of the hydrogel layer depends on the time in which the Ca^{2+} ions are able to diffuse into the top chamber. The longer they can diffuse, the further up they are able to cross-link the alginate in the top chamber. Thus, controlling the time of diffusion allows better control of the gel thickness that one wants to achieve. A thickness of about 200 µm was decided for imitation of a mucus layer. To obtain this specific thickness, 10 min of diffusion were required during the 3rd step of the protocol of “Hydrogel formation” section (Fig. 4). Confocal imaging revealed that the formed hydrogel was 230 µm (± 20 µm) thick (Fig. 5A).

During the optimization of the hydrogel formation, several experiments allowed the determination of a diffusion time range: 5 min of Ca^{2+} diffusion generates approximately 100 µm of hydrogel (Fig. 5B) whereas 15 min fills up the top chamber (Fig. 5C).

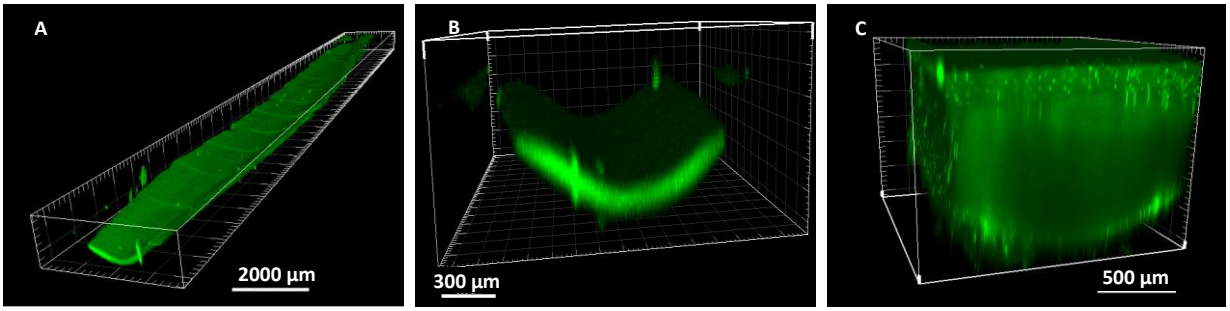

Fig. 5. A. Stained hydrogel characterized by CLSM B. 100 µm thick hydrogel obtained after 5 min of Ca^{2+} diffusion. C. Top chamber completely filled after 15 min of Ca^{2+} diffusion.

Co-culture of the Calu-3 epithelial cells and the *P. aeruginosa* PAO1 strain

The growth of the Calu-3 cells was successfully performed inside the microfluidic device. The cells reached a confluence of about 90% in 2 days (out of the 24 hours for attachment). To check the viability the cells were stained with Calcein AM and PI. Confocal microscopy revealed that less than 1% of the cells were necrotic after 3 days of culturing (Fig. 6). This resembles normal Calu-3 culturing viability in a regular tissue culture flask (data not shown).

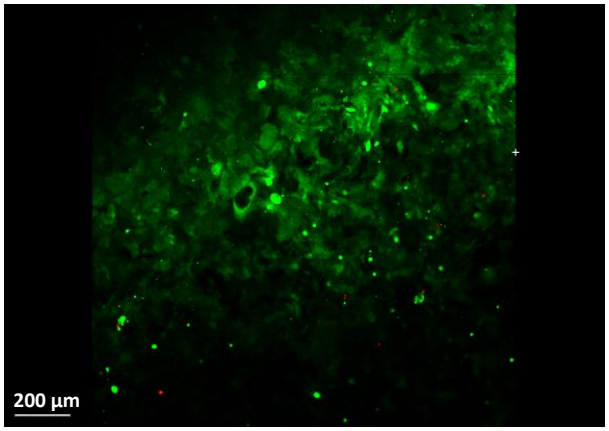

Fig. 6. Epithelial layer viability after 3 days of culture.

PA01 formed biofilm on top and inside the hydrogel layer (Fig. 7). Because the pores in the calcium alginate are much bigger (raging from tens to hundreds of microns) [20] than the size of bacteria, single bacteria can easily get inside and start forming microcolonies.

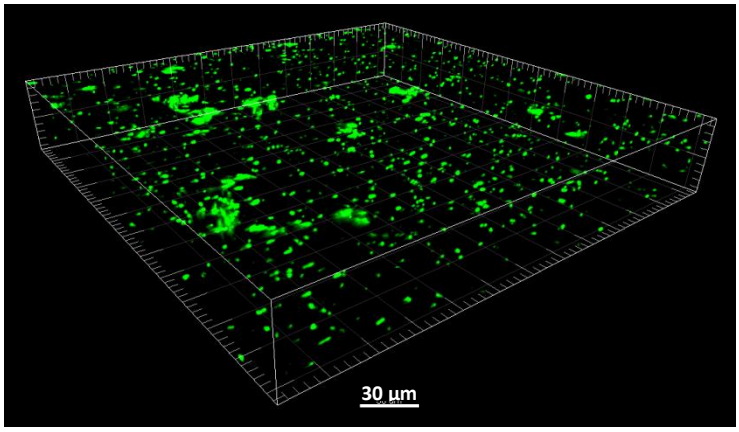

Fig. 7. 3D visualization of PA01-GFP embedded in the calcium alginate matrix at day 5.

Discussion

Membrane integration

We demonstrated a fast and easy way to integrate the PTFE porous membrane. No specific setup needs to be used or optimized if we compare to *in situ* membrane integration [21]. No alignment or specific treatment is required for this membrane regarding the bonding step. The surface treatment of polycarbonate parts using THF vapors and the thinness of the membrane (50 µm) enable strong and durable bonding, across the membrane, between the PC slides.

Hydrogel characterization

In this paper, the term “hydrogel thickness” includes the membrane size, the thickness of the gel below and above the membrane. The thickness below the membrane is though negligible (< 2 µm). Indeed because of due to the low diffusion coefficient of the alginate [22] a very low amount of it diffuses beneath the membrane and transforms into calcium alginate. Besides, the alginate does not affect the attachment and development of the Calu-3 cells.

Beyond flow cell and static culture

As mentioned in the introduction, there are two main ways to culture cells: the flow cell culture [11-13] and the static cell culture [14].

However, those types of culture do not reflect the conditions in which bacteria can develop in niches of the human body as in the severe case of the CF airways. As explained in the microfluidic model of the CF bronchi, the nutrients are provided to the bacteria by diffusion across different bio-layers from a cyclic flow (i.e. the blood stream). With this in mind, the proposed microfluidic system represents a significant step forward in the study of lung infections since such mimicry has not been reported in the literature yet.

Eventually, this *in vitro* chip makes microscopy observation possible which is not the case when using *in vivo* models. Moreover, there is a very strong pressure from public societies, states, international organizations and from the industry to replace, reduce and refine the research conducted with the use of animals [23, 24]. This strategy is known as the “3 Rs” principle [25, 26]. Therefore, our developed microfluidic system can play an important role in the replacement of animal models used for medical experiments.

A new strategy for drug tests in the CF airways.

The chip provides a new way to simulate bacterial infections in the airways. In the future, it can also provide a novel bio-mimetic approach regarding drug treatment. Antibiotics can be delivered in two different manners. One would be using a gaseous form that would be delivered to the upper chamber to reproduce treatment using spray antibiotics. On the other hand, a liquid form of the antibiotic injected in the lower chamber would simulate intravenous delivery through the blood stream.

The device offers great opportunities to improve the bio-mimicry. The biological resemblance between the mucus and the hydrogel can be enhanced by altering the composition of additives as mucins and DNA [27, 28]. Such improvement will offer a better model for studying the response of a biofilm community to drug treatments [29]. In addition, the chip could be coupled with our previous system [30] to recreate the different type of dissolved oxygen conditions inside the airways. Finally our device brings great promises in the mimicry of other human organs where the mucus is involved, e.g. the gut or the stomach.

Summary & Conclusion

In this paper, we have demonstrated the fabrication of a robust and reliable microfluidic device. This device enables the setup of an *in vitro* microfluidic chip based mimicry of an infected human CF bronchus. The recreation of the scenario leading infection of the bronchi is based on a new approach of bacteria culture to be closer to their *in vivo* growth: nutrients diffuse through different bio-layers to feed the bacteria embedded in the mucus-like matrix.

Inside the system, the imitation of the CF bronchus has been performed by incorporating Calu-3 cells and hydrogel, respectively beneath and on top of a microporous membrane. The formation of the hydrogel has been controlled in order to mimic a mucus layer as thick as 200 µm. Calu-3 cells, mimicking the epithelial tissue, have been cultured for 3 days to reach 90% of confluence. A bacterial infection has been simulated by inoculating *P. aeruginosa* PA01 in the hydrogel. The formation of bacterial microcolonies has been observed 2 days later. Confocal microscopy allowed *in vitro* imaging of the different cells to assess of their well growth and good viability.

For future experiments, such device can enable to simulate and observe the biofilm response to drug treatments taken by oral or intravenous ways. Also, mucin and DNA can be added in the hydrogel to study the impact of the mucus composition on the bacterial infection.

Acknowledgment

We would like to acknowledge for the funding of PhD stipends by the Technical University of Denmark. Furthermore we would like to thank Betinna Dinitzen, Maria Læssøe Pedersen and associate professor Hanne Mørck Nielsen from the Faculty of Pharmaceutical Sciences at the University of Copenhagen, for their help and supply of the Calu-3 cell line.

References

1. Maria Ciminelli, B., et al., *Anthropological features of the CFTR gene: Its variability in an African population.* Ann Hum Biol, 2011. **38**(2): p. 203-9.
2. Jih, K.Y., et al., *The most common cystic fibrosis-associated mutation destabilizes the dimeric state of the nucleotide-binding domains of CFTR.* Journal of Physiology-London, 2011. **589**(11): p. 2719-2731.
3. Boucher, R.C., *Evidence for airway surface dehydration as the initiating event in CF airway disease.* J Intern Med, 2007. **261**(1): p. 5-16.
4. Antunes, M.B. and N.A. Cohen, *Mucociliary clearance--a critical upper airway host defense mechanism and methods of assessment.* Curr Opin Allergy Clin Immunol, 2007. **7**(1): p. 5-10.
5. Song, Z.J., et al., *Pseudomonas aeruginosa alginate is refractory to Th1 immune response and impedes host immune clearance in a mouse model of acute lung infection.* Journal of Medical Microbiology, 2003. **52**(9): p. 731-740.
6. Bjarnsholt, T., *Pseudomonas aeruginosa Biofilms in the Lungs of Cystic Fibrosis Patients*, in *Biofilm infections*. 2010, Springer: New York ; London :. p. 167.
7. Huh, D., et al., *Reconstituting organ-level lung functions on a chip.* Science, 2010. **328**(5986): p. 1662-8.
8. Huh, D., et al., *Acoustically detectable cellular-level lung injury induced by fluid mechanical stresses in microfluidic airway systems.* Proc Natl Acad Sci U S A, 2007. **104**(48): p. 18886-91.
9. Tavana, H., et al., *Dynamics of liquid plugs of buffer and surfactant solutions in a micro-engineered pulmonary airway model.* Langmuir, 2010. **26**(5): p. 3744-52.
10. Kim, S.H., et al., *Mucin (MUC5AC) expression by lung epithelial cells cultured in a microfluidic gradient device.* Electrophoresis, 2011. **32**(2): p. 254-60.
11. Bjarnsholt, T., et al., *Pseudomonas aeruginosa tolerance to tobramycin, hydrogen peroxide and polymorphonuclear leukocytes is quorum-sensing dependent.* Microbiology, 2005. **151**(Pt 2): p. 373-83.
12. Christensen, B.B., et al., *Molecular tools for study of biofilm physiology.* Methods Enzymol, 1999. **310**: p. 20-42.
13. Weiss Nielsen, M., et al., *Pseudomonas aeruginosa and Saccharomyces cerevisiae biofilm in flow cells.* J Vis Exp, 2011(47).
14. Flickinger, S.T., et al., *Quorum sensing between Pseudomonas aeruginosa biofilms accelerates cell growth.* J Am Chem Soc, 2011. **133**(15): p. 5966-75.
15. Moir, L.M., J.P.T. Ward, and S.J. Hirst, *Contractility and phenotype of human bronchiole smooth muscle after prolonged fetal bovine serum exposure.* Experimental Lung Research, 2003. **29**(6): p. 339-359.
16. Koch, C., *Early infection and progression of cystic fibrosis lung disease.* Pediatr Pulmonol, 2002. **34**(3): p. 232-6.
17. Braschler, T., et al., *Fluidic microstructuring of alginate hydrogels for the single cell niche.* Lab Chip, 2010. **10**(20): p. 2771-7.
18. Holloway, B.W., *Genetic recombination in Pseudomonas aeruginosa.* J Gen Microbiol, 1955. **13**(3): p. 572-81.

19. Klausen, M., et al., *Biofilm formation by Pseudomonas aeruginosa wild type, flagella and type IV pili mutants.* Mol Microbiol, 2003. **48**(6): p. 1511-24.

20. Pathak, T.S., et al., *Preparation of Alginic Acid and Metal Alginate from Algae and their Comparative Study.* Journal of Polymers and the Environment, 2008. **16**(3): p. 198-204.

21. Bentley, W.E., et al., *In situ generation of pH gradients in microfluidic devices for biofabrication of freestanding, semi-permeable chitosan membranes.* Lab on a Chip, 2010. **10**(1): p. 59-65.

22. Braschler, T., et al., *Link between alginate reaction front propagation and general reaction diffusion theory.* Anal Chem, 2011. **83**(6): p. 2234-42.

23. Creton, S., et al., *Improved risk assessment of chemicals through the application of toxicokinetic information: Opportunities for the replacement, reduction and refinement of animal use.* Toxicology, 2009. **262**(1): p. 10-11.

24. Hendriksen, C.F.M., *Replacement, reduction and refinement alternatives to animal use in vaccine potency measurement.* Expert Review of Vaccines, 2009. **8**(3): p. 313-322.

25. Flecknell, P., *Replacement, reduction and refinement.* Altex-Alternativen Zu Tierexperimenten, 2002. **19**(2): p. 73-78.

26. Lucken, R.N., *The five Rs: Refinement, reduction, replacement. A regulatory revolution.* Replacement, Reduction and Refinement of Animal Experiments in the Development and Control of Biological Products, 1996. **86**: p. 67-72.

27. Lethem, M.I., et al., *The origin of DNA associated with mucus glycoproteins in cystic fibrosis sputum.* Eur Respir J, 1990. **3**(1): p. 19-23.

28. Shah, P.L., et al., *The effects of recombinant human DNase on neutrophil elastase activity and interleukin-8 levels in the sputum of patients with cystic fibrosis.* European Respiratory Journal, 1996. **9**(3): p. 531-534.

29. Ryu, J.H., C.H. Kim, and J.H. Yoon, *Innate immune responses of the airway epithelium.* Mol Cells, 2010. **30**(3): p. 173-83.

30. Skolimowski, M., et al., *Microfluidic dissolved oxygen gradient generator biochip as a useful tool in bacterial biofilm studies.* Lab on a Chip, 2010. **10**(16): p. 2162-2169.

9 Summary and conclusions

9.1 Key findings

Microfluidic airways model systems that can successfully simulate the changes in oxygen tension in different compartments of the CF airways, have been designed, developed and presented. These microfluidic systems were applied for studying of infections with *P. aeruginosa*, the bacteria that is responsible for most of the recurrent CF related infections.

The two different approaches to the system have been successfully developed. In the first approach (paper III and IV), a monolithic microfluidic chip was used. The layer-by-layer design allowed the incorporation of several desirable elements as the integrated gas permeable membrane, which was exploited by an oxygen scavenging liquid to produce the desired oxygen environments. The oxygen gradients were generated within the culture chambers and monitored by a thin film oxygen sensing layer. The oxygen concentrations were monitored by photoluminescence lifetime measurements. This specific way of monitoring oxygen concentration is compatible with several different detection methods as micro plate readers and fluorescence lifetime imaging microscopes. The designed system was applied to support growth of *P. aeruginosa* PAO1 biofilm. PAO1 responded to the low oxygen concentration environment by a reduced number of attached cells to the surface of the microchamber and lower rate of biomass growth.

In the second approach (paper V), the advantages of a highly complex modular microfluidic system that mimics the different compartments of the CF airways have been exploited. Integration of different modules, bringing in such important functionalities as multichannel fluid control, bubble trapping, gas control - exchange and bacterial culturing on a microfluidic lab-on-a-chip system, has been shown to be successfully achieved. The developed passive micromixer (paper I and II) has been utilised to enhance the oxygen exchange in the gas control module.

In contrast to the monolithic system described previously (paper III and IV), in the modular system, the culture microchambers with distinct oxygen concentration were used. In this way, it was possible to observe a migration of the cells between the compartments with different oxygen tension, as it is hypothesised to happen in the patients airways. The application of the system for studying *P. aeruginosa* PAO1 under different oxygen levels in response to treatment with ciprofloxacin in nitrate supplemented media has been demonstrated. It has been shown that the

effect of the presence of nitrate, which serves as final electron acceptor for anaerobic nitrate respiration utilized by *P. aeruginosa*, is not favoured in the presence of oxygen and drives the migration towards the higher oxygen gradient. It can mimic the reinoculation of the lower respiratory tract, previously cleared with the antibiotic treatment from the sinuses. This effect is hypothesised as the main reason for recurrent infections in CF patients. It has been shown that the system is an asset in reliable and controllable biofilm evaluations for treatment with antibiotics at reduced oxygen concentrations.

A complex model of the cystic fibrosis bronchi was also developed, which allows to simulate the CF epithelia covered with a thick and viscous mucus layer (paper VI and VII). This system allows to co-culturing the epithelial and bacterial cells in the environment close to that spotted in the CF bronchi and studying the biofilm growth under these conditions. This is a considerable advancement towards the development of an artificial CF bronchi model from the standard flow cell based systems and static co-cultures of mammalian and bacterial cells.

9.2 Future perspectives

The further research conducted with the described systems should try to answer the following question: are the bacteria in the three compartments identical phenotypically and genetically? Is there a detectable change in phenotype on the passage from one compartment to another? Do the sinuses represent a reservoir for intermittent infections of the same bacterium? Can the reinfections be efficiently blocked by addressing the sinus reservoirs?

The results expected from this should be a better understanding of the problems in the treatment of the chronically infected CF patient. Hopefully the knowledge obtained can help in the prevention and treatment of these infections which severely affect the life quality of the CF patients.

10 References

1. Aust, R. and B. Drettner, *Oxygen tension in the human maxillary sinus under normal and pathological conditions.* Acta oto-laryngologica., 1974. **78**(3-4): p. 264-269.
2. Mintz, M.L., *Anatomy and Physiology of the Respiratory Tract*, in *Disorders of the respiratory tract: common challenges in primary care*. 2006, Humana Press: Totowa, NJ :. p. 11.
3. Laufer, A.S., et al., *Microbial Communities of the Upper Respiratory Tract and Otitis Media in Children.* mBio, 2011. **2**(1).
4. Murphy, T.F., L.O. Bakaletz, and P.R. Smeesters, *Microbial Interactions in the Respiratory Tract.* Pediatric Infectious Disease Journal, 2009. **28**(10, Suppl. S): p. S121-S126.
5. Ciminelli, B.M., et al., *Anthropological features of the CFTR gene: Its variability in an African population.* Annals of Human Biology, 2011. **38**(2): p. 203-209.
6. Jih, K.-Y., et al., *The most common cystic fibrosis-associated mutation destabilizes the dimeric state of the nucleotide-binding domains of CFTR.* J Physiol, 2011. **589**(11): p. 2719-2731.
7. Moskowitz, S.M., et al., *Clinical practice and genetic counseling for cystic fibrosis and CFTR-related disorders.* Genetics in Medicine, 2008. **10**(12): p. 851-68.
8. O'Sullivan, B.P. and S.D. Freedman, *Cystic fibrosis.* Lancet, 2009. **373**(9678): p. 1891-904.
9. Riordan, J.R., et al., *Identification of the cystic fibrosis gene: cloning and characterization of complementary DNA.* Science, 1989. **245**(4922): p. 1066-73.
10. Bompadre, S.G. and T.C. Hwang, *Cystic fibrosis transmembrane conductance regulator: a chloride channel gated by ATP binding and hydrolysis.* Sheng li xue bao : [Acta physiologica Sinica], 2007. **59**(4): p. 431-42.
11. Reisin, I.L., et al., *The cystic fibrosis transmembrane conductance regulator is a dual ATP and chloride channel.* The Journal of biological chemistry, 1994. **269**(32): p. 20584-91.
12. Sheppard, D.N. and M.J. Welsh, *Effect of ATP-sensitive K+ channel regulators on cystic fibrosis transmembrane conductance regulator chloride currents.* The Journal of general physiology, 1992. **100**(4): p. 573-91.
13. Stutts, M.J., et al., *CFTR as a cAMP-dependent regulator of sodium channels.* Science, 1995. **269**(5225): p. 847-50.
14. Vankeerberghen, A., H. Cuppens, and J.J. Cassiman, *The cystic fibrosis transmembrane conductance regulator: an intriguing protein with pleiotropic functions.* Journal of cystic fibrosis : official journal of the European Cystic Fibrosis Society, 2002. **1**(1): p. 13-29.

15. *Cystic Fibrosis Mutation Database*. Available from: http://www.genet.sickkids.on.ca.

16. Wilschanski, M., et al., *Correlation of sweat chloride concentration with classes of the cystic fibrosis transmembrane conductance regulator gene mutations.* The Journal of Pediatrics, 1995. **127**(5): p. 705-10.

17. Anderson, M.P., et al., *Generation of cAMP-activated chloride currents by expression of CFTR.* Science, 1991. **251**(4994): p. 679-682.

18. Rowe, S.M., et al., *ΔF508 CFTR processing correction and activity in polarized airway and non-airway cell monolayers.* Pulmonary Pharmacology and Therapeutics, 2010. **23**(4): p. 268-278.

19. Welsh, M.J. and A.E. Smith, *Molecular mechanisms of CFTR chloride channel dysfunction in cystic fibrosis.* Cell, 1993. **73**(7): p. 1251-1254.

20. Lyczak, J.B., C.L. Cannon, and G.B. Pier, *Lung infections associated with cystic fibrosis.* Clinical Microbiology Reviews, 2002. **15**(2): p. 194-222.

21. Stern, R.C., *The diagnosis of cystic fibrosis.* The New England journal of medicine, 1997. **336**(7): p. 487-91.

22. Durieu, I., et al., *Increased sweat chloride concentrations in adult patients with pancreatic insufficiency: cystic fibrosis phenotype or lack of specificity of sweat test?* Scandinavian Journal of Gastroenterology, 1999. **34**(12): p. 1260.

23. Dork, T., et al., *Cystic fibrosis with three mutations in the cystic fibrosis transmembrane conductance regulator gene.* Human Genetics, 1991. **87**(4): p. 441-6.

24. Eisenhut, M., *Malnutrition causes a reduction in alveolar epithelial sodium and chloride transport which predisposes to death from lung injury.* Medical Hypotheses, 2007. **68**(2): p. 361-363.

25. Goralski, J.L., R.C. Boucher, and B. Button, *Osmolytes and ion transport modulators: new strategies for airway surface rehydration.* Current Opinion in Pharmacology, 2010. **10**(3): p. 294-9.

26. Boucher, R.C., *Evidence for airway surface dehydration as the initiating event in CF airway disease.* Journal of Internal Medicine, 2007. **261**(1): p. 5-16.

27. Smith, J.J., et al., *Cystic fibrosis airway epithelia fail to kill bacteria because of abnormal airway surface fluid.* Cell, 1996. **85**(2): p. 229-36.

28. Zabner, J., et al., *Loss of CFTR chloride channels alters salt absorption by cystic fibrosis airway epithelia in vitro.* Molecular Cell, 1998. **2**(3): p. 397-403.

29. Tarran, R., et al., *Normal and cystic fibrosis airway surface liquid homeostasis. The effects of phasic shear stress and viral infections.* The Journal of biological chemistry, 2005. **280**(42): p. 35751-9.

30. Smith, D.J., E.A. Gaffney, and J.R. Blake, *Modelling mucociliary clearance.* Respiratory Physiology & Neurobiology, 2008. **163**(1-3): p. 178-188.

31. Davis, C.W. and B.F. Dickey, *Regulated airway goblet cell mucin secretion.* Annual Review of Physiology, 2008. **70**: p. 487-512.

32. Norton, M.M., R.J. Robinson, and S.J. Weinstein, *Model of ciliary clearance and the role of mucus rheology.* Physical Review E: Statistical, Nonlinear, and Soft Matter Physics, 2011. **83**(1).

33. Antunes, M. and N. Cohen, *Mucociliary clearance - a critical upper airway host defense mechanism and methods of assessment.* Current Opinion in Allergy and Clinical Immunology, 2007. **7**(1).

34. Bjarnsholt, T., *Pseudomonas aeruginosa Biofilms in the Lungs of Cystic Fibrosis Patients*, in *Biofilm infections*. 2010, Springer: New York ; London :. p. 167.

35. Permin, H., et al., *Ceftazidime Treatment of Chronic Pseudomonas-Aeruginosa Respiratory-Tract Infection in Cystic-Fibrosis.* Journal of Antimicrobial Chemotherapy, 1983. **12**: p. 313-323.

36. Ratjen, F., et al., *Pharmacokinetics of inhaled colistin in patients with cystic fibrosis.* The Journal of antimicrobial chemotherapy, 2006. **57**(2): p. 306-11.

37. Gibson, R.L., et al., *Significant microbiological effect of inhaled tobramycin in young children with cystic fibrosis.* American Journal of Respiratory and Critical Care Medicine, 2003. **167**(6): p. 841-9.

38. Geller, D.E., et al., *Pharmacokinetics and bioavailability of aerosolized tobramycin in cystic fibrosis.* Chest, 2002. **122**(1): p. 219-26.

39. Burns, J.L., et al., *Longitudinal assessment of Pseudomonas aeruginosa in young children with cystic fibrosis.* The Journal of infectious diseases, 2001. **183**(3): p. 444-52.

40. Moreau-Marquis, S., B.A. Stanton, and G.A. O'Toole, *Pseudomonas aeruginosa biofilm formation in the cystic fibrosis airway.* Pulmonary Pharmacology & Therapeutics, 2008. **21**(4): p. 595-599.

41. Rosenfeld, M., B.W. Ramsey, and R.L. Gibson, *Pseudomonas acquisition in young patients with cystic fibrosis: pathophysiology, diagnosis, and management.* Current opinion in pulmonary medicine, 2003. **9**(6): p. 492-7.

42. Green, S.K., et al., *Agricultural Plants and Soil as a Reservoir for Pseudomonas-Aeruginosa.* Applied Microbiology, 1974. **28**(6): p. 987-991.

43. Speert, D.P., et al., *Pseudomonas-Aeruginosa Colonization of the Gastrointestinal-Tract in Patients with Cystic-Fibrosis.* Journal of Infectious Diseases, 1993. **167**(1): p. 226-229.

44. Heijerman, H., *Infection and inflammation in cystic fibrosis: a short review.* Journal of cystic fibrosis : official journal of the European Cystic Fibrosis Society, 2005. **4 Suppl 2**: p. 3-5.

45. Tsuneda, S., et al., *Extracellular polymeric substances responsible for bacterial adhesion onto solid surface.* FEMS Microbiology Letters, 2003. **223**(2): p. 287-92.

46. Jahn, A. and P.H. Nielsen, *Cell biomass and exopolymer composition in sewer biofilms.* Water Science and Technology, 1998. **37**(1): p. 17-24.

47. Sutherland, I.W., *The biofilm matrix - an immobilized but dynamic microbial environment.* Trends in Microbiology, 2001. **9**(5): p. 222-227.

48. Simoes, M., L.C. Simoes, and M.J. Vieira, *A review of current and emergent biofilm control strategies.* LWT-Food Science and Technology, 2010. **43**(4): p. 573-583.

49. Nicolas, G.G. and M.C. Lavoie, *Streptococcus mutans and streptococci in oral plaque.* Canadian Journal of Microbiology, 2011. **57**(1): p. 1-20.

50. Hoiby, N., et al., *Pseudomonas aeruginosa and the in vitro and in vivo biofilm mode of growth.* Microbes and infection / Institut Pasteur, 2001. **3**(1): p. 23-35.

51. Monroe, D., *Looking for chinks in the armor of bacterial biofilms.* PLoS Biology, 2007. **5**(11): p. e307.

52. Baltimore, R.S., C.D.C. Christie, and G.J.W. Smith, *Immunohistopathologic Localization of Pseudomonas-Aeruginosa in Lungs from Patients with Cystic-Fibrosis - Implications for the Pathogenesis of Progressive Lung Deterioration.* American Review of Respiratory Disease, 1989. **140**(6): p. 1650-1661.

53. Singh, P.K., et al., *Quorum-sensing signals indicate that cystic fibrosis lungs are infected with bacterial biofilms.* Nature, 2000. **407**(6805): p. 762-764.

54. Worlitzsch, D., et al., *Effects of reduced mucus oxygen concentration in airway Pseudomonas infections of cystic fibrosis patients.* Journal of Clinical Investigation, 2002. **109**(3): p. 317-325.

55. Lam, J., et al., *Production of mucoid microcolonies by Pseudomonas aeruginosa within infected lungs in cystic fibrosis.* Infection and Immunity, 1980. **28**(2): p. 546-56.

56. Costerton, J.W., P.S. Stewart, and E.P. Greenberg, *Bacterial biofilms: a common cause of persistent infections.* Science (New York, N.Y.), 1999. **284**(5418): p. 1318-1322.

57. Walters, M.C., et al., *Contributions of antibiotic penetration, oxygen limitation, and low metabolic activity to tolerance of Pseudomonas aeruginosa biofilms to ciprofloxacin and tobramycin.* Antimicrobial Agents and Chemotherapy, 2003. **47**(1): p. 317-23.

58. Bjarnsholt, T., *Antibiotic Tolerance and Resistance in Biofilms*, in *Biofilm infections*. 2010, Springer: New York ; London :. p. 216.

59. Jedlicka, S.S., J.L. Rickus, and D. Zemlyanov, *Controllable Surface Expression of Bioactive Peptides Incorporated into a Silica Thin Film Matrix.* The Journal of Physical Chemistry C, 2010. **114**(1): p. 342-344.

60. Lewis, K., *Persister cells, dormancy and infectious disease.* Nature reviews. Microbiology, 2007. **5**(1): p. 48-56.

61. Stewart, P.S., *Theoretical aspects of antibiotic diffusion into microbial biofilms.* Antimicrobial Agents and Chemotherapy, 1996. **40**(11): p. 2517-2522.

62. Rasmussen, K. and Z. Lewandowski, *Microelectrode measurements of local mass transport rates in heterogeneous biofilms.* Biotechnology and Bioengineering, 1998. **59**(3): p. 302-309.

63. Aanaes, K., et al., *Decreased mucosal oxygen tension in the maxillary sinuses in patients with cystic fibrosis.* Journal of Cystic Fibrosis, 2011. **10**(2): p. 114-120.

64. Guss, A.M., et al., *Phylogenetic and metabolic diversity of bacteria associated with cystic fibrosis.* The ISME journal, 2011. **5**(1): p. 20-29.

65. Bjarnsholt, T., et al., *Pseudomonas aeruginosa biofilms in the respiratory tract of cystic fibrosis patients.* Pediatric pulmonology, 2009. **44**(6): p. 547-58.

66. Kim, J., et al., *Tolerance of dormant and active cells in Pseudomonas aeruginosa PA01 biofilm to antimicrobial agents.* Journal of Antimicrobial Chemotherapy, 2009. **63**(1): p. 129-135.

67. Tolker-Nielsen, T., et al., *Tolerance to the antimicrobial peptide colistin in Pseudomonas aeruginosa biofilms is linked to metabolically active cells, and depends on the pmr and mexAB-oprM genes.* Molecular Microbiology, 2008. **68**(1): p. 223-240.

68. Kanj, S.S. and Z.A. Kanafani, *Current concepts in antimicrobial therapy against resistant gram-negative organisms: extended-spectrum beta-lactamase-producing Enterobacteriaceae, carbapenem-resistant Enterobacteriaceae, and multidrug-resistant Pseudomonas aeruginosa.* Mayo Clinic proceedings. Mayo Clinic, 2011. **86**(3): p. 250-9.

69. Falagas, M.E., A. Michalopoulos, and E.I. Metaxas, *Pulmonary drug delivery systems for antimicrobial agents: facts and myths.* International Journal of Antimicrobial Agents, 2010. **35**(2): p. 101-6.

70. Brooun, A., S. Liu, and K. Lewis, *A dose-response study of antibiotic resistance in Pseudomonas aeruginosa biofilms.* Antimicrobial Agents and Chemotherapy, 2000. **44**(3): p. 640-6.

71. Michiels, J., et al., *Novel persistence genes in Pseudomonas aeruginosa identified by high-throughput screening.* FEMS Microbiology Letters, 2009. **297**(1): p. 73-79.

72. Spoering, A.L. and K. Lewis, *Biofilms and planktonic cells of Pseudomonas aeruginosa have similar resistance to killing by antimicrobials.* Journal of Bacteriology, 2001. **183**(23): p. 6746-6751.

73. Brooun, A., S.H. Liu, and K. Lewis, *A dose-response study of antibiotic resistance in Pseudomonas aeruginosa biofilms.* Antimicrobial Agents and Chemotherapy, 2000. **44**(3): p. 640-646.

74. Mutschler, H., et al., *A novel mechanism of programmed cell death in bacteria by toxin-antitoxin systems corrupts peptidoglycan synthesis.* PLoS Biology, 2011. **9**(3): p. e1001033.

75. Murakami, K., et al., *Role for rpoS gene of Pseudomonas aeruginosa in antibiotic tolerance.* FEMS Microbiology Letters, 2005. **242**(1): p. 161-7.

76. Viducic, D., et al., *Functional analysis of spoT, relA and dksA genes on quinolone tolerance in Pseudomonas aeruginosa under nongrowing condition.* Microbiology and Immunology, 2006. **50**(4): p. 349-57.

77. De Groote, V.N., et al., *Novel persistence genes in Pseudomonas aeruginosa identified by high-throughput screening.* FEMS Microbiology Letters, 2009. **297**(1): p. 73-9.

78. Gerdes, K., S.K. Christensen, and A. Lobner-Olesen, *Prokaryotic toxin-antitoxin stress response loci.* Nature reviews. Microbiology, 2005. **3**(5): p. 371-82.

79. Hayes, F., *Toxins-antitoxins: plasmid maintenance, programmed cell death, and cell cycle arrest.* Science, 2003. **301**(5639): p. 1496-9.

80. Hayes, C.S. and R.T. Sauer, *Toxin-antitoxin pairs in bacteria: killers or stress regulators?* Cell, 2003. **112**(1): p. 2-4.

81. Nariya, H. and M. Inouye, *MazF, an mRNA interferase, mediates programmed cell death during multicellular Myxococcus development.* Cell, 2008. **132**(1): p. 55-66.

82. Bagge, N., et al., *Rapid development in vitro and in vivo of resistance to ceftazidime in biofilm-growing Pseudomonas aeruginosa due to chromosomal beta-lactamase.* APMIS, 2000. **108**(9): p. 589-600.

83. Bagge, N., et al., *Dynamics and spatial distribution of beta-lactamase expression in Pseudomonas aeruginosa biofilms.* Antimicrobial Agents and Chemotherapy, 2004. **48**(4): p. 1168-1174.

84. Moskowitz, S.M., et al., *Clinically feasible biofilm susceptibility assay for isolates of Pseudomonas aeruginosa from patients with cystic fibrosis.* Journal of Clinical Microbiology, 2004. **42**(5): p. 1915-1922.

85. Zhang, L. and T.F. Mah, *Involvement of a novel efflux system in biofilm-specific resistance to antibiotics.* Journal of Bacteriology, 2008. **190**(13): p. 4447-52.

86. Mah, T.F., et al., *A genetic basis for Pseudomonas aeruginosa biofilm antibiotic resistance.* Nature, 2003. **426**(6964): p. 306-10.

87. Li, Z., et al., *Longitudinal development of mucoid Pseudomonas aeruginosa infection and lung disease progression in children with cystic fibrosis.* JAMA : the journal of the American Medical Association, 2005. **293**(5): p. 581-8.

88. Yoon, S.S., et al., *Anaerobic killing of mucoid Pseudomonas aeruginosa by acidified nitrite derivatives under cystic fibrosis airway conditions.* Journal of Clinical Investigation, 2006. **116**(2): p. 436-446.

89. Koch, C., *Early infection and progression of cystic fibrosis lung disease.* Pediatric pulmonology, 2002. **34**(3): p. 232-6.

90. Hoiby, N., *Prospects for the prevention and control of pseudomonal infection in children with cystic fibrosis.* Paediatric drugs, 2000. **2**(6): p. 451-63.

91. McPherson, H., M. Rosenthal, and A. Bush, *Can Mucoid Pseudomonas aeruginosa Be Eradicated in Children With Cystic Fibrosis?* Pediatric pulmonology, 2010. **45**(6): p. 566-568.

92. Armstrong, D.S., et al., *Lower airway inflammation in infants and young children with cystic fibrosis.* American Journal of Respiratory and Critical Care Medicine, 1997. **156**(4 Pt 1): p. 1197-204.

93. Armstrong, D.S., et al., *Lower airway inflammation in infants with cystic fibrosis detected by newborn screening.* Pediatric pulmonology, 2005. **40**(6): p. 500-10.

94. Ciofu, O., et al., *Investigation of the algT operon sequence in mucoid and non-mucoid Pseudomonas aeruginosa isolates from 115 Scandinavian patients with cystic fibrosis and in 88 in vitro non-mucoid revertants.* Microbiology, 2008. **154**(Pt 1): p. 103-13.

95. Song, Z.J., et al., *Pseudomonas aeruginosa alginate is refractory to Th1 immune response and impedes host immune clearance in a mouse model of acute lung infection.* Journal of Medical Microbiology, 2003. **52**(9): p. 731-740.

96. Jensen, P.O., et al., *Rapid necrotic killing of polymorphonuclear leukocytes is caused by quorum-sensing-controlled production of rhamnolipid by Pseudomonas aeruginosa.* Microbiology, 2007. **153**(Pt 5): p. 1329-38.

97. Bjarnsholt, T., et al., *Pseudomonas aeruginosa tolerance to tobramycin, hydrogen peroxide and polymorphonuclear leukocytes is quorum-sensing dependent.* Microbiology, 2005. **151**(Pt 2): p. 373-83.

98. Wu, H., et al., *Pseudomonas aeruginosa mutations in lasI and rhlI quorum sensing systems result in milder chronic lung infection.* Microbiology, 2001. **147**(Pt 5): p. 1105-13.

99. Goldstein, W. and G. Doring, *Lysosomal enzymes from polymorphonuclear leukocytes and proteinase inhibitors in patients with cystic fibrosis.* The American review of respiratory disease, 1986. **134**(1): p. 49-56.

100. West, J.B., *Pulmonary physiology and pathophysiology : an integrated, case-based approach*. 2nd ed. 2007, Philadelphia: Wolters Kluwer Health/Lippincott Williams & Wilkins. vii, 150 p.

101. Rosenbluth, D.B., et al., *Lung function decline in cystic fibrosis patients and timing for lung transplantation referral.* Chest, 2004. **126**(2): p. 412-9.

102. Boverhof, D.R., et al., *Transgenic animal models in toxicology: historical perspectives and future outlook.* Toxicological sciences : an official journal of the Society of Toxicology, 2011. **121**(2): p. 207-33.

103. Kukavica-Ibrulj, I. and R.C. Levesque, *Animal models of chronic lung infection with Pseudomonas aeruginosa: useful tools for cystic fibrosis studies.* Laboratory Animals, 2008. **42**(4): p. 389-412.

104. Pedersen, S.S., et al., *Induction of experimental chronic Pseudomonas aeruginosa lung infection with P. aeruginosa entrapped in alginate microspheres.* APMIS : acta pathologica, microbiologica, et immunologica Scandinavica, 1990. **98**(3): p. 203-11.

105. Cash, H.A., et al., *A rat model of chronic respiratory infection with Pseudomonas aeruginosa.* The American review of respiratory disease, 1979. **119**(3): p. 453-9.

106. Sato, A., et al., *Study of the effects of AM-1155 in a rat chronic respiratory tract infection model with Pseudomonas aeruginosa.* Drugs, 1995. **49 Suppl 2**: p. 253-5.

107. Pennington, J.E., et al., *Active immunization with lipopolysaccharide Pseudomonas antigen for chronic Pseudomonas bronchopneumonia in guinea pigs.* The Journal of clinical investigation, 1981. **68**(5): p. 1140-8.

108. Thomassen, M.J., et al., *Pulmonary cellular response to chronic irritation and chronic Pseudomonas aeruginosa pneumonia in cats.* Infection and Immunity, 1984. **45**(3): p. 741-7.

109. Cheung, A.T., et al., *Chronic Pseudomonas aeruginosa endobronchitis in rhesus monkeys: I. Effects of pentoxifylline on neutrophil influx.* Journal of Medical Primatology, 1992. **21**(7-8): p. 357-62.

110. Cheung, A.T., et al., *Chronic Pseudomonas aeruginosa endobronchitis in rhesus monkeys: II. A histopathologic analysis.* Journal of Medical Primatology, 1993. **22**(4): p. 257-62.

111. Starke, J.R., et al., *A mouse model of chronic pulmonary infection with Pseudomonas aeruginosa and Pseudomonas cepacia.* Pediatric Research, 1987. **22**(6): p. 698-702.

112. Morissette, C., E. Skamene, and F. Gervais, *Endobronchial inflammation following Pseudomonas aeruginosa infection in resistant and susceptible strains of mice.* Infection and Immunity, 1995. **63**(5): p. 1718-24.

113. Stevenson, M.M., et al., *In vitro and in vivo T cell responses in mice during bronchopulmonary infection with mucoid Pseudomonas aeruginosa.* Clinical and Experimental Immunology, 1995. **99**(1): p. 98-105.

114. Stotland, P.K., D. Radzioch, and M.M. Stevenson, *Mouse models of chronic lung infection with Pseudomonas aeruginosa: models for the study of cystic fibrosis.* Pediatric pulmonology, 2000. **30**(5): p. 413-24.

115. Swords, W.E., et al., *Sialylation of lipooligosaccharides promotes biofilm formation by nontypeable Haemophilus influenzae.* Infection and Immunity, 2004. **72**(1): p. 106-13.

116. Bjarnsholt, T., *In Vivo Models of Biofilm Infection*, in *Biofilm infections*. 2010, Springer: New York ; London :. p. 267.

117. Tata, F., et al., *Cloning the mouse homolog of the human cystic fibrosis transmembrane conductance regulator gene.* Genomics, 1991. **10**(2): p. 301-7.

118. Du, M., et al., *Aminoglycoside suppression of a premature stop mutation in a Cftr-/- mouse carrying a human CFTR-G542X transgene.* Journal of molecular medicine, 2002. **80**(9): p. 595-604.

119. Davidson, D.J. and J.R. Dorin, *The CF mouse: an important tool for studying cystic fibrosis.* Expert Reviews in Molecular Medicine, 2001. **2001**: p. 1-27.

120. Committee on the Use of Animals in, R., S. National Academy of, and M. Institute of, *Science, medicine, and animals*. 1991, Washington, D.C. :: National Academy Press. 1-vii, 30 p.

121. O'Toole, G.A. and R. Kolter, *Initiation of biofilm formation in Pseudomonas fluorescens WCS365 proceeds via multiple, convergent signalling pathways: a genetic analysis.* Molecular Microbiology, 1998. **28**(3): p. 449-461.

122. O'Toole, G.A. and R. Kolter, *Flagellar and twitching motility are necessary for Pseudomonas aeruginosa biofilm development.* Molecular Microbiology, 1998. **30**(2): p. 295-304.

123. Bjarnsholt, T., *Different Methods for Culturing Biofilms In Vitro*, in *Biofilm infections*. 2010, Springer: New York ; London :. p. 251.

124. Weiss Nielsen, M., et al., *Pseudomonas aeruginosa and Saccharomyces cerevisiae biofilm in flow cells.* Journal of visualized experiments., 2011(47).

125. Heydorn, A., et al., *Quantification of biofilm structures by the novel computer program COMSTAT.* Microbiology, 2000. **146 (Pt 10)**: p. 2395-407.

126. Molin, S., et al., *Differentiation and distribution of colistin- and sodium dodecyl sulfate-tolerant cells in Pseudomonas aeruginosa biofilms.* Journal of Bacteriology, 2007. **189**(1): p. 28-37.

127. Klausen, M., et al., *Involvement of bacterial migration in the development of complex multicellular structures in Pseudomonas aeruginosa biofilms.* Molecular Microbiology, 2003. **50**(1): p. 61-8.

128. Pamp, S.J., C. Sternberg, and T. Tolker-Nielsen, *Insight into the Microbial Multicellular Lifestyle via Flow-Cell Technology and Confocal Microscopy.* Cytometry Part A, 2009. **75A**(2): p. 90-103.

129. Tolker-Nielsen, T., et al., *Roles of type IV pili, flagellum-mediated motility and extracellular DNA in the formation of mature multicellular structures in Pseudomonas aeruginosa biofilms.* Environmental Microbiology, 2008. **10**(9): p. 2331-2343.

130. Hekiert, A.M., et al., *Biofilms correlate with TH1 inflammation in the sinonasal tissue of patients with chronic rhinosinusitis.* Otolaryngology - Head and Neck Surgery, 2009. **141**(4): p. 448-453.

131. Lipinski, C. and A. Hopkins, *Navigating chemical space for biology and medicine.* Nature, 2004. **432**(7019): p. 855-61.

132. Creton, S., et al., *Improved risk assessment of chemicals through the application of toxicokinetic information: Opportunities for the replacement, reduction and refinement of animal use.* Toxicology, 2009. **262**(1): p. 10-11.

133. Hendriksen, C.F.M., *Replacement, reduction and refinement alternatives to animal use in vaccine potency measurement.* Expert Review of Vaccines, 2009. **8**(3): p. 313-322.

134. Flecknell, P., *Replacement, reduction and refinement.* ALTEX, 2002. **19**(2): p. 73-8.

135. Lucken, R.N., *The five Rs: refinement, reduction, replacement. A regulatory revolution.* Developments in biological standardization, 1996. **86**: p. 67-72.

136. Davila, J.C., et al., *Predictive value of in vitro model systems in toxicology.* Annual Review of Pharmacology and Toxicology, 1998. **38**: p. 63-96.

137. Ingber, D.E., *Cellular mechanotransduction: putting all the pieces together again.* The FASEB journal : official publication of the Federation of American Societies for Experimental Biology, 2006. **20**(7): p. 811-27.

138. van Midwoud, P.M., E. Verpoorte, and G.M. Groothuis, *Microfluidic devices for in vitro studies on liver drug metabolism and toxicity.* Integrative biology : quantitative biosciences from nano to macro, 2011. **3**(5): p. 509-21.

139. van Midwoud, P.M., et al., *Hydrogel embedding of precision-cut liver slices in a microfluidic device improves drug metabolic activity.* Biotechnology and Bioengineering, 2011. **108**(6): p. 1404-12.

140. van Midwoud, P.M., et al., *A microfluidic approach for in vitro assessment of interorgan interactions in drug metabolism using intestinal and liver slices.* Lab on a Chip, 2010. **10**(20): p. 2778-86.

141. van Midwoud, P.M., et al., *Microfluidic biochip for the perifusion of precision-cut rat liver slices for metabolism and toxicology studies.* Biotechnology and Bioengineering, 2010. **105**(1): p. 184-94.

142. Whitesides, G.M., et al., *Soft lithography in biology and biochemistry.* Annual Review of Biomedical Engineering, 2001. **3**: p. 335-73.

143. El-Ali, J., P.K. Sorger, and K.F. Jensen, *Cells on chips.* Nature, 2006. **442**(7101): p. 403-11.

144. Shin, M., et al., *Endothelialized networks with a vascular geometry in microfabricated poly(dimethyl siloxane).* Biomedical Microdevices, 2004. **6**(4): p. 269-78.

145. Jang, K., et al., *Development of an osteoblast-based 3D continuous-perfusion microfluidic system for drug screening.* Analytical and Bioanalytical Chemistry, 2008. **390**(3): p. 825-32.

146. Lam, M.T., et al., *Microfeature guided skeletal muscle tissue engineering for highly organized 3-dimensional free-standing constructs.* Biomaterials, 2009. **30**(6): p. 1150-5.

147. Carraro, A., et al., *In vitro analysis of a hepatic device with intrinsic microvascular-based channels.* Biomedical Microdevices, 2008. **10**(6): p. 795-805.

148. Lee, P.J., P.J. Hung, and L.P. Lee, *An artificial liver sinusoid with a microfluidic endothelial-like barrier for primary hepatocyte culture.* Biotechnology and Bioengineering, 2007. **97**(5): p. 1340-6.

149. Powers, M.J., et al., *A microfabricated array bioreactor for perfused 3D liver culture.* Biotechnology and Bioengineering, 2002. **78**(3): p. 257-69.

150. Khetani, S.R. and S.N. Bhatia, *Microscale culture of human liver cells for drug development.* Nature Biotechnology, 2008. **26**(1): p. 120-6.

151. Park, J.W., et al., *Microfluidic culture platform for neuroscience research.* Nature Protocols, 2006. **1**(4): p. 2128-36.

152. Shuler, M.L., et al., *Characterization of a Gastrointestinal Tract Microscale Cell Culture Analog Used to Predict Drug Toxicity.* Biotechnology and Bioengineering, 2009. **104**(1): p. 193-205.

153. Baudoin, R., et al., *Development of a renal microchip for in vitro distal tubule models.* Biotechnology Progress, 2007. **23**(5): p. 1245-53.

154. Jang, K.J. and K.Y. Suh, *A multi-layer microfluidic device for efficient culture and analysis of renal tubular cells.* Lab on a Chip, 2010. **10**(1): p. 36-42.

155. Song, J.W., et al., *Computer-controlled microcirculatory support system for endothelial cell culture and shearing.* Analytical Chemistry, 2005. **77**(13): p. 3993-9.

156. Harris, S.G. and M.L. Shuler, *Growth of endothelial cells on microfabricated silicon nitride membranes for an in vitro model of the blood-brain barrier.* Biotechnology and Bioprocess Engineering, 2003. **8**(4): p. 246-251.

157. Huh, D., et al., *Acoustically detectable cellular-level lung injury induced by fluid mechanical stresses in microfluidic airway systems.* Proceedings of the National Academy of Sciences of the United States of America, 2007. **104**(48): p. 18886-91.

158. Tavana, H., et al., *Dynamics of liquid plugs of buffer and surfactant solutions in a micro-engineered pulmonary airway model.* Langmuir : the ACS journal of surfaces and colloids, 2010. **26**(5): p. 3744-52.

159. Huh, D., et al., *Reconstituting organ-level lung functions on a chip.* Science, 2010. **328**(5986): p. 1662-1668.

160. Hoganson, D.M., et al., *Lung assist device technology with physiologic blood flow developed on a tissue engineered scaffold platform.* Lab on a Chip, 2011. **11**(4): p. 700-707.

161. Charati, S.G. and S.A. Stern, *Diffusion of Gases in Silicone Polymers: Molecular Dynamics Simulations.* Macromolecules, 1998. **31**: p. 5529-5535.

162. Merkel, T.C., et al., *Gas Sorption, Diffusion, and Permeation in Poly(dimethylsiloxane).* Journal of Polymer Science, Part B: Polymer Physics, 2000. **38**: p. 415–434.

163. Mehta, G., et al., *Quantitative measurement and control of oxygen levels in microfluidic poly(dimethylsiloxane) bioreactors during cell culture.* Biomedical Microdevices, 2007. **9**(2): p. 123 - 134.

164. Mata, A., A.J. Fleischman, and S. Roy, *Characterization of Polydimethylsiloxane (PDMS) Properties for Biomedical Micro/Nanosystems.* Biomedical Microdevices, 2005. **7**: p. 281–293.

165. Kim, L., et al., *A practical guide to microfluidic perfusion culture of adherent mammalian cells.* Lab on a Chip, 2007. **7**: p. 681–694.

166. McDonald, J.C., et al., *Fabrication of microfluidic systems in poly(dimethylsiloxane).* Electrophoresis, 2000. **21**(1): p. 27-40.

167. Smith, G.D., et al., *Characterization and resolution of evaporation-mediated osmolality shifts that constrain microfluidic cell culture in poly(dimethylsiloxane) devices.* Analytical Chemistry, 2007. **79**(3): p. 1126-1134.

168. Beebe, D.J. and M.W. Toepke, *PDMS absorption of small molecules and consequences in microfluidic applications.* Lab on a Chip, 2006. **6**(12): p. 1484-1486.

169. Regehr, K.J., et al., *Biological implications of polydimethylsiloxane-based microfluidic cell culture.* Lab on a Chip, 2009. **9**(15): p. 2132-2139.

170. Lee, J.N., et al., *Compatibility of mammalian cells on surfaces of poly(dimethylsiloxane).* Langmuir, 2004. **20**(26): p. 11684-11691.

171. Lee, G.B., M.H. Wu, and S.B. Huang, *Microfluidic cell culture systems for drug research.* Lab on a Chip, 2010. **10**(8): p. 939-956.

172. Harsha, A.P. and U.S. Tewari, *The effect of fibre reinforcement and solid lubricants on abrasive wear behavior of polyetheretherketone composites.* Journal of Reinforced Plastics and Composites, 2003. **22**(8): p. 751-767.

173. Katzer, A., et al., *Polyetheretherketone - cytotoxicity and mutagenicity in vitro.* Biomaterials, 2002. **23**(8): p. 1749-1759.

174. Gronowicz, G.A., et al., *The in vitro response of human osteoblasts to polyetheretherketone (PEEK) substrates compared to commercially pure titanium.* Biomaterials, 2008. **29**(11): p. 1563-1572.

175. Hwang, W., et al., *Polyether ether ketone microstructures for chemical analytics.* Microsystem Technologies-Micro-and Nanosystems-Information Storage and Processing Systems, 2008. **14**(9-11): p. 1699-1700.

176. Muhlberger, H., et al., *Polymer Lab-on-a-Chip system with electrical detection.* Ieee Sensors Journal, 2008. **8**(5-6): p. 572-579.

177. Beebe, D.J., et al., *Rapid Prototyping of Arrayed Microfluidic Systems in Polystyrene for Cell-Based Assays.* Analytical Chemistry, 2011. **83**(4): p. 1408-1417.

178. Hansen, T.S., D. Selmeczi, and N.B. Larsen, *Fast prototyping of injection molded polymer microfluidic chips.* Journal of Micromechanics and Microengineering, 2010. **20**(1).

179. Stangegaard, M., et al., *A biocompatible micro cell culture chamber (microCCC) for the culturing and on-line monitoring of eukaryote cells.* Lab on a Chip, 2006. **6**(8): p. 1045-51.

180. Brown, L., et al., *Fabrication and characterization of poly(methylmethacrylate) microfluidic devices bonded using surface modifications and solvents.* Lab on a Chip, 2006. **6**(1): p. 66-73.

181. Kallepalli, D.L.N., N.R. Desai, and V.R. Soma, *Fabrication and optical characterization of microstructures in poly(methylmethacrylate) and poly(dimethylsiloxane) using femtosecond pulses for photonic and microfluidic applications.* Applied Optics, 2010. **49**(13): p. 2475-2489.

182. Garstecki, P., et al., *Bonding of microfluidic devices fabricated in polycarbonate.* Lab on a Chip, 2010. **10**(10): p. 1324-1327.

183. Park, J., et al., *A microsystem for sensing and patterning oxidative microgradients during cell culture.* Lab on a Chip, 2006. **6**: p. 611–622.

184. Aitken, C.E.a., R.A. Marshall, and J.D. Puglisi, *An Oxygen Scavenging System for Improvement of Dye Stability in Single-Molecule Fluorescence Experiments.* Biophysical Journal, 2008. **94**(5): p. 1826-1835.

185. Shaikh, A.A. and S.M.J. Zaidi, *Kinetics of catalytic oxidation of aqueous sodium sulfite.* Reaction Kinetics and Catalysis Letters, 1998. **64**(2): p. 343-349.

186. Shams el Din, A.M. and R.A. Arain, *Kinetics of oxygen scavenging by catalysed hydrazine.* Corrosion Science, 1989. **29**(4): p. 445-453.

187. Polinkovsky, M., et al., *Fine temporal control of the medium gas content and acidity and on-chip generation of series of oxygen concentrations for cell cultures.* Lab on a Chip, 2009. **9**(8): p. 1073-84.

188. Vollmer, A.P., et al., *Development of an integrated microfluidic platform for dynamic oxygen sensing and delivery in a flowing medium.* Lab on a Chip, 2005. **5**(10): p. 1059-66.

189. Adler, M., et al., *Generation of oxygen gradients with arbitrary shapes in a microfluidic device.* Lab on a Chip, 2010. **10**(3): p. 388-91.

190. Marianne Reist, K.-A.M.P.J., *Toxic Effects of Sulphite in Combination with Peroxynitrite on Neuronal Cells.* Journal of Neurochemistry, 1998. **71**(6): p. 2431-2438.

191. Wu, C.-C., et al., *Fabrication of miniature Clark oxygen sensor integrated with microstructure.* Sensors and Actuators, B: Chemical, 2005. **110**: p. 342–349.

192. Lee, J.-H., et al., *Needle-type dissolved oxygen microelectrode array sensors for in situ measurements.* Sensors and Actuators, B: Chemical, 2007. **128**(1): p. 179-185.

193. Park, J., et al., *2 X 3 array oxygen sensor for measuring cellular respiration level.* 4th IEEE International Conference on Nano/Micro Engineered and Molecular Systems, NEMS 2009, 2009: p. 1054-1057.

194. Jerónimo, P.C.A., A.N. Araújo, and M. Conceição B.S.M. Montenegro, *Optical sensors and biosensors based on sol-gel films.* Talanta, 2007. **72**(1): p. 13-27.

195. O'Riordan, T.C., et al., *Analysis of Intracellular Oxygen and Metabolic Responses of Mammalian Cells by Time-Resolved Fluorometry.* Analytical Chemistry, 2007. **79**: p. 9414-9419.

196. Carraway, E.R. and J.N. Demas, *Luminescence Quenching Mechanism for Microheterogeneous Systems.* Analytical Chemistry, 1991. **63**: p. 332-336.

197. Jorge, P.A.S., et al., *Optical fiber probes for fluorescence based oxygen sensing.* Sensors and Actuators, B: Chemical, 2004. **103**(1-2): p. 290-299.

198. McEvoy, A.K., C.M. McDonagh, and B.D. MacCraith, *Dissolved Oxygen Sensor Based on FIuorescence Quenching of Oxygen-sensitive Ruthenium Complexes Immobilized in Sol-Gel-derived Porous Silica Coatings.* The Analyst, 1997. **121**: p. 785-788.

199. Klimant, l. and O.S. Wolfbeis, *Oxygen-Sensitive Luminescent Materials Based on Silicone-Soluble Ruthenium Diimine Complexes.* Analytical Chemistry, 1995. **67**: p. 3160-3166.

200. Pieper, S.B., et al., *Phosphorescence characteristics of ruthenium complex as an optical transducer for biosensors.* Applied Physics Letters, 2008. **92**(8): p. 081915-3.

201. Yeh, T.-S., C.-S. Chu, and Y.-L. Lo, *Highly sensitive optical fiber oxygen sensor using Pt(II) complex embedded in sol–gel matrices.* Sensors and Actuators, B: Chemical, 2006. **119**: p. 701–707.

202. Basu, B.J., *Optical oxygen sensing based on luminescence quenching of platinum porphyrin dyes doped in ormosil coatings.* Sensors and Actuators, B: Chemical, 2007. **123**: p. 568–577.

203. Amao, Y., T. Miyashita, and I. Okura, *Optical oxygen sensing based on the luminescence change of metalloporphyrins immobilized in styrene–pentafluorostyrene copolymer film.* The Analyst, 2000. **125**: p. 871–875.

204. Lee, S.-K. and I. Okura, *Optical Sensor for Oxygen Using a Porphyrin-doped Sol–Gel Glass.* The Analyst, 1997. **122**: p. 81–84.

205. Amao, Y., T. Miyashita, and I. Okura, *Novel optical oxygen sensing material: platinum octaethylporphyrin immobilized in a copolymer film of isobutyl methacrylate and tetrafluoropropyl methacrylate.* Reactive & Functional Polymers, 2001. **47**: p. 49–54.

206. Amao, Y., T. Miyashita, and I. Okura, *Platinum tetrakis(pentafuorophenyl)porphyrin immobilized in polytrifluoroethylmethacrylate film as a photostable optical oxygen detection material.* Journal of Fluorine Chemistry, 2001(107): p. 101-106.

207. Schmaelzlin, E., et al., *An Optical Multifrequency Phase-Modulation Method Using Microbeads for Measuring Intracellular Oxygen Concentrations in Plants.* Biophysical Journal, 2005. **89**: p. 1339–1345.

208. Gillanders, R.N., et al., *A composite sol–gel/fluoropolymer matrix for dissolved oxygen optical sensing.* Journal of Photochemistry and Photobiology, A: Chemistry, 2004. **163**: p. 193–199.

209. Dunbar, R.A., J.D. Jordan, and F.V. Bright, *Development of Chemical Sensing Platforms Based on Sol-Gel-Derived Thin Films: Origin of Film Age vs Performance Trade-Offs.* Analytical Chemistry, 1996. **68**: p. 604-610.

210. Tang, Y., et al., *Sol-Gel-Derived Sensor Materials That Yield Linear Calibration Plots, High Sensitivity, and Long-Term Stability.* Analytical Chemistry, 2003. **75**(10): p. 2407-2413.

211. Lin, J. and C.W. Brown, *Sol-gel glass as a matrix for chemical and biochemical sensing.* TrAC Trends in Analytical Chemistry, 1997. **16**(4): p. 200-211.

212. Madou, M.J., *Fundamentals of microfabrication : the science of miniaturization*. 2nd ed. 2002, Boca Raton: CRC Press. 723 p.

213. Chin, C.D., V. Linder, and S.K. Sia, *Lab-on-a-chip devices for global health: Past studies and future opportunities.* Lab on a Chip, 2007. **7**(1): p. 41-57.

214. Becker, H. and C. Gartner, *Polymer microfabrication methods for microfluidic analytical applications.* Electrophoresis, 2000. **21**(1): p. 12-26.

215. Fischer, R., et al., *Cell Cultures in Microsystems: Biocompatibility Aspects.* Biotechnology and Bioengineering, 2011. **108**(3): p. 687-693.

216. Nunes, P.S., et al., *Cyclic olefin polymers: emerging materials for lab-on-a-chip applications.* Microfluidics and Nanofluidics, 2010. **9**(2-3): p. 145-161.

217. Becker, H. and C. Gartner, *Polymer microfabrication technologies for microfluidic systems.* Analytical and Bioanalytical Chemistry, 2008. **390**(1): p. 89-111.

218. Rotting, O., et al., *Polymer microfabrication technologies.* Microsystem Technologies, 2002. **8**(1): p. 32-36.

219. *Performance Micro Tool*. 2011; Available from: http://www.pmtnow.com.

220. Chae, J., S.S. Park, and T. Freiheit, *Investigation of micro-cutting operations.* International Journal of Machine Tools & Manufacture, 2006. **46**(3-4): p. 313-332.

221. Tansel, I.N., et al., *Tool wear estimation in micro-machining. Part I: tool usage-cutting force relationship.* International Journal of Machine Tools & Manufacture, 2000. **40**(4): p. 599-608.

222. Tansel, I.N., et al., *Tool wear estimation in micro-machining. Part II: neural-network-based periodic inspector for nonmetals.* International Journal of Machine Tools & Manufacture, 2000. **40**(4): p. 609-620.

223. Lee, K.H. and D.A. Dornfeld, *Micro-burr formation and minimization through process control.* Precision Engineering-Journal of the International Societies for Precision Engineering and Nanotechnology, 2005. **29**(2): p. 246-252.

224. Matsumura, T., et al., *Deburring of micro-scale structures machined in milling.* Proceedings Of The ASME International Manufacturing Science And Engineering Conference, 2011. **1**: p. 105-112.

225. Aramcharoen, A. and P.T. Mativenga, *Size effect and tool geometry in micromilling of tool steel.* Precision Engineering-Journal of the International Societies for Precision Engineering and Nanotechnology, 2009. **33**(4): p. 402-407.

226. Ogilvie, I.R.G., et al., *Reduction of surface roughness for optical quality microfluidic devices in PMMA and COC.* Journal of Micromechanics and Microengineering, 2010. **20**(6): p. -.

227. Kafka, J., et al., *Fabrication of an all-polymer electrochemical sensor by using a one-step hot embossing procedure.* Microelectronic Engineering, 2010. **87**(5-8): p. 1239-1241.

228. Chantiwas, R., et al., *Simple replication methods for producing nanoslits in thermoplastics and the transport dynamics of double-stranded DNA through these slits.* Lab on a Chip, 2010. **10**(23): p. 3255-3264.

229. Wilson, M.E., et al., *Fabrication of circular microfluidic channels by combining mechanical micromilling and soft lithography.* Lab on a Chip, 2011. **11**(8): p. 1550-1555.

230. Bogue, R., *Fifty years of the laser: its role in material processing.* Assembly Automation, 2010. **30**(4): p. 317-322.

231. Jensen, M.F., et al., *Microstructure fabrication with a CO2 laser system: characterization and fabrication of cavities produced by raster scanning of the laser beam.* Lab on a Chip, 2003. **3**(4): p. 302-307.

232. Snakenborg, D., H. Klank, and J.P. Kutter, *Microstructure fabrication with a CO2 laser system.* Journal of Micromechanics and Microengineering, 2004. **14**(2): p. 182-189.

233. Klank, H., J.P. Kutter, and O. Geschke, *CO2-laser micromachining and back-end processing for rapid production of PMMA-based microfluidic systems.* Lab on a Chip, 2002. **2**: p. 242-246.

234. Bowden, M., et al., *CO2 laser microfabrication of an integrated polymer microfluidic manifold for the determination of phosphorus.* Lab on a Chip, 2003. **3**(4): p. 221-223.

235. Lander, M.R., et al., *Biomimetic Membrane Arrays on Cast Hydrogel Supports.* Langmuir, 2011. **27**(11): p. 7002-7007.

236. Hansen, J.S., et al., *Large scale biomimetic membrane arrays.* Analytical and Bioanalytical Chemistry, 2009. **395**(3): p. 719-727.

237. Hansen, J.S., et al., *Development of an automation technique for the establishment of functional lipid bilayer arrays.* Journal of Micromechanics and Microengineering, 2009. **19**(2): p. -.

238. Vogel, J., et al., *A support structure for biomimetic applications.* Journal of Micromechanics and Microengineering, 2009. **19**(2): p. -.

239. Chung, C.K., Y.C. Lin, and G.R. Huang, *Bulge formation and improvement of the polymer in CO2 laser micromachining.* Journal of Micromechanics and Microengineering, 2005. **15**(10): p. 1878-1884.

240. Li, Y., et al., *Integration of isoelectric focusing with parallel sodium dodecyl sulfate gel electrophoresis for multidimensional protein separations in a plastic microfludic network.* Analytical Chemistry, 2004. **76**(3): p. 742-748.

241. Park, D.S.W., et al., *A titer plate-based polymer microfluidic platform for high throughput nucleic acid purification.* Biomedical Microdevices, 2008. **10**(1): p. 21-33.

242. Nikcevic, I., et al., *Characterization and performance of injection molded poly(methylmethacrylate) microchips for capillary electrophoresis.* Journal of Chromatography A, 2007. **1154**(1-2): p. 444-453.

243. Hsu, Y.C. and T.Y. Chen, *Applying Taguchi methods for solvent-assisted PMMA bonding technique for static and dynamic mu-TAS devices.* Biomedical Microdevices, 2007. **9**(4): p. 513-522.

244. Ng, S.H., et al., *Thermally activated solvent bonding of polymers.* Microsystem Technologies-Micro-and Nanosystems-Information Storage and Processing Systems, 2008. **14**(6): p. 753-759.

245. Tsao, C.W. and D.L. DeVoe, *Bonding of thermoplastic polymer microfluidics.* Microfluidics and Nanofluidics, 2009. **6**(1): p. 1-16.

246. Witek, M.A., et al., *Cell transport via electromigration in polymer-based microfluidic devices.* Lab on a Chip, 2004. **4**(5): p. 464-472.

247. Shenton, M.J., M.C. Lovell-Hoare, and G.C. Stevens, *Adhesion enhancement of polymer surfaces by atmospheric plasma treatment.* Journal of Physics D-Applied Physics, 2001. **34**(18): p. 2754-2760.

248. Nath, P., et al., *Rapid prototyping of robust and versatile microfluidic components using adhesive transfer tapes.* Lab on a Chip, 2010. **10**(17): p. 2286-2291.